CELLULAR AND MOLECULAR ANALYSIS OF AXON DEVELOPMENT IN ZEBRAFISH

by

Lingyan Xing

A dissertation submitted to the faculty of
The University of Utah
in partial fulfillment of the requirements for the degree of

Doctor of Philosophy

Interdepartmental Program in Neuroscience

The University of Utah

December 2015

The University of Utah Graduate School

STATEMENT OF DISSERTATION APPROVAL

The dissertation of **Lingyan Xing**

has been approved by the following supervisory committee members:

Joshua Bonkowsky	, Chair	**July 15th 2015** Date Approved
Richard Dorsky	, Member	**July 15th 2015** Date Approved
Adam Douglass	, Member	**July 15th 2015** Date Approved
Kristen Keefe	, Member	**July 15th 2015** Date Approved
Michael Bastiani	, Member	**July 15th 2015** Date Approved

and by **Richard Dorsky** , Chair/Dean of

the Department/College/School of **Interdepartmental Program in Neuroscience**

and by David B. Kieda, Dean of The Graduate School.

ABSTRACT

Brain wiring is critical for normal brain function, and brain connection defects have been described in many neurodevelopmental disorders. Accurate central nervous system connectivity relies on precise axon navigation. The cellular and molecular mechanisms governing axon guidance during development are important but not well understood.

In this dissertation, I utilize zebrafish, a powerful vertebrate model in developmental and genetic studies, to determine the molecular mechanisms regulating axon guidance *in vivo*. We specifically determine the role of the two molecules FoxP2 and serotonin (5-HT) in axon guidance. We demonstrate that FoxP2, a forkhead-domain transcription factor, is not required for axon guidance, but it reduces the expression levels of a synaptic protein Cntnap2. We also establish that 5-HT and its receptor Htr2a are important for axon guidance. The regulation of 5-HT on axon guidance is mediated by the tyrosine kinase Ephrinb2a. Moreover, we discover that axon guidance defects induced by environmental hypoxia can be rescued by serotonin reuptake inhibitor fluoxetine. I have also developed and implemented a PCR-based high resolution melting analysis (HRMA) for large-scale genotype screening and characterization of genes involved in axon development. Taken together, this work identifies a novel mechanism involved in central nervous system connectivity, and indicates raphe 5-HT neurons act as a sensor to alterations in the developmental environment.

TABLE OF CONTENTS

LIST OF FIGURES

ACKNOWLEDGEMENTS

I wish to express my sincere thanks to my advisor, Dr. Joshua Bonkowsky, for his excellent guidance and patience. I'm also grateful to my co-mentor, Dr. Richard Dorsky, for his great suggestions and help. I would also like to thank my other committee members: Dr. Adam Douglass, Dr. Kristen Keefe and Dr. Michael Bastiani.

I would like to give thanks to individuals who have contributed to this work. These include Tamara Stevenson, Esther Fujimoto, Jong-Hyun Son, Tiffanie Dahl and Tyler Quist. I also appreciate the help I got from other Bonkowsky lab members: Matthew Keefe, Jingxia Gao and Lauren Strachan.

I would also like to thank my parents, my grandparents and my parents-in-law. Last but not least, I would to thank my husband Liulei Cao for his unconditional support and love.

CHAPTER 1

INTRODUCTION

Overview

Neurodevelopmental disorders are a group of conditions characterized by impairments in central nervous system (CNS) development. These disorders typically manifest in childhood or adolescence. Neurodevelopmental disorders include, but are not limited to, autism spectrum disorders, intellectual disability, attention deficit hyperactivity disorder (ADHD), and cerebral palsy. In many patients with neurodevelopmental disorders, disruption of brain connectivity has been observed (van Ewijk et al., 2012; Minshew and Williams, 2007; Sundaram et al., 2014; Thomas et al., 2005).

Intact brain connectivity depends on accurate axon navigation, which requires the appropriate interaction between axon guidance molecules and their receptors. Therefore, disrupted signaling induced by genetic or environmental factors during axon development may have devasting results in early brain circuit formation and later behavior. Revealing the molecular mechanisms underlying axon guidance will provide more insight in understanding and treating neurodevelopmental disorders.

Axon guidance is a critical developmental process by which neurons send axon projections to the correct targets. Growing axons have a highly specialized and dynamic

structure located at each axon tip called the growth cone. Receptors on the growth cone can sense environmental signaling or guidance cues, promoting the reorganization of the cytoskeleton. Each receptor acts and responds to different guidance cues. Various guidance molecule pairs have been discovered, including the four best-described "canonical" signaling pairs: Slit-Robo, Netrin-DCC/Unc5, Ephrin-Eph, and Semaphorin-Plexin/Neuropilin (Barton et al., 2004; Bashaw and Klein, 2010, Figure 1.1). Appropriate interaction between axon guidance molecules and receptors ensures accurate axon pathfinding during development. Therefore, it is critical to understand the regulation of axon guidance molecules and their receptors by endogenous and exogenous stimuli.

Though many studies have focused on molecular signaling in early development, many questions still remain. These questions include how the mRNA or protein levels of axon guidance receptors are regulated by upstream signaling during the guidance of axons to the correct targets. In this dissertation, two potential regulators, FoxP2 and serotonin (5-HT), are discussed. I follow the standard nomenclature used to refer to the protein in different species: FOXP2 in human, Foxp2 in mouse, and FoxP2 in other chordates. Gene names are in italic (Vernes et al., 2011).

FOXP2 in language and brain development

FOXP2, a forkhead-box transcription factor, is well known for its role in language development. It was originally identified in a family with a severe speech and language disorder, and has subsequently been identified in other patients with language defects as well (Feuk et al., 2006; Lai et al., 2001; Lennon et al., 2007; MacDermot et al., 2005; Shriberg et al., 2006; Watkins et al., 2002a; Zeesman et al., 2006). Further studies

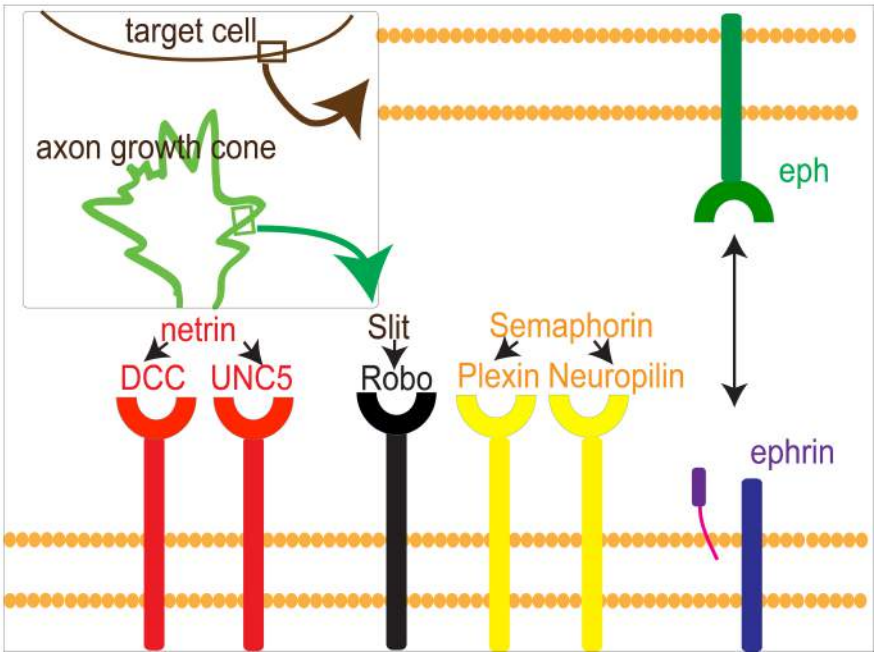

Figure 1.1. Diagram of major axon guidance molecules and their receptors.

showed that haploinsufficiency for *FOXP2* in humans leads to defects in grammatical language construction, as well as in the sequencing of orofacial movements required for speech articulation (Vargha-Khadem et al., 2005).

Individuals with language impairments from human *FOXP2* mutant pedigrees have altered neural activity in Broca's area and abnormal grey matter in the basal ganglia and prefrontal cortex, as shown by functional and volumetric magnetic resonance imaging (MRI) (Belton et al., 2003; Liégeois et al., 2003; Watkins et al., 2002b). However, how FOXP2 deficiency contributes to the brain abnormalities is not well understood.

Evidence from other species also indicates that FOXP2 plays an important role in brain development. In mice, *Foxp2* heterozygotes have impaired motor learning (Groszer et al., 2008), while homozygotes have a smaller cerebellum (Groszer et al., 2008), disorganization of the Purkinje cell layer in the cerebellum, and reduced ultrasonic vocalization (Shu et al., 2005). In songbirds, *FoxP2* is required for normal vocal learning or imitation of tutor songs during a juvenile sensitive period (Haesler et al., 2004; Teramitsu et al., 2004).

In addition, studies indicate that Foxp2 is necessary for intact synaptic function: *Foxp2* nulls have impaired synaptic plasticity and knock in of the human version of *FOXP2* in mice increases long-term depression in medium spiny neurons (Enard et al., 2009; Groszer et al., 2008). This evidence supports a role for Foxp2 in the development of brain connectivity. Nevertheless, the underlying developmental process that FOXP2 is involved in is not well characterized.

A few studies have suggested that FOXP2 may contribute to axon development.

In vitro chromatin immunoprecipitation (ChIP) showed that FOXP2 regulates multiple molecules involved in axon guidance, including EPHA2 and SEMA3B (Spiteri et al., 2007; Vernes et al., 2007). Cell culture shows that FOXP2 is necessary for axon outgrowth, consistent with the finding that FOXP2 can regulate the gene networks involved in controlling the length and branching of neuronal projections (Vernes et al., 2011). However, little information is available about the role of FOXP2 in axon pathfinding *in vivo*. In Chapter 3, I examine whether axon guidance is disrupted in zebrafish *FoxP2* mutants (Figure 1.2).

As a transcription factor, FOXP2 targets and regulates many downstream transcripts. Genome-wide chromatin immunoprecipitation (ChIP) has identified hundreds of DNA promoters bound by FOXP2 (Vernes et al., 2011), many of which function in early brain development. This study also shows that contactin-associated protein-like 2 (*CNTNAP2*), a member of the neurexin family, is a target of FOXP2 (Vernes et al., 2011). Genome-wide analysis has linked the gene *CNTNAP2* to both specific language impairment and autism (Alarcón et al., 2008; Arking et al., 2008; Peñagarikano et al., 2011; Whitehouse et al., 2011). Genetic variation in *CNTNAP2* is associated with altered CNS connectivity (Scott-Van Zeeland et al., 2010). During brain development, *CNTNAP2* is highly enriched in the frontal and anterior lobes, striatum, dorsal thalamus, and Broca's area (Rodenas-Cuadrado et al., 2014), consistent with its role in language development and cognitive function. The protein product of *CNTNAP2* facilitates cell-cell interaction in the nervous system (Rodenas-Cuadrado et al., 2014). Therefore, I hypothesized that misregulation of *CNTNAP2* by FOXP2 may, at least partially, account for the brain developmental defects that were observed in humans and rodents with

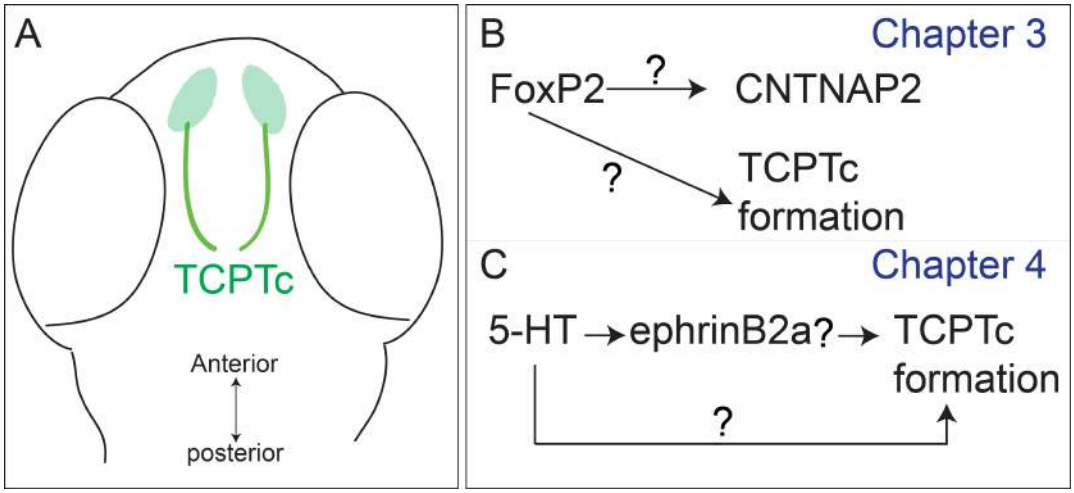

Figure 1.2. Development of TCPT axons and the molecular signaling tested. A). TCPT commissure axons starting to cross the midline. B) Diagram of the major hypothesis tested in Chapter 3 and Chapter 4.

FOXP2 mutations. However, whether the FOXP2/*CNTNAP2* signaling pathway exists *in vivo* has not been clarified. In Chapter 3, I determine the role of FoxP2 in axon development and further test whether the FoxP2/*CNTNAP2* signaling pathway is conserved in zebrafish (Figure 1.2).

The *FOXP2* gene is highly conserved in vertebrates. Mouse and human *FOXP2* orthologs only differ by three amino acids. The zebrafish FoxP2 protein has 86% homology with the human protein. The *FoxP2* expression pattern in the CNS is also conserved in vertebrates, as shown in mice, songbirds, and humans (Bonkowsky and Chien, 2005; Ferland et al., 2003; Haesler et al., 2004; Lai et al., 2003; Takahashi et al., 2003). Therefore, dissecting the role of FoxP2 in zebrafish development may provide insight into the mechanism by which FOXP2 functions in the development of human brain architecture.

5-HT and brain development

In the adult CNS, the neurotransmitter 5-HT acts as a molecular modulator of the strength of synaptic signals (Lesch and Waider, 2012). Many studies have addressed the role of 5-HT in adult physiological processes and behavior including, but not limited to, sleeping, appetite, emotion, and memory consolidation (Gingrich et al., 2003). Therefore, perturbation of the serotonergic system by drugs or adverse environment can lead to deficits in biological physiology and behavior.

Intriguingly, accumulated evidence shows a nonclassical role for 5-HT during development. 5-HT and its receptors have been detected during vertebrate CNS development, prior to the development of behaviors requiring 5-HT (Gaspar et al., 2003).

Loss of 5-HT neurons or other components of 5-HT signaling in early development leads to broad CNS abnormalities with a wide range of behavioral phenotypes (van Kleef et al., 2012). A genetic model that temporally regulates HTR1A (5-HT receptor 1A) demonstrates that the serotonergic system acts during development, not the adult stage, to establish normal anxiety-like behavior (Gross et al., 2002).

Work in rodent models provides more evidence supporting a role for 5-HT in early brain development. Impaired barrel cortex is observed in serotonin transporter (5-HTT) knockout mice (Persico et al., 2001); the number of synapses in the visual cortex is decreased followed by drug-induced 5-HT depletion (Matsukawa et al., 2003); neurons in the somatosensory cortex display a reduced dendritic arborization when 5-HT is depleted (Vitalis et al., 2007); either exogenous 5-HT or a 5-HTR6 (serotonin receptor 6) agonist can block embryonic cortical interneuron migration (Riccio et al., 2009). However, these studies did not exclude the possibility that these defects observed following serotonergic signaling disruption may derive from the secondary effects caused by perturbations in normal brain development.

A potential role for 5-HT in axon pathfinding has been observed, as well as its role in axon branching, synapse formation, dendrite arborization, and interneuron migration. In mouse thalamocortical neuron explants, application of 5-HT caused a repulsive response to netrin-1 and overexpression of the 5-HT receptor *htr1b/1d* caused dorso-ventral shifting of the axon tracts (Bonnin et al., 2007). In rat raphe neuron explants, knockdown of the 5-HT transporter led to altered fasciculation and projections of axons (Witteveen et al., 2013). However, evidence for a cell-autonomous role of 5-HT receptors in axon pathfinding is lacking. Moreover, the direct mechanism by which 5-HT

regulates axon guidance *in vivo* is not well understood. Axon guidance receptors are critical in recognizing guidance cues leading to the possibility that 5-HT could regulate guidance receptors and further contribute to the development of axon connectivity. In Chapter 4, I test the role of 5-HT in axon guidance and investigate the potential mechanism involved in the process.

Ephrin/eph signaling in axon guidance

As mentioned in the overview, ephrin/eph signaling is one of the four best-described "canonical" pathways involved in axon guidance. Ephrins are glycosylphosphatdylinostol (GPI) anchored transmembrane proteins. They are known to interact with EphA or EphB receptors, the largest receptor-tyrosine kinases (RTK) families. When acting as ligands, ephrins induce an intracellular signaling cascade in eph-expressing cells (Bashaw and Klein, 2010). This is known as "forward signaling". As membrane-bound proteins (Pasquale, 2008), ephrins can also induce "reverse signaling", in which signals transfer from ephs to ephrins, activating the downstream signaling in ephrin-expressing cells. As opposed to a variety of other axon guidance cues/receptors, signal transduction between ephrins and ephs requires cell-cell interaction. Therefore, one feature of ephrin/eph signals is that interactions occur only at adjacent cells (Bashaw and Klein, 2010).

Several studies have demonstrated that ephrinBs and their receptors play an important role in regulating midline axon crossing (Cramer et al., 2006; Frisén et al., 1999; Henkemeyer et al., 1996; Kullander et al., 2001; Nakagawa et al., 2000). For example, ephrinB expressed at the midline optic chiasm repels ipsilateral retinal axons

crossing the midline (Nakagawa et al., 2000) and *ephB2* expressed in the brainstem prohibits axons crossing back over the midline (Cramer et al., 2006). Consistent with a critical role of ephrinB2 in axon guidance, misregulated ephrinB in early development leads to axon guidance disruptions. Our lab observed that increased ephrinB2a contributes to midline axon guidance defects under hypoxic conditions (Stevenson et al., 2012). Interestingly, this is mediated by ephrins/ephs "reverse signaling" (Stevenson et al., 2012).

Based on the potential role of 5-HT in axon development (Bonnin et al., 2007; Witteveen et al., 2013) and the fact that ephrinB2a is expressed in TCPTc (Stevenson et al., 2012), I hypothesize that 5-HT regulates axon guidance through ephrinB2a. I test the hypothesis in Chapter 4 (Figure 1.2).

5-HT as an environmental sensor

Neural circuitry development in the vertebrate brain is governed not only by genetic, but also by environmental factors. For example, during perinatal sensitive periods, early-life stress, nutrition, and maternal care affect brain structure and function (Korosi and Baram, 2009; Lucassen et al., 2013; Weinstock, 2008). However, how neural circuits are manipulated by environmental stimuli remains elusive.

Studies have found that environmental stimuli including hypoxia, pH, and chemicals can modify the serotonergic system (Bosker et al., 1994; Davis, 1975; Eddahibi et al., 1999; Hickner et al., 2014; Kellum et al., 1983; Pocock and Hobert, 2010a; Rahman and Thomas, 2009, 2014). In *C. elegans*, hypoxia activates an additional, previously unrecognized neural circuit for chemosensory perception (Pocock and Hobert,

2010b). Interestingly, enhanced sensory perception is mediated by 5-HT and its receptor ser-7. (Pocock and Hobert, 2010a). These studies suggest that 5-HT is a potential intrinsic modulator responsive to exogenous developmental or environmental cues (Chaouluff, 2000).

However, the neural circuits modified by 5-HT under hypoxia are not well characterized. Hypoxia is a key adverse environmental factor in early development, especially for premature infants with underdeveloped lungs and cardiovascular system at birth. Children born prematurely are more likely to suffer from neurological disorders (Bass *et al*., 2004; Barrett *et al*., 2007; Mathiasen *et al*., 2011; Raman *et al*., 2006). Based on diffusion tension imaging data, premature birth could lead to CNS connectivity disruption (Yeatman *et al*., 2009). Specific axon guidance defects have also been observed following hypoxia in both zebrafish and *C. elegans* (Stevenson *et al*., 2012 and Pocock & Hobert, 2009). However, whether 5-HT contributes to axon connectivity disruption in response to developmental hypoxia is still unexplored.

Based on the fact that hypoxia could affect the serotonergic system in vertebrates (Davis, 1975; Rahman and Thomas, 2009) and because of a potential role of 5-HT in axon development (Bonnin et al., 2007; Witteveen et al., 2013), I hypothesize that 5-HT contributes to axon guidance defects under hypoxia. I test this hypothesis in Chapter 4. A role of 5-HT in sensing exogenous stimuli and further altering neural circuits during development may explain neurobehavioral repertoire changes in response to parental or developmental exposures.

In this dissertation, I take advantage of the ease of use of the zebrafish model and apply pharmacological, genetic and molecular tools, including high-resolution melting

analysis (HRMA), to promote our understanding of the molecular mechanisms involved in axon guidance.

Advantages of zebrafish in developmental studies

The zebrafish is a widely used vertebrate model in genetic and developmental studies due to its transparent embryos, rapid developmental process, external fertilization, and powerful genetic tools, including numerous mutant and easy to generate transgenic lines. In this dissertation, the transgenic line Tg(*foxP2-enhancerA.2:egfp-caax*)^{zc69} is utilized to monitor axon development in zebrafish. Tg(*foxP2-enhancerA.2:egfp-caax*) labels neurons in the telencephalon, and their axons with assistance of the membrane-targeted motif caax. Axons either form the anterior commissure, the diencephalic tract of the commissure of the posterior tuberculum (TCPTc) (Wilson et al., 1990), or longitudinal axons (Figure 1.3). In this dissertation, I focus on the molecular mechanisms involved in TCPTc development. The axons forming TCPTc extend around 24 hpf (hours post-fertilization), start to cross the midline at 36-48 hpf, and most axons have crossed by 72 hpf.

High-resolution melting analysis (HRMA) in genotyping

Traditional genotyping approaches have limitations in rapid and large-scale screening. PCR followed by gel electrophoresis, sometimes combined with restriction enzyme digestion, is time-consuming and less sensitive for small deletions or insertions. The TaqMan probe assay is expensive and requires careful optimization, and sequencing

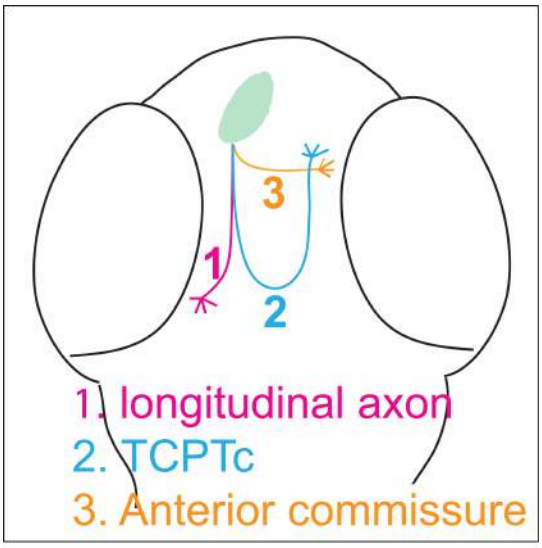

Figure 1.3. The axons labeled by *foxP2-enhancer A.2:egfp-caax*. *In the dissertation, we will focus on the* diencephalic tract of the commissure of the posterior tuberculum (TCPTc).

PCR products is tedious and not suitable for large-scale screening.

HRMA, a closed-tube post-PCR analysis method, has been developed for screening large numbers of animals. HRMA is a rapid, sensitive, and inexpensive approach for genotyping. HRMA is based on thermal denaturation of double-stranded DNAs—each PCR amplicon has a unique dissociation (melt) characteristic. Samples can be discriminated based on their different nucleotides, GC content, or length, typically in combination with a fluorescent dye that only binds to double-stranded DNA. HRMA can be used to detect SNPs, mutations, and transgenes (Dahlem et al., 2012; Liew et al., 2004; Vossen et al., 2009). Since HRMA uses low-cost reagents and is a single-step post-PCR process, it is amenable to high-throughput screening.

HRMA has been applied in many organisms and systems, including cell lines, mice, and humans (Carrillo et al. 2013; Thomsen et al. 2012; Vorkas et al. 2010). Its use has recently been described in zebrafish to detect mutations induced by zinc finger nucleases (ZFNs) or transcription activator-like effector nucleases (TALENs) (Dahlem et al., 2012; Xing et al., 2012).

Chapter 2 is a peer-reviewed paper and video discussing how to apply HRMA in both embryonic and adult fish to detect transgenes and mutations. This helps the scientific research community see exactly how this technique works. I first apply HRMA in fin clips of embryos prior to phenotype analysis. This is extremely useful when homozygotes are not viable or fertile. Though the *foxP2* nulls I obtained are fertile, almost all were female for unidentified reasons; therefore it was necessary to intercross heterozygotes and genotype individual embryos by fin clip prior to analyzing their phenotypes. In this thesis, I applied two different strategies to generate knockout fish:

zinc finger nucleases (ZFNs) and the Clustered Regularly Interspaced Short Palindromic Repeats (CRISPR). HRMA greatly facilitates genotyping multiple genetic lines or mutant lines, maximizing the power of mutagenesis tools.

Summary

CNS connectivity is altered in patients with specific language impairment and in other neurodevelopmental disorders including autism spectrum disorders, intellectual disability, ADHD, and cerebral palsy (van Ewijk et al., 2012; Minshew and Williams, 2007; Sundaram et al., 2014; Thomas et al., 2005). Connections between different brain regions rely on accurate axonal and synaptic development. Thus, unraveling the genetic pathways and neural circuitry involved in axon pathfinding, an important process for CNS connectivity, will facilitate understanding the pathogenic mechanisms in neurodevelopmental disorders. In this dissertation, I have used the zebrafish as a model, combined with different experimental strategies, including pharmacological, genetic and molecular tools to study whether FoxP2 and/or 5-HT is involved in axon pathfinding. I have also tested whether FoxP2 and 5-HT regulate CNTNAP2 and ephrinB2a in Chapter 3 and Chapter 4, respectively (Figure 1.2). In Chapter 2, I have applied HRMA for large-scale genotype screening in zebrafish, which helps facilitate the characterization of genes involved in axon development. Taken together, this dissertation contributes to a better understanding of the molecular mechanisms involved in axon guidance.

References

Alarcón, M., Abrahams, B.S., Stone, J.L., Duvall, J.A., Perederiy, J. V., Bomar, J.M., Sebat, J., Wigler, M., Martin, C.L., Ledbetter, D.H., et al. (2008). linkage, association, and gene-expression analyses identify CNTNAP2 as an autism-susceptibility gene. Am. J. Hum. Genet. *82*, 150–159.

Arking, D.E., Cutler, D.J., Brune, C.W., Teslovich, T.M., West, K., Ikeda, M., Rea, A., Guy, M., Lin, S., Cook, E.H., et al. (2008). A common genetic variant in the neurexin superfamily member CNTNAP2 increases familial risk of autism. Am. J. Hum. Genet. *82*, 160–164.

Barton, W.A., Himanen, J.-P., Antipenko, A., and Nikolov, D.B. (2004). Structures of axon guidance molecules and their neuronal receptors. Adv. Protein Chem. *68*, 65–106.

Bashaw, G.J., and Klein, R. (2010). Signaling from axon guidance receptors. Cold Spring Harb. Perspect. Biol. *2*, a001941.

Belton, E., Salmond, C.H., Watkins, K.E., Vargha-Khadem, F., and Gadian, D.G. (2003). Bilateral brain abnormalities associated with dominantly inherited verbal and orofacial dyspraxia. Hum. Brain Mapp. *18*, 194–200.

Bonkowsky, J.L., and Chien, C.-B. (2005). Molecular cloning and developmental expression of foxP2 in zebrafish. Dev. Dyn. *234*, 740–746.

Bonnin, A., Torii, M., Wang, L., Rakic, P., and Levitt, P. (2007). Serotonin modulates the response of embryonic thalamocortical axons to netrin-1. Nat. Neurosci. *10*, 588–597.

Bosker, F., Klompmakers, A., and Westenberg, H. (1994). Extracellular 5-hydroxytryptamine in median raphe nucleus of the conscious rat is decreased by nanomolar concentrations of 8-hydroxy-2-(di-n-propylamino) tetralin and is sensitive to tetrodotoxin. J. Neurochem. *63*, 2165–2171.

Cramer, K.S., Cerretti, D.P., and Siddiqui, S.A. (2006). EphB2 regulates axonal growth at the midline in the developing auditory brainstem. Dev. Biol. *295*, 76–89.

Dahlem, T.J., Hoshijima, K., Jurynec, M.J., Gunther, D., Starker, C.G., Locke, A.S., Weis, A.M., Voytas, D.F., and Grunwald, D.J. (2012). Simple methods for generating and detecting locus-specific mutations induced with TALENs in the zebrafish genome. PLoS Genet. *8*, e1002861.

Davis, J.N. (1975). Adaptation of brain monoamine synthesis to hypoxia in the rat. J. Appl. Physiol. *39*, 215–220.

Eddahibi, S., Fabre, V., Boni, C., Martres, M.P., Raffestin, B., Hamon, M., and Adnot, S. (1999). Induction of Serotonin Transporter by Hypoxia in Pulmonary Vascular Smooth

Muscle Cells : Relationship With the Mitogenic Action of Serotonin. Circ. Res. *84*, 329–336.

Enard, W., Gehre, S., Hammerschmidt, K., Hölter, S.M., Blass, T., Somel, M., Brückner, M.K., Schreiweis, C., Winter, C., Sohr, R., et al. (2009). A humanized version of Foxp2 affects cortico-basal ganglia circuits in mice. Cell *137*, 961–971.

Van Ewijk, H., Heslenfeld, D.J., Zwiers, M.P., Buitelaar, J.K., and Oosterlaan, J. (2012). Diffusion tensor imaging in attention deficit/hyperactivity disorder: A systematic review and meta-analysis. Neurosci. Biobehav. Rev. *36*, 1093–1106.

Ferland, R.J., Cherry, T.J., Preware, P.O., Morrisey, E.E., and Walsh, C.A. (2003). Characterization of Foxp2 and Foxp1 mRNA and protein in the developing and mature brain. J. Comp. Neurol. *460*, 266–279.

Feuk, L., Kalervo, A., Lipsanen-Nyman, M., Skaug, J., Nakabayashi, K., Finucane, B., Hartung, D., Innes, M., Kerem, B., Nowaczyk, M.J., et al. (2006). Absence of a paternally inherited FOXP2 gene in developmental verbal dyspraxia. Am. J. Hum. Genet. *79*, 965–972.

Frisén, J., Holmberg, J., and Barbacid, M. (1999). Ephrins and their Eph receptors: multitalented directors of embryonic development. EMBO J. *18*, 5159–5165.

Gaspar, P., Cases, O., and Maroteaux, L. (2003). The developmental role of serotonin: news from mouse molecular genetics. Nat. Rev. Neurosci. *4*, 1002–1012.

Gingrich, J.A., Ansorge, M.S., Merker, R., Weisstaub, N., and Zhou, M. (2003). New lessons from knockout mice: The role of serotonin during development and its possible contribution to the origins of neuropsychiatric disorders. CNS Spectr. *8*, 572–577.

Gross, C., Zhuang, X., Stark, K., Ramboz, S., Oosting, R., Kirby, L., Santarelli, L., Beck, S., and Hen, R. (2002). Serotonin1A receptor acts during development to establish normal anxiety-like behaviour in the adult. Nature *416*, 396–400.

Groszer, M., Keays, D.A., Deacon, R.M.J., de Bono, J.P., Prasad-Mulcare, S., Gaub, S., Baum, M.G., French, C.A., Nicod, J., Coventry, J.A., et al. (2008). Impaired synaptic plasticity and motor learning in mice with a point mutation implicated in human speech deficits. Curr. Biol. *18*, 354–362.

Haesler, S., Wada, K., Nshdejan, A., Morrisey, E.E., Lints, T., Jarvis, E.D., and Scharff, C. (2004). FoxP2 expression in avian vocal learners and non-learners. J. Neurosci. *24*, 3164–3175.

Henkemeyer, M., Orioli, D., Henderson, J.T., Saxton, T.M., Roder, J., Pawson, T., and Klein, R. (1996). Nuk Controls Pathfinding of Commissural Axons in the Mammalian Central Nervous System. Cell *86*, 35–46.

Hickner, S., Hussain, N., Angoa-Perez, M., Francescutti, D.M., Kuhn, D.M., and Mateika, J.H. (2014). Ventilatory long-term facilitation is evident after initial and repeated exposure to intermittent hypoxia in mice genetically depleted of brain serotonin. J. Appl. Physiol. *116*, 240–250.

Kellum, J., McCabe, M., Schneier, J., and Donowitz, M. (1983). Neural control of acid-induced serotonin release from rabbit duodenum. Am. J. Physiol. *245*, G824–G831.
Van Kleef, E.S.B., Gaspar, P., and Bonnin, A. (2012). Insights into the complex influence of 5-HT signaling on thalamocortical axonal system development. Eur. J. Neurosci. *35*, 1563–1572.

Korosi, A., and Baram, T.Z. (2009). The pathways from mother's love to baby's future. Front. Behav. Neurosci. *3*, 27.

Kullander, K., Croll, S.D., Zimmer, M., Pan, L., McClain, J., Hughes, V., Zabski, S., DeChiara, T.M., Klein, R., Yancopoulos, G.D., et al. (2001). Ephrin-B3 is the midline barrier that prevents corticospinal tract axons from recrossing, allowing for unilateral motor control. Genes Dev. *15*, 877–888.

Lai, C.S.L., Fisher, S.E., Hurst, J.A., Vargha-Khadem, F., and Monaco, A.P. (2001). A forkhead-domain gene is mutated in a severe speech and language disorder. Nature *413*, 519–523.

Lai, C.S.L., Gerrelli, D., Monaco, A.P., Fisher, S.E., and Copp, A.J. (2003). FOXP2 expression during brain development coincides with adult sites of pathology in a severe speech and language disorder. Brain *126*, 2455–2462.

Lennon, P.A., Cooper, M.L., Peiffer, D.A., Gunderson, K.L., Patel, A., Peters, S., Cheung, S.W., and Bacino, C.A. (2007). Deletion of 7q31.1 supports involvement of FOXP2 in language impairment: clinical report and review. Am. J. Med. Genet. A *143A*, 791–798.

Lesch, K.-P., and Waider, J. (2012). Serotonin in the modulation of neural plasticity and networks: implications for neurodevelopmental disorders. Neuron *76*, 175–191.

Liégeois, F., Baldeweg, T., Connelly, A., Gadian, D.G., Mishkin, M., and Vargha-Khadem, F. (2003). Language fMRI abnormalities associated with FOXP2 gene mutation. Nat. Neurosci. *6*, 1230–1237.

Liew, M., Pryor, R., Palais, R., Meadows, C., Erali, M., Lyon, E., and Wittwer, C. (2004). Genotyping of single-nucleotide polymorphisms by high-resolution melting of small amplicons. Clin. Chem. *50*, 1156–1164.

Lucassen, P.J., Naninck, E.F.G., van Goudoever, J.B., Fitzsimons, C., Joels, M., and Korosi, A. (2013). Perinatal programming of adult hippocampal structure and function; emerging roles of stress, nutrition and epigenetics. Trends Neurosci. *36*, 621–631.

MacDermot, K.D., Bonora, E., Sykes, N., Coupe, A.-M., Lai, C.S.L., Vernes, S.C., Vargha-Khadem, F., McKenzie, F., Smith, R.L., Monaco, A.P., et al. (2005). Identification of FOXP2 truncation as a novel cause of developmental speech and language deficits. Am. J. Hum. Genet. *76*, 1074–1080.

Matsukawa, M., Nakadate, K., Ishihara, I., and Okado, N. (2003). Synaptic loss following depletion of noradrenaline and/or serotonin in the rat visual cortex: a quantitative electron microscopic study. Neuroscience *122*, 627–635.

Minshew, N.J., and Williams, D.L. (2007). The new neurobiology of autism: cortex, connectivity, and neuronal organization. Arch. Neurol. *64*, 945–950.

Nakagawa, S., Brennan, C., Johnson, K.G., Shewan, D., Harris, W.A., and Holt, C.E. (2000). Ephrin-B regulates the Ipsilateral routing of retinal axons at the optic chiasm. Neuron *25*, 599–610.

Pasquale, E.B. (2008). Eph-ephrin bidirectional signaling in physiology and disease. Cell *133*, 38–52.

Peñagarikano, O., Abrahams, B.S., Herman, E.I., Winden, K.D., Gdalyahu, A., Dong, H., Sonnenblick, L.I., Gruver, R., Almajano, J., Bragin, A., et al. (2011). Absence of CNTNAP2 leads to epilepsy, neuronal migration abnormalities, and core autism-related deficits. Cell *147*, 235–246.

Persico, A.M., Mengual, E., Moessner, R., Hall, F.S., Revay, R.S., Sora, I., Arellano, J., DeFelipe, J., Gimenez-Amaya, J.M., Conciatori, M., et al. (2001). Barrel pattern formation requires serotonin uptake by thalamocortical afferents, and not vesicular monoamine release. J. Neurosci. *21*, 6862–6873.

Pocock, R., and Hobert, O. (2010). Hypoxia activates a latent circuit for processing gustatory information in C. elegans. Nat. Neurosci. *13*, 610–614.

Rahman, M.S., and Thomas, P. (2009). Molecular cloning, characterization and expression of two tryptophan hydroxylase (TPH-1 and TPH-2) genes in the hypothalamus of Atlantic croaker: down-regulation after chronic exposure to hypoxia. Neuroscience *158*, 751–765.

Rahman, M.S., and Thomas, P. (2014). Restoration of tryptophan hydroxylase functions and serotonin content in the Atlantic croaker hypothalamus by antioxidant treatment during hypoxic stress. Front. Neurosci. *8*, 130.
Riccio, O., Potter, G., Walzer, C., Vallet, P., Szabó, G., Vutskits, L., Kiss, J.Z., and Dayer, A.G. (2009). Excess of serotonin affects embryonic interneuron migration through activation of the serotonin receptor 6. Mol. Psychiatry *14*, 280–290.

Rodenas-Cuadrado, P., Ho, J., and Vernes, S.C. (2014). Shining a light on CNTNAP2: complex functions to complex disorders. Eur. J. Hum. Genet. *22*, 171–178.

Scott-Van Zeeland, A.A., Abrahams, B.S., Alvarez-Retuerto, A.I., Sonnenblick, L.I., Rudie, J.D., Ghahremani, D., Mumford, J.A., Poldrack, R.A., Dapretto, M., Geschwind, D.H., et al. (2010). Altered functional connectivity in frontal lobe circuits is associated with variation in the autism risk gene CNTNAP2. Sci. Transl. Med. *2*, 56ra80.

Shriberg, L.D., Ballard, K.J., Tomblin, J.B., Duffy, J.R., Odell, K.H., and Williams, C.A. (2006). Speech, prosody, and voice characteristics of a mother and daughter with a 7;13 translocation affecting FOXP2. J. Speech. Lang. Hear. Res. *49*, 500–525.

Shu, W., Cho, J.Y., Jiang, Y., Zhang, M., Weisz, D., Elder, G.A., Schmeidler, J., De Gasperi, R., Sosa, M.A.G., Rabidou, D., et al. (2005). Altered ultrasonic vocalization in mice with a disruption in the Foxp2 gene. Proc. Natl. Acad. Sci. U. S. A. *102*, 9643–9648.

Spiteri, E., Konopka, G., Coppola, G., Bomar, J., Oldham, M., Ou, J., Vernes, S.C., Fisher, S.E., Ren, B., and Geschwind, D.H. (2007). Identification of the Transcriptional Targets of FOXP2, a Gene Linked to Speech and Language, in Developing Human Brain. Am. J. Hum. Genet. *81*, 1144–1157.

Stevenson, T.J., Trinh, T., Kogelschatz, C., Fujimoto, E., Lush, M.E., Piotrowski, T., Brimley, C.J., and Bonkowsky, J.L. (2012). Hypoxia disruption of vertebrate CNS pathfinding through ephrinB2 Is rescued by magnesium. PLoS Genet. *8*, e1002638.

Sundaram, S., Huq, A.H.M., Hsia, T., and Chugani, H. (2014). Exome sequencing and diffusion tensor imaging in developmental disabilities. Pediatr. Res. *75*, 443–447.

Takahashi, K., Liu, F.-C., Hirokawa, K., and Takahashi, H. (2003). Expression of Foxp2, a gene involved in speech and language, in the developing and adult striatum. J. Neurosci. Res. *73*, 61–72.

Teramitsu, I., Kudo, L.C., London, S.E., Geschwind, D.H., and White, S.A. (2004). Parallel FoxP1 and FoxP2 expression in songbird and human brain predicts functional interaction. J. Neurosci. *24*, 3152–3163.

Thomas, B., Eyssen, M., Peeters, R., Molenaers, G., Van Hecke, P., De Cock, P., and Sunaert, S. (2005). Quantitative diffusion tensor imaging in cerebral palsy due to periventricular white matter injury. Brain *128*, 2562–2577.

Vargha-Khadem, F., Gadian, D.G., Copp, A., and Mishkin, M. (2005). FOXP2 and the neuroanatomy of speech and language. Nat. Rev. Neurosci. *6*, 131–138.

Vernes, S.C., Spiteri, E., Nicod, J., Groszer, M., Taylor, J.M., Davies, K.E., Geschwind, D.H., and Fisher, S.E. (2007). High-throughput analysis of promoter occupancy reveals direct neural targets of FOXP2, a gene mutated in speech and language disorders. Am. J. Hum. Genet. *81*, 1232–1250.

Vernes, S.C., Oliver, P.L., Spiteri, E., Lockstone, H.E., Puliyadi, R., Taylor, J.M., Ho, J., Mombereau, C., Brewer, A., Lowy, E., et al. (2011). Foxp2 regulates gene networks implicated in neurite outgrowth in the developing brain. PLoS Genet. *7*, e1002145.

Vitalis, T., Cases, O., Passemard, S., Callebert, J., and Parnavelas, J.G. (2007). Embryonic depletion of serotonin affects cortical development. Eur. J. Neurosci. *26*, 331–344.

Vossen, R.H.A.M., Aten, E., Roos, A., and den Dunnen, J.T. (2009). High-resolution melting analysis (HRMA): more than just sequence variant screening. Hum. Mutat. *30*, 860–866.

Watkins, K.E., Dronkers, N.F., and Vargha-Khadem, F. (2002). Behavioural analysis of an inherited speech and language disorder: comparison with acquired aphasia. Brain *125*, 452–464.

Watkins, K.E., Vargha-Khadem, F., Ashburner, J., Passingham, R.E., Connelly, A., Friston, K.J., Frackowiak, R.S.J., Mishkin, M., and Gadian, D.G. (2002b). MRI analysis of an inherited speech and language disorder: structural brain abnormalities. Brain *125*, 465–478.

Weinstock, M. (2008). The long-term behavioural consequences of prenatal stress. Neurosci. Biobehav. Rev. *32*, 1073–1086.

Whitehouse, A.J.O., Bishop, D.V.M., Ang, Q.W., Pennell, C.E., and Fisher, S.E. (2011). CNTNAP2 variants affect early language development in the general population. Genes. Brain. Behav. *10*, 451–456.

Wilson, S.W., Ross, L.S., Parrett, T., and Easter, S.S. (1990). The development of a simple scaffold of axon tracts in the brain of the embryonic zebrafish, Brachydanio rerio. Development *108*, 121–145.

Witteveen, J.S., Middelman, A., van Hulten, J.A., Martens, G.J.M., Homberg, J.R., and Kolk, S.M. (2013). Lack of serotonin reuptake during brain development alters rostral raphe-prefrontal network formation. Front. Cell. Neurosci. *7*, 143.

Xing, L., Hoshijima, K., Grunwald, D.J., Fujimoto, E., Quist, T.S., Sneddon, J., Chien, C.-B., Stevenson, T.J., and Bonkowsky, J.L. (2012). Zebrafish foxP2 zinc finger nuclease mutant has normal axon pathfinding. PLoS One *7*, e43968.

Zeesman, S., Nowaczyk, M.J.M., Teshima, I., Roberts, W., Cardy, J.O., Brian, J., Senman, L., Feuk, L., Osborne, L.R., and Scherer, S.W. (2006). Speech and language impairment and oromotor dyspraxia due to deletion of 7q31 that involves FOXP2. Am. J. Med. Genet. A *140*, 509–514.

CHAPTER 2

RAPID AND EFFICIENT ZEBRAFISH GENOTYPING USING PCR WITH HIGH-RESOLUTION MELT ANALYSIS

The following chapter is reprinted with permission from the Journal of Visualized Experiments. Xing, L., Quist, T. S., Stevenson, T. J., Dahlem, T. J., Bonkowsky, J. L. Rapid and Efficient Zebrafish Genotyping Using PCR with High-resolution Melt Analysis. *J. Vis. Exp.* (84), e51138, doi:10.3791/51138 (2014).

jove Journal of Visualized Experiments www.jove.com

Video Article

Rapid and Efficient Zebrafish Genotyping Using PCR with High-resolution Melt Analysis

Lingyan Xing[1,2,3], Tyler S. Quist[1], Tamara J. Stevenson[1], Timothy J. Dahlem[4], Joshua L. Bonkowsky[1,2,3,5]

[1]Division of Pediatric Neurology, Department of Pediatrics, University of Utah School of Medicine

[2]Department of Neurobiology and Anatomy, University of Utah School of Medicine

[3]Interdepartmental Program in Neurosciences, University of Utah School of Medicine

[4]Mutation Generation and Detection Core, HSC Core Research Facility, University of Utah School of Medicine

[5]Department of Neurology, University of Utah School of Medicine

Correspondence to: Joshua L. Bonkowsky at Joshua.Bonkowsky@hsc.utah.edu

URL: http://www.jove.com/video/51138
DOI: doi:10.3791/51138

Keywords: Basic Protocol, Issue 84, genotyping, high-resolution melting analysis (HRMA), PCR, zebrafish, mutation, transgenes

Date Published: 2/5/2014

Citation: Xing, L., Quist, T.S., Stevenson, T.J., Dahlem, T.J., Bonkowsky, J.L. Rapid and Efficient Zebrafish Genotyping Using PCR with High-resolution Melt Analysis. *J. Vis. Exp.* (84), e51138, doi:10.3791/51138 (2014).

Abstract

Zebrafish is a powerful vertebrate model system for studying development, modeling disease, and performing drug screening. Recently a variety of genetic tools have been introduced, including multiple strategies for inducing mutations and generating transgenic lines. However, large-scale screening is limited by traditional genotyping methods, which are time-consuming and labor-intensive. Here we describe a technique to analyze zebrafish genotypes by PCR combined with high-resolution melting analysis (HRMA). This approach is rapid, sensitive, and inexpensive, with lower risk of contamination artifacts. Genotyping by PCR with HRMA can be used for embryos or adult fish, including in high-throughput screening protocols.

Video Link

The video component of this article can be found at http://www.jove.com/video/51138/

Introduction

Zebrafish (*Danio rerio*) is a vertebrate model system widely used for studies of development and disease modeling. Recently, numerous transgenic and mutation technologies have been developed for zebrafish. Rapid transgenesis techniques, usually based on a Tol2 transposon system[1], have been combined with improved cloning options for multiple DNA fragment assembly[2]. Zinc-finger nucleases (ZFNs) and transcription activator-like effector nucleases (TALENs) have been used to target loci in both somatic and germline cells in zebrafish[3,4]. These techniques can efficiently generate genetically modified animals, with high-frequency mutation creation and germ-line transmission[3,4].

Despite these advances, traditional genotyping techniques in zebrafish limit the full power of the mutagenesis and transgenesis tools. PCR followed by gel electrophoresis, sometimes combined with restriction enzyme digestion, is widely used to detect genome modification, but is time-consuming and less sensitive to identify small insertions or deletions. TaqMan probe assays have high initial costs and require careful optimization. Sequencing of PCR products can take several days and is not practical for large-scale screening. Restriction fragment length polymorphism (RFLP) analysis can only discriminate SNPs affecting a limited range of restriction enzyme recognition sites.

High-resolution melting analysis (HRMA), a closed-tube post-PCR analysis method, is a recently developed method that is rapid, sensitive, inexpensive, and amenable to screening large numbers of samples. HRMA can be used to detect SNPs, mutations, and transgenes[5-7]. HRMA is based on thermal denaturation of double-stranded DNAs, and each PCR amplicon has a unique dissociation (melt) characteristic[5]. Samples can be discriminated due to their different nucleotide composition, GC content, or length, typically in combination with a fluorescent dye that only binds double-stranded DNA[8]. Thus, HRMA can distinguish different genotypes based on the different melt-curve characteristics. Because HRMA uses low-cost reagents and is a single-step post-PCR process, it can be used for high-throughput strategies. HRMA is nondestructive, so following analysis the PCR amplicons can be used for other applications. HRMA has been applied in many organisms and systems, including cell lines, mice, and humans[9-11]. Its use has recently been described in zebrafish to detect mutations induced by zinc finger nucleases (ZFNs) and TALENs[6,12,13].

In this paper, we describe how to perform PCR-based HRMA in embryonic and adult zebrafish (**Figure 1**). This protocol is suitable for detecting SNPs, transgenes, and mutations, including single base-pair changes, insertions, or deletions.

jove Journal of Visualized Experiments www.jove.com

Protocol

1. DNA Preparation

1. Prepare DNA lysis buffer: 50 mM KCl, 10 mM Tris-HCl pH 8.3, 0.3% Tween 20, 0.3% NP40. Add fresh Proteinase K to a final concentration of 1 mg/ml on the day of use[12].
2. Tissue collection:
    1. For adult fish fin clip:
        1. Anesthetize fish: Place the fish in 0.004% MS-222 (tricaine) solution. Wait until gill movement slows.
        2. Put fish on a stack of 5-10 Kimwipes and cut a small piece of the tail fin, about 2-3 mm, with a sterile razor blade.
        3. Quickly place the fish in a labeled tank with fresh water for recovery; carefully label both the tank and corresponding tube that will contain the fin clip. Change the water and feed the fish every other day.
        4. Pick up the fin clip with a sterile pipette tip and transfer it into a tube filled with 100 µl DNA lysis buffer.
        5. Discard the pipette tip, and discard the razor blade into a sharps container.
    2. For embryo tail clip:
        1. Place embryos into 0.004% MS-222 (tricaine) solution. Wait 2 min.
        2. Cut a piece of tail with forceps under a dissecting microscope.
        3. Put the tail into a labeled tube filled with 30 µl DNA lysis buffer.
        4. Quickly put the embryo into a tube containing 100 µl 4% paraformaldehyde.
        5. Label tubes with embryos and their corresponding tail tubes.
        6. Store the tubes with embryos at 4 °C overnight for fixation.
        7. Clean the forceps using Milli-Q water and Kimwipes between each embryo to minimize contamination.
    3. For whole embryos:
        1. Place embryos into 0.004% MS-222 (tricaine) solution. Wait 2 min.
        2. Put 1-5 embryos in a tube filled with 100 µl DNA lysis buffer. Dechorionation is not necessary.
3. DNA digestion
   Incubate tubes with tissue (fin or tail clips or embryos) at 55 °C for 4 hr up to overnight[12].
4. Inactivate the Proteinase K
   Heat tubes to 95 °C for 15 min[12]. DNA should be used for PCR immediately, or stored at -20 °C for up to 3 months.

2. PCR

1. Design Primers either manually or by primer design software (*e.g.* Lightscanner Primer Design Software- Biofire). PCR products for HRMA are usually 50-200 bp; PCR products for SNP detection should be smaller, typically 50-80 bp.
2. PCR
    1. Perform PCR reaction in a 96-well or 384-well plate.
    2. Use 10 µl total volume: 4 µl LightScanner master mix (0.1 U hot-start Taq-AB polymerase, buffer, 0.2 mM dNTPs, 2 mM magnesium chloride, and 1x fluorescent double-stranded DNA-binding dye); 5 pmol each primer, and 1 µl genomic DNA template extracted from adult tail fin or 3 µl genomic DNA from embryonic tail[13].
    3. Cover samples with 30 µl mineral oil.
    4. Cover the plate with an optically-transparent adhesive seal.
    5. Optimize PCR cycling conditions- typical conditions are 95 °C for 5 min and 30 cycles of 10 sec at 95 °C, 25 sec at 60 °C, 30 sec at 72 °C, ending with 95 °C for 30 sec and cooled to 15 °C.
    6. Store PCR plates at 4 °C or continue directly to HRMA.
    7. Confirm our PCR product by analysis of its size using agarose gel electrophoresis during initial optimization of PCR; and if indicated, by sequencing of the PCR product.

3. HRMA

1. Heat plates
    1. Place plate in a melt analysis system.
    2. Open the software (LightScanner Software Call-IT 2.0).
    3. Heat plates from 60-95 °C.
    4. Create a new data storage file.
2. Analyze HRMA data (**Figure 2**).
   Multiple steps of analysis are possible. We show the most commonly used set of data manipulations.
    1. Subset setting
       Click Subset tab. Select the wells with samples.
    2. Normalization

1. Select the **Normalize** tab in the left panel. To eliminate fluorescence variance, manually position the parallel double-line in pre- (initial) and post (final) -melt regions as illustrated (**Figure 2C**, arrowheads) and normalize premelt and post-melt fluorescence signals of all samples to 1 and 0, respectively[14].
2. Adjust the positioning of the lines so that the melt region is in the region between the pre- and post-melt lines, but not selected. In general, the Lower Min and Lower Max (and Upper Min and Upper Max) temperature lines should be placed approximately 1 °C apart.
3. Choose temperature positions for normalization such that all samples have maximum or full (100%) fluorescence for the premelt region and minimum or no (0%) fluorescence for the post-melt region (as best as possible). Normalization should result in a near-horizontal line at the maximum fluorescence of 1 that extends until the melt point and then a near-horizontal line from the melt point at the minimum fluorescence of 0; there should not be fluorescence levels above 1 or below 0. For example, in **Figure 2C**, normalize the premelting curves using temperature ranges of 79-80 °C.

3. Grouping/Clustering
   Distinguish genotypes based on their melting temperature (**Figure 2C**, green box). Select **Grouping**.
   1. Select **Autogroup** from the **Standards** selection list under the **Grouping** section.
   2. Select **Normal** or **High** for melting profiles with single transitions or multiple transitions respectively from the **Sensitivity** selection list under the Grouping section.
   3. Select **Compute Groups** under the **Grouping** section.
   4. Go to the **File** menu and click **Save** to save the results.

Representative Results

The protocol can be performed during a single day or separated in steps over several days (flow diagram of work is shown in **Figure 1**). DNA extraction is followed by the melt and analysis of PCR amplicons. The temperatures for the melt of the amplicon depend on the size and GC-content, but generally start and end temperatures of 50 ˚C and 95 ˚C are appropriate (**Figures 2A** and **2B**). Once the melt is performed, analysis of the fluorescence melt curves typically requires normalization of the variation of the different sample curves, using pre- and post-melt regions as standards (**Figure 2C**). This improves comparison of results from different samples in which the variation of fluorescence is related to minor experimental variations. Each pair of temperature lines for normalization should be placed approximately 1 ˚C apart (**Figure 2C**, arrowheads). Grouping of data results is represented in two different ways: an upper graph that shows melt curve profiles, and a lower graph that shows a subtractive difference plot in comparison to a reference sample (**Figure 2D**).

HRMA analysis can be used to detect mutations (**Figures 3A** and **3B**) or transgenes (**Figure 3C**). In **Figure 3A**, two different mutations in *eif2b5* gene are shown (red and blue curves in **Figure 3A**) by subtracting the normalized fluorescence data of the wild-type sample. It does not matter which genotype is chosen for reference. More subtle or confusing differences in melt-curves can be distinguished by using the subtractive difference plot. In **Figure 3B**, an example of four different genotypes in a single collection of embryos is shown.

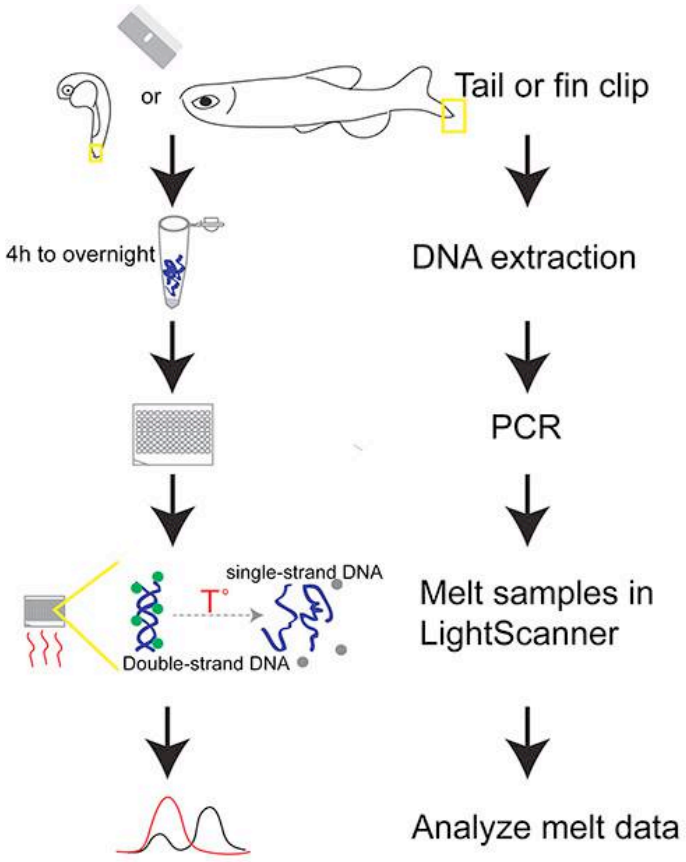

Figure 1. Outline of protocol for PCR-based HRMA of zebrafish genomic DNA. DNA extraction from whole tissue (fin-clip or embryo) is followed by PCR amplification in the presence of a fluorescent double-stranded DNA-binding dye. The PCR amplicon is denatured and fluorescence signal is recorded, followed by melt-curve analysis, to detect the amplicon and/or to differentiate genotypes.

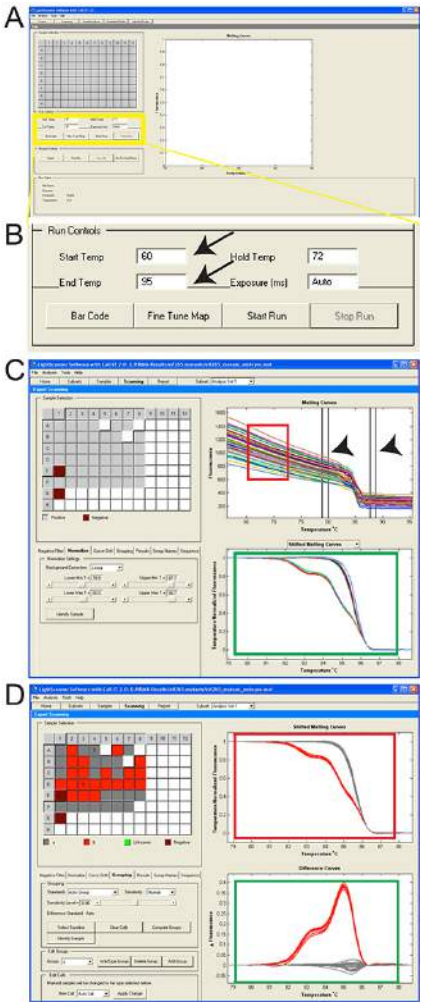

Figure 2. Screen-shots of software to perform HRMA and analyze results. A. Screen shot of LightScanner software; yellow box is magnified in "**B**". **B**. Magnified view of boxed region in "**A**". Setting Start and End Temp are shown (arrows). **C**. Position the premelt and post-melt parallel lines for normalization (arrowheads). Notice the fluorescence variance in pre- and post-melting regions (red box). Lower graph (green box) shows melt-curves derived from the raw data plots following normalization. **D**. Upper graph shows melt curve profiles after automatic grouping; different genotypes are illustrated in different colors (red box). Lower graph (green box) shows the *fluorescence difference curve*. Click here to view larger image.

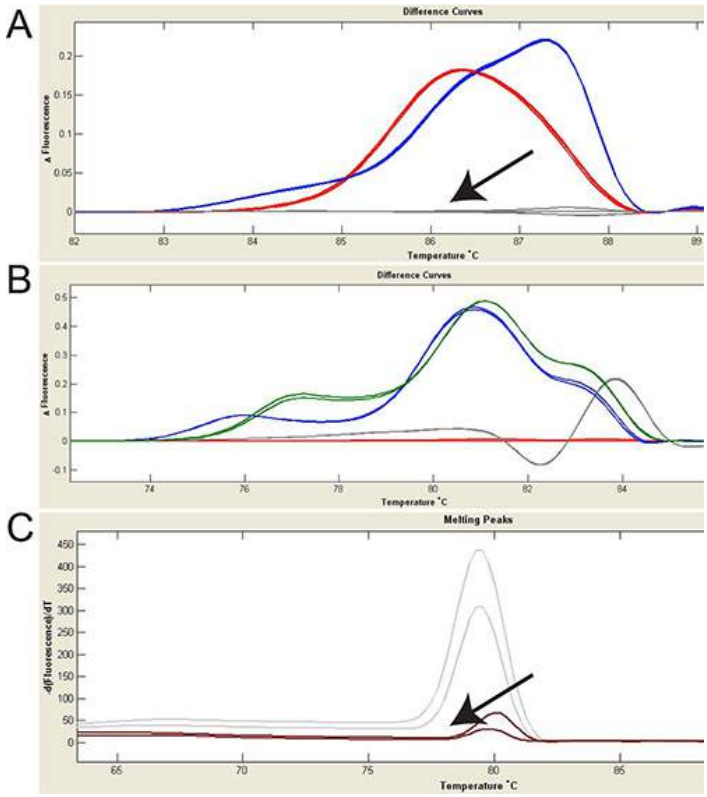

Figure 3. Using HRMA to identify mutations and transgenes. *Fluorescence difference curves* are shown; change in fluorescence (y-axis) to temperature (x-axis) is shown. **A**. HRMA was used to detect fish carrying mutations in the *eif2b5* gene. Wild type is shown in grey (arrow). Red and blue colors represent two different *eif2b5* mutations, confirmed by sequencing of the PCR product. **B**. Four different *foxP2* mutant alleles are identified with HRMA. Red: zc82/+ (8 bp deletion), green: zc83/+ (17 bp deletion), blue: zc82/zc83 (8bp deletion/17bp deletion), grey: zc83/zc83 (17bp deletion homozygotes). **C**. Gal4 transgenic fish (grey curves) can be distinguished from wild type (brown curve, arrow). Notice that for transgene detection, normalization should not be performed. Click here to view larger image.

Discussion

PCR combined with HRMA is a powerful technology for zebrafish genotyping. The advantages of this approach are its speed, robustness, and sensitivity to detect even point mutations. The entire protocol, from fin-clip to melt-curve analysis, can be performed in less than eight hours by a single individual. In addition, the technique is amenable for high-throughput screening; does not require the use of ethidium bromide; and is sealed for all PCR and analysis steps which helps minimize contamination issues.

A critical step for this technique is PCR amplicon and primer design. Typical length for PCR products in HRMA is 50-200 bp. Short amplicons increase sensitivity and are ideal for detecting single nucleotide changes. If melt-curves of closely related PCR product species can not be distinguished easily, a small oligonucleotide complementary to the SNP and blocked at the 3' end can be included in the PCR reaction (Lunaprobes; probes). The probes are generated by asymmetric PCR using different concentration of the forward and reverse primers, with a 3' C3 blocker to prevent probe extension in the subsequent HRMA PCR. The probe is then included in the HRMA PCR reaction. HRMA then occurs with the probe, in which the asymmetric probe binds to the PCR product and generates probe-target duplexes with different melt-curves that can be used to distinguish alleles.

Several companies offer melt-curve analysis systems. These include the Biofire Lightscanner, the Roche LightcyclerVR 480 and the Qiagen Rotor-Gene Q. Several fluorescent, DNA-binding dyes are available, including LC Green PLUS and SYT09 EvaGreen. There is some variation in sensitivity in mutation detection based on different fluorescent dyes and melt-curve machines[8,15]. Nonsaturating dyes, for example, SYBR Green I, are unsuitable for most HRMA applications: at high concentrations, SYBR Green I inhibits the activity of DNA polymerase; and at

lower concentrations, SYBR Green I cannot precisely measure melting behavior due to its redistribution from melted regions back to regions of dsDNA[16]. In general most existing Real Time PCR platforms are capable of preforming HRMA using a software package add-on and a second-generation fluorescent DNA binding dye. While technical details of the software and sequence of experimental steps vary slightly between platforms, the overall scientific concepts are essentially identical.

Our lab and others have demonstrated that HRMA can be used in both embryonic and adult zebrafish to detect transgenes, and mutations induced by ZFNs and TALENs[6,12,13]. HRMA has been used to discover polymorphisms in zebrafish[6,12]. Our lab uses HRMA both for initial screening of TALEN-induced mutations as well as for sorting of established lines (TSQ and JLB, unpublished). Other potential applications that could be applied to zebrafish include methylation-sensitive HRMA (ms-HRMA)[17], quantification of copy-number variants[5]; and pathogen detection in vivariums[18].

Disclosures

The authors have nothing to disclose.

Acknowledgements

We thank members of the Blaschke, Grunwald, and Wittwer labs for advice and technical assistance. This work is supported by the PCMC Foundation, NIH R01 MH092256 and DP2 MH100008, and the March of Dimes Foundation research grant #1-FY13-425, to JLB.

References

1. Kawakami, K., Takeda, H., Kawakami, N., Kobayashi, M., Matsuda, N. & Mishina, M. A transposon-mediated gene trap approach identifies developmentally regulated genes in zebrafish. *Dev. Cell.* **7**(1), 133-144 (2004).
2. Kwan, K. M., Fujimoto, E., *et al.* The Tol2kit: a multisite gateway-based construction kit for Tol2 transposon transgenesis constructs. *Dev. Dyn.* **236**(11), 3088-3099 (2007).
3. Sander, J. D., Cade, L., *et al.* Targeted gene disruption in somatic zebrafish cells using engineered TALENs. *Nat. Biotechnol.* **29**(8), 697-698 (2011).
4. Huang, P., Xiao, A., Zhou, M., Zhu, Z., Lin, S. & Zhang, B. Heritable gene targeting in zebrafish using customized TALENs. *Nat. Biotechnol.* **29**(8), 699-700 (2011).
5. Vossen, R. H. A. M., Aten, E., Roos, A. & Den Dunnen, J. T. High-resolution melting analysis (HRMA): more than just sequence variant screening. *Hum. Mutation.* **30**(6), 860-866 (2009).
6. Dahlem, T. J., Hoshijima, K., *et al.* Simple methods for generating and detecting locus-specific mutations induced with TALENs in the zebrafish genome. *PLoS Genet.* **8**(8), e1002861 (2012).
7. Liew, M., Pryor, R., *et al.* Genotyping of single-nucleotide polymorphisms by high-resolution melting of small amplicons. *Clin. Chem.* **50**(7), 1156-1164 (2004).
8. Herrmann, M. G., Durtschi, J. D., Bromley, L. K., Wittwer, C. T. & Voelkerding, K. V Amplicon DNA melting analysis for mutation scanning and genotyping: cross-platform comparison of instruments and dyes. *Clin. Chem.* **52**(3), 494-503 (2006).
9. Carrillo, J., Martínez, P., *et al.* High resolution melting analysis for the identification of novel mutations in DKC1 and TERT genes in patients with dyskeratosis congenita. *Blood Cell. Mol. Dis.* **49**(3-4), 140-146 (2012).
10. Thomsen, N., Ali, R. G., Ahmed, J. N. & Arkell, R. M. High resolution melt analysis (HRMA); a viable alternative to agarose gel electrophoresis for mouse genotyping. *PloS one.* **7**(9), e45252 (2012).
11. Vorkas, P. A., Poumpouridou, N., Agelaki, S., Kroupis, C., Georgoulias, V. & Lianidou, E. S. PIK3CA hotspot mutation scanning by a novel and highly sensitive high-resolution small amplicon melting analysis method. *J. Mol. Diagn.* **12**(5), 697-704 (2010).
12. Parant, J. M., George, S. A., Pryor, R., Wittwer, C. T. & Yost, H. J. A rapid and efficient method of genotyping zebrafish mutants. *Dev. Dyn.* **238**(12), 3168-3174 (2009).
13. Xing, L., Hoshijima, K., *et al.* Zebrafish foxP2 zinc finger nuclease mutant has normal axon pathfinding. *PloS one.* **7**(8), e43968 (2012).
14. Raghavendra, A., Siji, A., Sridhar, T. S., Phadke, K. & Vasudevan, A. Evaluation of High Resolution Melting analysis as an alternate tool to screen for risk alleles associated with small kidneys in Indian newborns. *BMC Nephrol.* **12**(1), 60 (2011).
15. Herrmann, M. G., Durtschi, J. D., Wittwer, C. T. & Voelkerding, K. V Expanded instrument comparison of amplicon DNA melting analysis for mutation scanning and genotyping. *Clin. Chem.* **53**(8), 1544-1548 (2007).
16. Wittwer, C. T. High-Resolution Genotyping by Amplicon Melting Analysis Using LCGreen. *Clin. Chem.* **49**(6), 853-860 (2003).
17. Dimitrakopoulos, L., Vorkas, P. A., Georgoulias, V. & Lianidou, E. S. A closed-tube methylation-sensitive high resolution melting assay (MS-HRMA) for the semi-quantitative determination of CST6 promoter methylation in clinical samples. *BMC Cancer.* **12**, 486 (2012).
18. Jeng, K., Gaydos, C. A., *et al.* Comparative analysis of two broad-range PCR assays for pathogen detection in positive-blood-culture bottles: PCR-high-resolution melting analysis versus PCR-mass spectrometry. *J. Clin. Microbiol.* **50**(10), 3287-3292 (2012).

CHAPTER 3

ZEBRAFISH FOXP2 ZINC FINGER NUCLEASE MUTANT HAS NORMAL AXON PATHFINDING

The following chapter is reprinted with permission from the Public Library of Science (PLOS). Xing L, Hoshijima K, Grunwald DJ, Fujimoto E, Quist TS, et al. (2012) Zebrafish foxP2 Zinc Finger Nuclease Mutant Has Normal Axon Pathfinding. *PLoS ONE* 7(8): e43968. doi:10.1371/journal.pone.0043968.

OPEN ACCESS Freely available online

PLOS ONE

Zebrafish *foxP2* Zinc Finger Nuclease Mutant Has Normal Axon Pathfinding

Lingyan Xing[1,2,3], Kazuyuki Hoshijima[5], David J. Grunwald[5], Esther Fujimoto[1], Tyler S. Quist[1], Jacob Sneddon[1], Chi-Bin Chien[2,3], Tamara J. Stevenson[1], Joshua L. Bonkowsky[1,2,3,4]*

1 Division of Pediatric Neurology, Department of Pediatrics, University of Utah School of Medicine, Salt Lake City, Utah, United States of America, **2** Department of Neurobiology and Anatomy, University of Utah School of Medicine, Salt Lake City, Utah, United States of America, **3** Interdepartmental Program in Neurosciences, University of Utah School of Medicine, Salt Lake City, Utah, United States of America, **4** Department of Neurology, University of Utah School of Medicine, Salt Lake City, Utah, United States of America, **5** Department of Human Genetics, University of Utah School of Medicine, Salt Lake City, Utah, United States of America

Abstract

foxP2, a forkhead-domain transcription factor, is critical for speech and language development in humans, but its role in the establishment of CNS connectivity is unclear. While *in vitro* studies have identified axon guidance molecules as targets of *foxP2* regulation, and cell culture assays suggest a role for *foxP2* in neurite outgrowth, *in vivo* studies have been lacking regarding a role for *foxP2* in axon pathfinding. We used a modified zinc finger nuclease methodology to generate mutations in the zebrafish *foxP2* gene. Using PCR-based high resolution melt curve analysis (HRMA) of G0 founder animals, we screened and identified three mutants carrying nonsense mutations in the 2nd coding exon: a 17 base-pair (bp) deletion, an 8bp deletion, and a 4bp insertion. Sequence analysis of cDNA confirmed that these were frameshift mutations with predicted early protein truncations. Homozygous mutant fish were viable and fertile, with unchanged body morphology, and no apparent differences in CNS apoptosis, proliferation, or patterning at embryonic stages. There was a reduction in expression of the known *foxP2* target gene *cntnap2* that was rescued by injection of wild-type *foxP2* transcript. When we examined axon pathfinding using a pan-axonal marker or transgenic lines, including a *foxP2*-neuron-specific enhancer, we did not observe any axon guidance errors. Our findings suggest that *foxP2* is not necessary for axon pathfinding during development.

Citation: Xing L, Hoshijima K, Grunwald DJ, Fujimoto E, Quist TS, et al. (2012) Zebrafish *foxP2* Zinc Finger Nuclease Mutant Has Normal Axon Pathfinding. PLoS ONE 7(8): e43968. doi:10.1371/journal.pone.0043968

Editor: Henry H. Roehl, University of Sheffield, United Kingdom

Received November 4, 2011; **Accepted** July 30, 2012; **Published** August 24, 2012

Funding: This work was supported by a Primary Children's Medical Center (PCMC) Foundation grant to JLB, National Institutes of Health (NIH) K12 5HD001410 and K08 DA024753 to JLB, and NIH P01 HD048886 to KH, DJG, and CBC. The funders had no role in study design, data collection and analysis, decision to publish, or preparation of the manuscript.

Competing Interests: The authors have declared that no competing interests exist.

* E-mail: joshua.bonkowsky@hsc.utah.edu

Introduction

Language impairment is central to autism and the autistic spectrum disorders, and is a major component in many neurodevelopmental disorders including Angelman syndrome and Fragile X syndrome [1]. Unraveling the genetic pathways and neural circuitry involved in language development is important for understanding these different disorders. However, only one gene, *FOXP2*, has been linked specifically with the normal development of language [2]. This gene, a forkhead-box transcription factor, was originally identified in a family with a severe speech and language disorder, and has subsequently been identified in other patients as well [2–8]. Haploinsufficiency for *FOXP2* in humans leads to defects in grammatical language construction, as well as in the sequencing of orofacial movements required for speech articulation [9]. Studies on the human *FOXP2* mutant pedigrees, using functional and volumetric magnetic resonance imaging (MRI), show abnormalities of the basal ganglia, cerebellum, and prefrontal cortex [10–12].

However, it is not clear what the primary role of *FOXP2* in the central nervous system (CNS) is, nor how that leads to impaired language development. Further, both pre- and post-natal functions for *FOXP2* have been proposed. In mice, *Foxp2* heterozygotes have impaired motor learning [13], while homozygotes have a smaller cerebellum [13] and a disorganized Purkinje cell layer in the cerebellum [14], suggesting a developmental role for *Foxp2*. In contrast, knockdown of *FoxP2* with lentivirus-mediated RNA interference (RNAi) in Area X of songbirds leads to inaccurate vocalizations [15], consistent with a post-natal role.

Additional support for a developmental function of *FOXP2* has come from studies implicating a role for *FOXP2* in axon pathfinding. First, *in vitro* chromatin immunoprecipitation (ChIP) showed that *CNTNAP2*, a member of the neurexin superfamily, was a target of *FOXP2* [16]. *CNTNAP2* is associated with specific language impairment as well as with autism [17–19]. *CNTNAP2*, as well as other autism-associated genes, show defects in the normal development of connectivity [19–21]. Second, ChIP analysis showed that *FOXP2* regulated genes involved in axon guidance, including *EPHA2* and *SEMA3B* [22,23]. Third, cell culture studies demonstrated that normal function of *Foxp2* was necessary for neurite outgrowth [24].

We decided to address whether *FOXP2* has a role in regulating axon guidance *in vivo*. We used a zebrafish model because of its rapid CNS development and relative ease for imaging and analysis of axon pathfinding. Zebrafish foxP2 has 86% protein similarity to

human FOXP2 [25], and its CNS expression pattern is conserved in the telencephalon, basal ganglia, and cerebellum to that of humans, mice, songbirds, and frogs [25–30]. Previously we had tried to knock down *foxP2* expression using morpholinos in zebrafish embryos. However, five different morpholinos had embryonic toxicity, leading to early lethality (JLB, unpublished data) that was not rescued using a morpholino against *p53* [31].

In this paper we generated and screened zinc finger nucleases (ZFNs) against zebrafish *foxP2* using a modified bacterial 1-hybrid screen. Mosaic G0 injected fish were identified using high resolution melt analysis (HRMA) PCR of somatic DNA (fin-clip), and we describe our use of HRMA PCR for screening and identification of mutants. We generated three frameshift *foxP2* mutant alleles: an 8 bp deletion, a 17 bp deletion, and a 4 bp insertion. The three mutant alleles were homozygous mutant and fertile, and characterization of CNS development revealed no changes in apoptosis, proliferation, patterning, or specification. To analyze pathfinding we used both pan-axonal immunohistochemistry, as well as neuron-type specific transgenic reporter lines. We found that disruption of *foxP2* in zebrafish did not affect axon pathfinding during development. Our results demonstrate the importance of *in vivo* validation of ChIP and *in vitro* studies, and are concordant with other studies suggesting a role for *foxP2* in synapse development [13,32].

Results

Zinc Finger Nuclease (ZFN) Generation, Injection, and Screening

We designed ZFNs against a region in exon 2 of the zebrafish *foxP2* cDNA using the target prediction program ZiFiT (http://bindr.gdcb.iastate.edu/ZiFiT) (Figure 1A). The site in exon 2 was the only ZFN target 5′ of the functional domains including the forkhead domain and zinc finger domain, as the other acceptable ZFN sites were 3′ to these domains. OPEN pool PCR amplification, generation of the three-finger zinc finger protein libraries, reporter plasmid preparation, and bacterial 1-hybrid screening was performed as described [33]. We screened bacterial 1-hybrid libraries with titers of 2.8×10^7 and 1.1×10^7 cells/plate, for the right and left fingers, respectively. We picked and sequenced the selected zinc finger proteins for 10 clones for each ZFN clone (20 clones total) and compared the amino acid sequences (Figure 1B, B'). The recovered clones from the library screening were selected from plates with middle to high stringency: the concentration of carbenicillin was 100 μg/mL and the concentration of 3-AT ranged from 20–30 mM. For our final choice of clones for the left and right ZFNs, we chose the clones that had the highest percentage of amino acids in common with the other clones at the specific positions in the zinc finger (Figure 1C). We hypothesized that this conservation was indicative of a relative selection for this amino acid at a particular position. For the "left" ZFN clone (clone #21), every amino acid was found in at least 50% of the selected clones, and in half of the positions every clone shared 100% identity. The right ZFN clone (clone #37) had less conservation, but still 1/3rd of the sites had perfect conservation.

Clones #37 and #21 were subcloned into the pCS2-FokI-DD and -RR FokI nuclease expression vectors (pCS2-Flag-TTGZFP-FokI-DD and pCS2-HA-GAAZFP-FokI-RR [34]), and injected as mRNA into zebrafish embryos (Figure 2A). Initially we injected 20, 80, and 250 pg of each ZFN into 1-cell stage embryos, and at 48 hours post-fertilization (hpf) assessed the percentage of embryos that showed a dysmorphic or "monster" appearance [34]. We found that injections at 80pg each resulted in approximately 50% dysmorphic embryos, and we used this amount for subsequent experiments. We confirmed by HRMA PCR (discussed below) performed on pools of 4–10 embryos each (Figure 2B), and by subsequent selection of individual clones for sequencing, that we were inducing mutations in the *foxP2* target locus. We raised 25 G0 injected embryos to adulthood, and screened by HRMA PCR on fin-clip DNA samples. We identified four G0 fish with abnormal melt-curves in somatic DNA; these fish were crossed to wild-type fish, and pools of 4 embryos each were screened again by HRMA PCR. Two of the identified G0 fish did not yield any mutant offspring, while two fish (of the four) produced mutant offspring, and were crossed to subsequently give rise to the three different *foxP2* alleles. For the two G0 fish which did not yield mutant offspring, the mutation may not have been present in the germline, it may have been present at very low rates, or the HRMA PCR result may have been falsely abnormal. In the F1 offspring of the two mutant G0 parents, the relative frequency of mutant offspring was 7% and 25%.

HRMA PCR was performed by designing a small amplicon centered on the *foxP2* ZFN target locus, and performing PCR and melt-curve analysis of the PCR product [35]. Following amplification in the presence of a fluorescent dye that binds double-stranded DNA, a "melt" of the PCR product either yields a single peak (Figure 2B, asterisk) corresponding to a single wild-type product, or to multiple peaks and/or a broader, shifted peak corresponding to heteroduplexes of wild-type and mutant PCR product (Figure 2B, arrows), which melt at a lower temperature [36]. By performing a dilution analysis of mutant DNA into wild-type DNA, we determined that we could reliably detect mutant samples when mutant DNA was present in a proportion of 1:20, but not to 1:50 (Figure 2C-C′, arrowheads). Thus, HRMA PCR will be able to detect founder G0 fish if mutant cells are present in more than 1/20–50th of the total cells. Similarly, screening F1 embryos should be limited to no more than 15–20 embryos concurrently (20 embryos = 40 copies of a genomic locus).

foxP2 Mutant Alleles

We identified three mutant alleles: *zc82* (8bp deletion), *zc83* (17bp deletion), and *zc84* (4bp insertion), which lead to out-of-frame proteins with early stop codons at amino acids 137, 134, or 164 (out of 697 amino acids) for each mutant (Figure 2D). The three different alleles each generate a different amino acid sequence downstream of the mutation prior to the stop, as the alleles each have a slightly different location of where the deletion or insertion has occurred. We outcrossed mutant alleles for successive generations to reduce the potential problem of off-target mutations [37]. We assessed both *in trans* heterozygous (hetero-allelic) and *in cis* homozygous mutants, but for the experiments shown here we used heteroallelic mutants in order to avoid possible off-target background effects. We performed experiments by crossing heteroallelic parents to one another, and genotyping their embryos with HRMA. The use of *foxP2* heteroallelic mutant parents prevented possible rescue or amelioration of effects due to maternal contribution of wild-type transcript from a heterozygous parent.

To demonstrate that the mutations led to disruption of the normal transcript we performed RT-PCR followed by sequencing of the products. We found a single transcript was generated in mutant embryos which included the mutated exon 2 (Figure 2E). We cloned and sequenced the PCR product from exon 1–2 amplification, and found that the mutation led to the predicted shift in codon reading frame. These results suggest that the ZFN-induced *foxP2* mutants will lead to expression of truncated, mutant protein products lacking the zinc-finger, leucine zipper, and

A *foxP2* Target Sequence

target sequence of *foxP2*: 5'-cTCCTACAGCAACCAGGCAGTGGCCt-3' [700 – 725nt on cDNA]

	zinc finger			
clone name	F3	F2	F1	*Target Sequence*
foxP2-ZFP-1L	GCT	GTA	GGAg	5'-tGCTGTAGGAg-3'
foxP2-ZFP-1R	GCA	GTG	GCCc/g	5'-gGCAGTGGCCt-3'

B Bacterial 1-Hybrid Screen Results

foxP2-ZFP-1L

		aa sequence
Finger F1		
clone	22	DNAHLA
	24	"
	26	"
	27	"
	21	DKTKLR
	25	"
	28	"
	29	"
	23	DKTKLN
	30	DRTKLR
Finger F2		
	22	QRSSLV
	26	"
	27	"
	30	"
	21	QSSSLV
	28	"
	25	"
	23	"
	29	"
	24	QSASLR
Finger F3		
	21	QRSDLH
	24	"
	25	"
	28	"
	23	"
	29	"
	30	"
	22	QRSSLV
	26	"
	27	"

foxP2-ZFP-1R

		aa sequence
Finger F1		
clone	31	DARGLL
	37	"
	36	DQSTLR
	38	"
	35	DSSTLA
	32	EKRSSL
	33	DGRGLE
	34	HRRDLD
	39	DAAGLV
	40	HRRDLI
Finger F2		
	37	RTEILR
	38	"
	34	RTEVLA
	35	RREVLS
	31	RTEVLT
	32	RSEVLA
	33	RREVLQ
	36	RGEILV
	39	RSEVLA
	40	RREVLE
Finger F3		
	33	QTATLK
	35	"
	37	"
	36	"
	39	"
	40	"
	31	QATTLR
	32	"
	34	QKVTLM
	38	QNGTLT

B'

foxP2-ZFP-1L

clone		F1	F2	F3
	22	DNAHLA	QRSSLV	QRSSLV
	23	DKTKLN	QSSSLV	QRSDLH
	24	DNAHLA	QSASLR	QRSDLH
	25	DKTKLR	QSSSLV	QRSDLH
	26	DNAHLA	QRSSLV	QRSSLV
	27	DNAHLA	QRSSLV	QRSSLV
	28	DKTKLR	QSSSLV	QRSDLH
	29	DKTKLR	QSSSLV	QRSDLH
	30	DRTKLR	QRSSLV	QRSDLH

foxP2-ZFP-1R

clone		F1	F2	F3
	31	DARGLL	RTEVLT	QATTLR
	32	DKTKLN	QSSSLV	QRSDLH
	33	DNAHLA	QSASLR	QRSDLH
	34	DKTKLR	QSSSLV	QRSDLH
	35	DNAHLA	QRSSLV	QRSSLV
	36	DNAHLA	QRSSLV	QRSSLV
	37	DKTKLR	QSSSLV	QRSDLH
	38	DKTKLR	QSSSLV	QRSDLH
	39	DRTKLR	QRSSLV	QRSDLH
	40	HRRDLI	RREVLE	QTATLK

C ZFN Clones for Injection

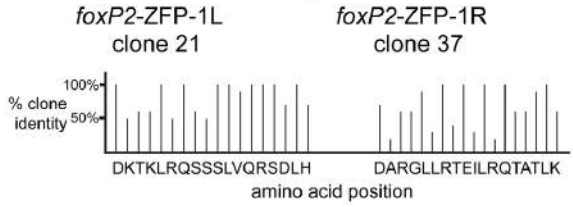

Figure 1. Targeting and selection of ZFNs. (A) *foxP2* cDNA sequence, nt 700–725, with target cleavage region in red, and ZFN binding targets underlined. Codons for design of the left and right zinc finger proteins (ZFP) are shown below with their respective target sequence. (B and B′) Amino acid sequences of the 10 clones from bacterial 1-hybrid selection, arranged by clone number, zinc finger, and left or right; or (B′) selected clones shown sequentially. (C) Graphical representation of the relative amino acid frequency compared to other selected ZFN clones, at each position, in the two ZFN clones chosen for injection.
doi:10.1371/journal.pone.0043968.g001

forkhead domains. Truncation of human *FOXP2* by a premature nonsense mutation prior to these domains has been shown to lead to loss of functional protein [38,39], suggesting that our mutations are in fact nulls.

Homozygous mutant fish were viable and fertile, including both heteroallelic (*foxP2* $^{zc82/zc83}$, *foxP2* $^{zc82/zc84}$, *foxP2* $^{zc83/zc84}$) and homozygous (*foxP2* $^{zc82/zc82}$, *foxP2* $^{zc83/zc83}$, *foxP2* $^{zc84/zc84}$) alleles. There were no obvious changes in overall body morphology of *foxP2* mutants. By *in situ* analysis, there was no change in *foxP2* expression pattern or overall intensity of expression in mutants (Figure 3 C, D), which is not unexpected since we expect normal production of mRNA transcript based on the nature of the alleles. We also measured brain size at 72hpf, and found that mutants had no difference compared to their wild-type siblings (325 vs. 323 µm, SEM 3.5 and 2.6, $p = 0.64$) (Figure 3A, B). Further, there were no changes in *foxP2* mutants in the CNS of apoptosis or of proliferation, as assayed using TUNEL (terminal deoxynucleotidyl transferase dUTP nick-end labeling) and anti-H3 phosphohistidine (H3P) antibody at 48hpf and 72hpf, respectively (Figure 4E-H).

CNS development and patterning

To broadly assess CNS patterning we performed *in situs* for *dlx2* and *zic2a* at 30hpf and 48hpf, respectively. *dlx2* and *zic2a* are widely expressed and regulate development of many cell types in the CNS [40–42]. No changes in expression patterns of *dlx2* and *zic2a* were detected in *foxP2* mutants compared to wild-type (Figure 3E-H). This suggests that *foxP2* does not have a role in overall CNS patterning.

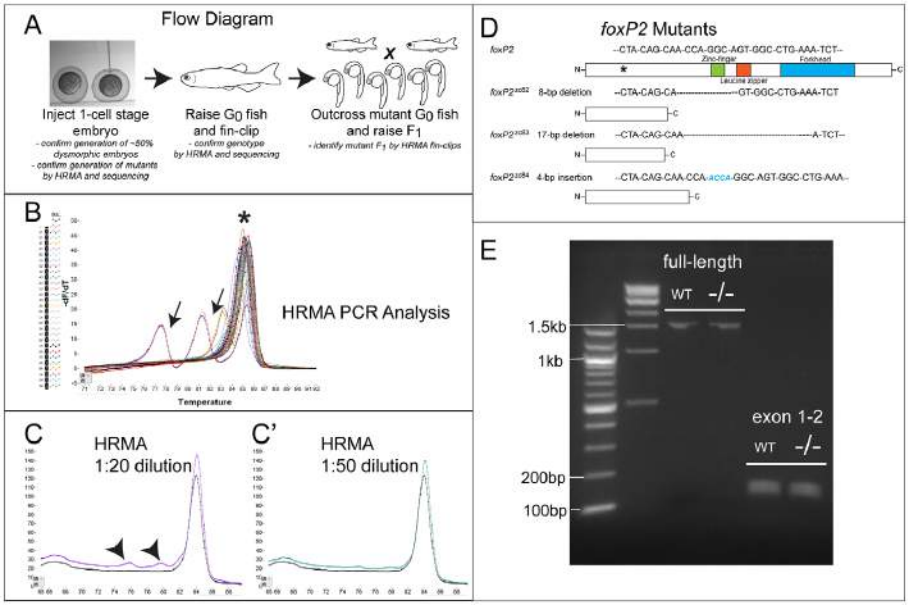

Figure 2. Flow diagram for generation of ZFN mutants, and HRMA analysis. (A) Flow diagram illustrating steps in generation and identification of fish carrying ZFN-induced mutation. (B) Illustrative melt-curve (“HRMA” high-resolution melt analysis) of F1 generation *foxP2* ZFN fish. Y-axis corresponds to the differential of the change (decrease) in fluorescence; X-axis is the temperature (°C). Each colored line is a different sample, arrows point to samples with mutations in the *foxP2* amplicon; asterisk is the wild-type product. There is some variability in the melt temperature of the wild-type amplicon because of minor variations in starting template amount and salt concentrations. (C-C′) Melt-curves of dilutions of mutant *foxP2* DNA. Abnormal melt curves (arrowheads) are detected at dilutions of 1:20 mutant:wild-type DNA, but not (or very minimally) at a dilution of 1:50. (D) Schematic diagram of foxP2 protein domains; asterisk shows the targeted region for ZFN mutagenesis; sequence above the picture is the nucleotide sequence targeted. Below are shown the three alleles, with the sequence of the mutation, and a picture of the predicted protein. (E) RT-PCR from wt or *foxP2* homozygous mutant embryos at 72hpf, with primers for the full-length transcript, or encompassing exons 1–2. No alternative splice variants were noted, and sequencing of the *foxP2* mutant PCR product showed that the mutations led to the predicted out-of-frame sequence.
doi:10.1371/journal.pone.0043968.g002

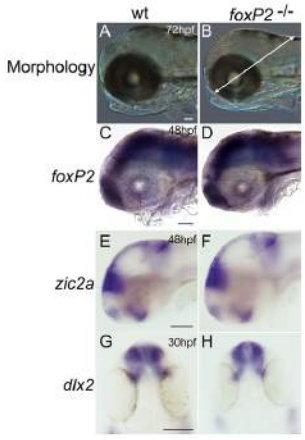

Figure 3. *foxP2* mutant has normal morphology and CNS patterning. Whole-mount embryos, brightfield images, scale bar = 50 μm. Lateral views, rostral to the left (A-F); dorsal views, rostral to the top (G, H). (A, B) Gross head morphology is unchanged in mutants at 72hpf. Arrow in (B) shows line used to measure brain size, from the midbrain-hindbrain boundary to the edge of the head by dissecting the midpoint of the lens. (C-D) mRNA expression of *foxP2* transcript is unchanged in intensity and pattern in *foxP2* mutants. (E-H) *in situ* expression patterns and intensity of *zic2a* and *dlx2* is unchanged in mutants compared to wild-type embryos.
doi:10.1371/journal.pone.0043968.g003

We examined neuron specification in detail for Purkinje cells and dopaminergic neurons, because of a proposed role for *FoxP2* in their development and function [10–14]. Using immunohistochemistry for calbindin to label Purkinje cells of the hindbrain, and for tyrosine hydroxylase to label dopaminergic neurons of the diencephalon, we found no apparent differences in cell morphology, number, or organization in *foxP2* mutants (Figure 4 A–D). Therefore, in zebrafish *foxP2* does not appear to have a role in development of cerebellar or dopaminergic neurons.

Foxp2 has also been proposed to regulate synapse formation [13,32]. We used immunohistochemistry for the pre-synaptic vesicle protein SV2 [43], and found no difference in neuropil development in *foxP2* mutants (Figure 4 I, J). However, *CNTNAP2*, a neurexin-family member identified as an *in vitro* target of *FOXP2* with a potential role in neuronal migration and development of CNS connectivity [16,19], had decreased expression at 36hpf (Figure 4K, L, arrows). This decrease was developmentally persistent and was confirmed by quantitative RT-PCR to be down-regulated to 72% of normal levels in 72hpf *foxP2* mutants (standard error of the mean 0.078; $p<0.05$) (Figure 4M). To confirm the specificity of this effect we injected *foxP2* transcript into mutant embryos at the 1-cell stage transcribed from a full-length cDNA clone [25]. At 72hpf RNA was prepared from embryos (wild-type, mutant, or mutant injected with mRNA) that were morphologically indistinguishable, and a resultant rescue of *cntnap2* levels was found (Figure 4M).

For both the *in situs* and the RT-PCR of *cntnap2* we used heteroallelic (trans-heterozygous) parents to generate the mutant off-spring (zc82/zc84×zc82/zc84). This was designed to: i. prevent any maternal mRNA contribution from obscuring results;

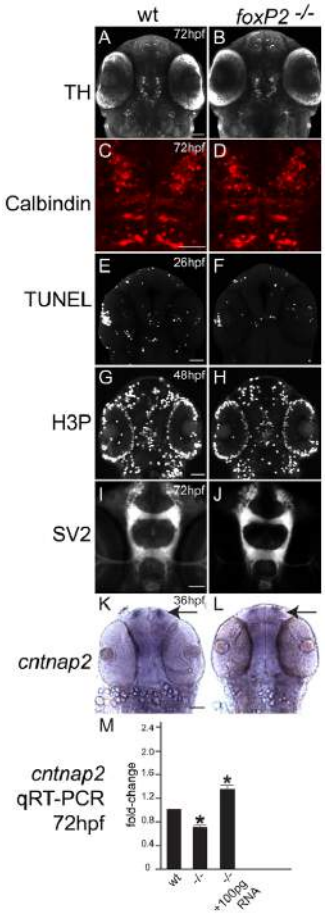

Figure 4. *foxP2* does not affect neuron specification, apoptosis, or proliferation, but does affect *cntnap2* expression levels. Confocal z-stack images, rostral to the top, scale bars 50 μm. (A, B, E-H, K-L) ventral views. (C, D) dorsal views. (*A, B*) TH immunohistochemistry at 72hpf shows no difference in WT and mutants in diencephalic dopaminergic neuron pattern or number. (C, D) Calbindin immunohistochemistry in the dorsal hindbrain at 72hpf shows similar patterns and numbers of Purkinje neurons in WT and mutants. (E, F) TUNEL staining for apoptotic cells at 26hpf in the brain shows no difference in pattern or number of cells between WT and mutants. (G, H) Detection of proliferation by H3P staining is similar in WT and mutants at 48hpf. (I, J) Neuropil distribution and intensity visualized with anti-SV2 synaptic vesicle protein antibody at 72hpf is similar in WT and mutants. (K, L) *cntnap2 in situ* expression pattern at 36hpf shows less expression in mutant embryos, more noticeably in the telencephalon (arrows). (M) quantitative RT-PCR at 72hpf confirms decreased expression of *cntnap2* in mutants, which is rescued by injection with full-length *foxP2* mRNA (* $p<0.05$). Y-axis indicates fold-change.
doi:10.1371/journal.pone.0043968.g004

and ii. to prevent any non-specific background effects of off-target mutations caused by the zinc-finger nucleases. The wild-types were generated by crosses between heteroallelic heterozygous parents (i.e. zc82/+× zc84/+), and confirmed by HRMA PCR. Thus although they were not "litter" (clutch) mates, they were of the same genetic background. Thus, our zebrafish *foxP2* mutant does recapitulate some aspects of CNS dysregulation noted in other systems.

Axon pathfinding

An outstanding question for *foxP2* is whether it regulates the development of CNS connectivity. To address this, we analyzed whether *foxP2* is required for normal axon pathfinding *in vivo*. We used both acetylated tubulin antibody and anti-SV2 to label all axon tracts, as well as enhancers that specifically express membrane-targeted GFP in subsets of neurons, including *foxP2* neurons (*foxP2-enhancerA.2:egfp-caax*) [44] and axons of diencephalic dopaminergic neurons (*otpb.A:egfp-caax*) [45,46]. We analyzed axon tracts at 24hpf and 72hpf, including the anterior and post-optic commissures, optic chiasm, tract of the commissure of the posterior tuberculum (TCPTc) [47], dopamine neuron projections, projections to the pituitary, reticulospinal axons, and spinal cord projections. We did not observe any axon pathfinding errors in *foxP2* mutants (Figure 5 A–R). Our findings show that *foxP2* does not play a role in pathfinding during development, assayed using a variety of markers for different axon tracts.

Discussion

Determining the function of *FOXP2* in the CNS has been difficult, and different groups [13,15,24,28,32] have proposed a variety of roles, including regulation of synaptic plasticity in striatal neurons, development of Purkinje cells for motor-skill learning, and the control of connectivity development [24]. However, studies have been constrained by the use of primarily *in vitro* data, or by a lack of analysis of early CNS development, including basic patterning. Further, no analysis has been done whether *FOXP2* controls the development of axon pathfinding. Since in humans language ability depends on connections between different language areas [48], we had hypothesized a role for *FOXP2* in axon guidance.

In the work we generated *foxP2* mutants in zebrafish using a modified zinc finger nuclease (ZFN) protocol [33], and recovered 3 mutants alleles from 25 injected G0 fish. The use of ZFN technology in zebrafish is important for analysis of gene function. For example, our own previous analysis of *foxP2* in zebrafish using morpholinos led to conflicting results: 5 of 6 different morpholinos had a severe, early embryonic phenotype with tissue necrosis that began shortly after gastrulation, whereas a 6th morpholino caused no observable phenotype. We demonstrated that in the *foxP2* mutant alleles we only had mutant mRNA transcript generated, with no evidence for alternate splicing. While we can not exclude the possibility that other *foxP2* splice variants might be generated that lack the ZFN-induced mutation of exon 2, at least during this critical time period of axon pathfinding we only obtain a single RT-PCR product that contains exon 2.

We tried a variety of commercially available antibodies generated against mouse and human FoxP2, as well as a polyclonal antibody directed against two different peptide epitopes from the zebrafish foxP2 protein, we were unable to find an antibody that was specific (JLB, LX, data not shown). In particular, with the polyclonal antibodies we raised against zebrafish peptide epitopes, there was no signal above background on whole-mount or cryostat section immunohistochemistry. On western blots, the zebrafish-directed antibodies gave numerous bands that did not correspond in size to the predicted zebrafish foxP2 protein. Following pre-incubation with the peptides used to raise the antibodies, there was no loss of an obvious band that might correspond to foxP2. The lack of demonstration of a protein null is a limitation. However, our indirect evidence based on RT-PCR and sequencing, as well as the down-regulation of *cntnap2* and the ability of full-length *foxP2* transcript to rescue the *cntnap2* phenotype, argue that our alleles are mutants.

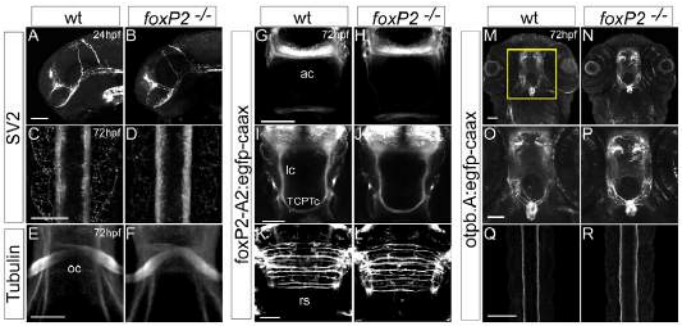

Figure 5. *foxP2* does not affect axon pathfinding. Confocal z-stack images of whole-mount embryos, scale bars 50 μm, show no difference between wild-type and *foxP2* mutant (−/−) embryos for axon pathfinding using a variety of axonal labels. (A–D) anti-SV2 immunohistochemistry at 24hpf, lateral views of the brain, rostral to the left (A, B) and 72hpf, dorsal views of the spinal cord, rostral to the top (C, D). (E, F) anti-acetylated tubulin immunohistochemistry at 72hpf, ventral views of the optic chiasm. (G-L) GFP immunohistochemistry at 72hpf in Tg(*foxP2-enhancerA.2:egfp-caax*) embryos that labels *foxP2* neurons show no pathfinding errors in anterior commissure (ac), longitudinal commissures (lc), tract of the commissure of the posterior tuberculum (TCPTc), or reticulospinal axons (rs). (M-R) GFP immunohistochemistry at 72hpf in Tg(*otpb.A:egfp-caax*) embryos for visualization of dopaminergic and neuroendocrine projections (M, N, with insets shown in O, P) in the brain, and dopaminergic axon tracts in spinal cord (Q, R).
doi:10.1371/journal.pone.0043968.g005

In addition, our ability to efficiently detect mutant fish was enhanced by our use of HRMA PCR analysis, including screening the G0 fish by analysis of somatic (fin-clip) DNA. This permitted us to analyze a subset of the G0 fish and limit the number of different animals that we needed to cross and screen. HRMA permits rapid genotyping, and we were able to use the patterns of the different melt-curves to distinguish between the different *foxP2* alleles we generated. Using fin-clip followed by HRMA PCR of G0 fish offers a potential short-cut to detect ZFN founders. However, in our experiments we did not examine the founder rate in G0 fish that were fin-clip PCR negative. Thus, we can not exclude the possibility that our method does not enrich for founders and instead reflects chance.

In contrast to work on *Foxp2* in mouse, we found that the *foxP2* mutant zebrafish were viable and fertile, with no changes in CNS patterning or specification, normal axon pathfinding, and minor changes in synapse development. We did not find any abnormalities in specification of Purkinje or dopamine neurons, or in cerebellar development [13,14,32]. We also examined in detail effects of loss of *foxP2* on apoptosis, patterning, and CNS patterning and specification, and found no effects in mutant animals. While we can not exclude that *foxP2* might exert more subtle effects on axon pathfinding that our assays did not detect, we have demonstrated that our transgenic lines can detect relatively minor axon pathfinding errors in other experimental paradigms [49].

What explains the difference in phenotypes from zebrafish to mouse? These results are unlikely to be explained by the presence of a second closely related protein in zebrafish, since genomic sequence data as well as our own RT-PCR results do not show any evidence for a second *foxP2* ortholog (JLB, unpublished). There are two *foxP1* orthologs in zebrafish (JLB, unpublished data; [50]), and as FoxP1 can act cooperatively with FoxP2 [51,52], it is possible that the *foxP1* orthologs in zebrafish could functionally compensate for loss of *foxP2*. However, it is not clear then why in mouse Foxp1 is unable to compensate for Foxp2 function. Finally, *foxP2*'s role in CNS development may have changed over evolution, with a critical role in mouse viability, for example in lung development [52].

Our two primary findings were first, that *foxP2* mutants did not have changes in axon pathfinding. This is in contrast to the results suggesting a role for *Foxp2* in neurite outgrowth, and in regulation of axon guidance genes [24]. This finding must be tempered in that we can not exclude an axon guidance role for *foxP2* that is compensated by one of the *foxP1* orthologs. Second, we found that in *foxP2* mutants there was a decrease in *cntnap2* expression levels, which is opposite to the cell culture results showing that loss of *FOXP2* led to an increase in *CNTNAP2* expression [16]. Our results suggest caution in interpretation of *in vitro* data, although it is possible that zebrafish *foxP2* has different CNS roles than mouse *Foxp2*. However, given the conservation of expression domains and protein similarity in zebrafish, argue at least in part against a widely divergent CNS function of *foxP2* in zebrafish. Future studies with *foxP2* will need to examine in greater detail its role in synaptic development, given our findings of decreased *cntnap2* expression levels, and data from mice and humans on this function [13,22,23].

Materials and Methods

Ethics Statement

All zebrafish experiments were performed with supervision and in strict accordance of guidelines from the University of Utah Institutional Animal Care and Use Committee (IACUC), regulated under federal law (the Animal Welfare Act and Public Health Services Regulation Act) by the U.S. Department of Agriculture (USDA) and the Office of Laboratory Animal Welfare at the NIH, and accredited by the Association for Assessment and Accreditation of Laboratory Care International (AAALAC). This study was approved by the University of Utah IACUC (protocol #11–06005).

Fish stocks and embryo raising

Adult fish were bred according to standard methods. Embryos were raised at 28.5°C in E3 embryo medium and staged by time and morphology [53]. For *in situ* or immunohistochemistry staining, embryos were fixed in 4% paraformaldehyde (PFA) (in PBS) overnight (O/N) at 4°C, washed briefly in PBS, dehydrated stepwise from PBS to 100% MeOH, and stored in 100% MeOH at −20°C until use.

Transgenic fish lines used in this paper were the following: Tg*(otpb.A:egfp-caax)* (official ZFIN nomenclature Tg(otpb:1EGFP)^{zc49}) [e3] and Tg*(foxP2-enhancerA.2:egfp-caax)*^{zc69} [44,49]. *foxP2* mutant alleles are *zc82* (8 bp deletion), *zc83* (17 bp deletion), and *zc84* (4 bp insertion) (Figure 2). Injection of DNA constructs and raising of stable transgenic lines was performed as described [44,54,55]. Lines are available upon request. Mutant allele sequences have been deposited in ZFIN.

In situ hybridization and Immunohistochemistry

Whole-mount *in situ* labeling and immunohistochemistry were performed as described [25,44]. Antibodies and dilutions were rabbit polyclonal anti-tyrosine hydroxylase 1:400 (Millipore); mouse anti-acetylated tubulin 1:250; goat anti-mouse Alexa 488 1:500 (Invitrogen); rabbit anti-calbindin 1:150 (Swant); rabbit anti-H3P (Millipore), 1:500; mouse anti-SV2 (Developmental Studies Hybridoma Bank) 1:300; and Cy-3 anti-rabbit 1:400. Apoptotic cells were stained with TUNEL (Millipore) as described [56].

Microscopy and image analysis

Image acquisition and analysis were performed as described previously [44]. Embryos were processed and placed in a solution of 80% glycerol/20% PBST, and mounted on a glass slide with a #0 coverslip. NIH ImageJ software was used to merge slices to create maximal intensity z-stack projections. Brain size was calculated using whole-mount images of embryos at 72hpf; distance was calculated in ImageJ from the midbrain-hindbrain boundary to the edge of the head by a line dissecting the midpoint of the lens (Figure 3B).

cDNA and quantitative RT-PCR

Total RNA from 72hpf embryos was extracted using Trizol (Invitrogen), purified (Qiagen RNeasy mini-columns), and reverse-transcribed (SuperscriptTM III First-strand Invitrogen kit). Primers for *foxP2* were used to amplify either the entire coding region (forward 5′-AGCAGTGAAGTAAGCGCAGTCGA-3′; reverse: 5′-AGCGGCAAAGTGGTCTCCGC-3′), or the region encompassing exons 1 and 2 (forward primer: 5′-AGCAGTGAAGTAAGCGCAGTCGA-3′; reverse primer: 5′-CGCTGTTTGTCGTTGTTCTTTGG-3′). PCR product of exon 1–2 amplification from *foxP2* homozygous mutants were cloned and sequenced.

RT-qPCR reaction for *cntnap2* was performed on 72hpf embryos on two separate occasions. The reaction mix included SYBR Green, primers, and cDNA templates; conditions were 95°C for 10 min, followed by 38 cycles of 95°C for 30 s, 60°C for 30 s and 72°C for 30 s. Each reaction was performed in triplicate

and the mean of replicates was calculated; results were normalized to the mRNA level of *cntnap2* in wild-type embryos with β-actin transcript levels as a control using the Pfaffl method [57]. Primers were forward 5′- CCAGCTGTTTGTAGGTGCTTCGGG-3′ and reverse 5′- CGCACCAGCGTCCCACTCTC-3′.

DNA preparation, Genomic DNA PCR, HRMA, and Dilution Analysis

Genomic DNA was prepared as described [35]. PCR reactions were performed in 96-well, hard-shell plates (Bio-Rad, Inc.) in 10 µl volume: 4µl master mix including Taq polymerase, dNTPs, magnesium chloride, and fluorescent double-stranded DNA binding dye (LCGreen PLUS) (Lightscanner Master Mix- Idaho Technology, Inc.), 5 pmol each primer (forward primer: 5′-CCTACAAGCAGCAAGGCA-3′; reverse primer: 5′-TGTCGTTGTTCTTTGGAGATT-3′), and genomic DNA template extracted from DNA lysis buffer [35]. PCR reactions were covered with 30 µl mineral oil. PCR cycling conditions were: 2 min at 95°C, followed by 28 cycles of 10s at 95°C, 25 s at 61°C, ending with 95°C for 30 s and cooled to 15°C. HRMA was performed on a LightScanner-96 instrument (Idaho Technology, Inc.), from 60°C to 97°C with a temperature transition rate of 0.1°C/s. The melt curves were normalized using temperature ranges of 74–75°C and 87–88°C. Genotypes can be distinguished on the basis of their respective melt temperatures [58]; following initial confirmation by DNA sequencing.

Dilution analyses were performed in triplicate. Genomic DNA was prepared in the standard fashion; DNA concentrations were determined, and corresponding amounts of wild-type and *foxP2* mutant DNA were then mixed. Dilutions of 1:2, 1:5, 1:10, 1:20, 1:50, and 1:100, mutant:wild-type DNA sample were prepared, and HRMA PCR was then performed.

OPEN selection of zinc finger arrays and bacterial 1-hybrid selection

We designed ZFNs against a region in exon 2 of the zebrafish *foxP2* cDNA using the target prediction program ZiFiT (http://bindr.gdcb.iastate.edu/ZiFiT) (Figure 1A). OPEN pool PCR amplification, generation of the three-finger zinc finger protein libraries, reporter plasmid preparation, and bacterial 1-hybrid screening was performed as described [33]. Final ZFN clones were prepared in pCS2-FokI-DD and pCS2-FokI-RR nuclease expression vectors (pCS2-Flag-TTGZFP-FokI-DD and pCS2-HA-GAAZFP-FokI-RR were from Addgene, plasmids #18755 and 18754); transcribed mRNA was injected into 1-cell stage zebrafish embryos at 80pg each.

Acknowledgments

We would like to thank A. Blaschke, C. Heyrend, and J. Parant for assistance in developing the HRMA PCR assay; C. Wittwer and R. Pryor for assistance with HRMA; and R. Dorsky for helpful discussions.

Author Contributions

Conceived and designed the experiments: JLB KH DJG CBC LX. Performed the experiments: JLB KH EF LX JS TSQ TJS. Analyzed the data: JLB KH DJG CBC LX TJS. Contributed reagents/materials/analysis tools: JLB KH DJG CBC LX. Wrote the paper: JLB LX.

References

1. Williams CA, Driscoll DJ, Dagli AI (2010) Clinical and genetic aspects of Angelman syndrome. Genet Med 12:385–95.
2. Lai CS, Fisher SE, Hurst JA, Vargha-Khadem F, Monaco AP (2001) A forkhead-domain gene is mutated in a severe speech and language disorder. Nature 413:519–23.
3. Watkins KE, Dronkers NF, Vargha-Khadem F (2002) Behavioural analysis of an inherited speech and language disorder: comparison with acquired aphasia. Brain 125:452–64.
4. MacDermot KD, Bonora E, Sykes N, Coupe AM, Lai CS, et al. (2005) Identification of FOXP2 truncation as a novel cause of developmental speech and language deficits. Am J Hum Genet 76:1074–80.
5. Feuk L, Kalervo A, Lipsanen-Nyman M, Skaug J, Nakabayashi K, et al. (2006) Absence of a paternally inherited FOXP2 gene in developmental verbal dyspraxia. Am J Hum Genet 79:965–72.
6. Zeesman S, Nowaczyk MJ, Teshima I, Roberts W, Cardy JO, et al. (2006) Speech and language impairment and oromotor dyspraxia due to deletion of 7q31 that involves FOXP2. Am J Hum Genet 140:509–14.
7. Shriberg LD, Ballard KJ, Tomblin JB, Duffy JR, Odell KH, et al. (2006) Speech, prosody, and voice characteristics of a mother and daughter with a 7;13 translocation affecting FOXP2. J Speech Lang Hear Res 49:500–25.
8. Lennon PA, Cooper ML, Peiffer DA, Gunderson KL, Patel A, et al. (2007) Deletion of 7q31.1 supports involvement of FOXP2 in language impairment: clinical report and review. Am J Med Genet A. 143A791–8.
9. Vargha-Khadem F, Gadian DG, Copp A, Mishkin M (2005) FOXP2 and the neuroanatomy of speech and language. Nat Rev Neurosci 6:131–8.
10. Watkins KE, Vargha-Khadem F, Ashburner J, Passingham RE, Connelly A, et al. (2002) MRI analysis of an inherited speech and language disorder: structural brain abnormalities. Brain 125:465–78.
11. Liégeois F, Baldeweg T, Connelly A, Gadian DG, Mishkin M, et al. (2003) Language fMRI abnormalities associated with FOXP2 gene mutation. Nat Neurosci 6:1230–7.
12. Belton E, Salmond CH, Watkins KE, Vargha-Khadem F, Gadian DG (2003) Bilateral brain abnormalities associated with dominantly inherited verbal and orofacial dyspraxia. Hum Brain Mapp 18:194–200.
13. Groszer M, Keays DA, Deacon RM, de Bono JP, Prasad-Mulcare S, et al. (2008) Impaired synaptic plasticity and motor learning in mice with a point mutation implicated in human speech deficits. Curr Biol 18:354–62.
14. Shu W, Cho JY, Jiang Y, Zhang M, Weisz D, et al. (2005) Altered ultrasonic vocalization in mice with a disruption in the Foxp2 gene. Proc Natl Acad Sci U S A 102:9643–8.
15. Haesler S, Rochefort C, Georgi B, Licznerski P, Osten P, et al. (2007) Incomplete and inaccurate vocal imitation after knockdown of FoxP2 in songbird basal ganglia nucleus Area X. PLoS Biol 5:e321.
16. Vernes SC, Newbury DF, Abrahams BS, Winchester L, Nicod J, et al. (2008) A functional genetic link between distinct developmental language disorders. N Engl J Med 359: 2337–45.
17. Arking DE, Cutler DJ, Brune CW, Teslovich TM, West K, et al. (2008) A common genetic variant in the neurexin superfamily member CNTNAP2 increases familial risk of autism. Am J Hum Genet 82:160–4.
18. Alarcón M, Abrahams BS, Stone JL, Duvall JA, Perederiy JV, et al. (2008) Linkage, association, and gene-expression analyses identify CNTNAP2 as an autism-susceptibility gene. Am J Hum Genet 82:150–9.
19. Peñagarikano O, Abrahams BS, Herman EI, Winden KD, Gdalyahu A, et al. (2011) Absence of CNTNAP2 Leads to Epilepsy, Neuronal Migration Abnormalities, and Core Autism-Related Deficits. Cell 147:235–46.
20. Bill BR, Geschwind DH (2009) Genetic advances in autism: heterogeneity and convergence on shared pathways. Curr Opin Genet Dev 19:271–8.
21. Scott-Van Zeeland AA, Abrahams BS, Alvarez-Retuerto AI, Sonnenblick LI, Rudie JD, et al. (2010) Altered functional connectivity in frontal lobe circuits is associated with variation in the autism risk gene CNTNAP2. Sci Transl Med 2:56ra80.
22. Spiteri E, Konopka G, Coppola G, Bomar J, Oldham M, et al. (2007) Identification of the transcriptional targets of FOXP2, a gene linked to speech and language, in developing human brain. Am J Hum Genet 81:1144–57.
23. Vernes SC, Spiteri E, Nicod J, Groszer M, Taylor JM, et al. (2007) High-throughput analysis of promoter occupancy reveals direct neural targets of FOXP2, a gene mutated in speech and language disorders. Am J Hum Genet 81:1232–50.
24. Vernes SC, Oliver PL, Spiteri E, Lockstone HE, Puliyadi R, et al. (2011) Foxp2 regulates gene networks implicated in neurite outgrowth in the developing brain. PLoS Genet 7:e1002145.
25. Bonkowsky JL, Chien CB (2005) Molecular cloning and developmental expression of foxP2 in zebrafish. Dev Dyn 234:740–6.
26. Lai CS, Gerrelli D, Monaco AP, Fisher SE, Copp AJ (2003) FOXP2 expression during brain development coincides with adult sites of pathology in a severe speech and language disorder. Brain 126:2455–62.
27. Takahashi K, Liu FC, Hirokawa K, Takahashi H (2003) Expression of Foxp2, a gene involved in speech and language, in the developing and adult striatum. J Neurosci Res 73:61–72.
28. Haesler S, Wada K, Nshdejan A, Morrisey EE, Lints T, et al. (2004) FoxP2 expression in avian vocal learners and non-learners. J Neurosci 24:3164–75.

29. Ferland RJ, Cherry TJ, Preware PO, Morrisey EE, Walsh CA (2003) Characterization of Foxp2 and Foxp1 mRNA and protein in the developing and mature brain. J Comp Neurol 460:266–79.
30. Schön C, Wochnik A, Rössner A, Donow C, Knöchel W (2006) The FoxP subclass in Xenopus laevis development. Dev Genes Evol 216:641–6.
31. Robu ME, Larson JD, Nasevicius A, Beiraghi S, Brenner C, et al. (2007) PLoS Genet 3:e78.
32. Enard W, Gehre S, Hammerschmidt K, Hölter SM, Blass T, et al. (2009) A humanized version of Foxp2 affects cortico-basal ganglia circuits in mice. Cell 137:961–71.
33. Hoshijima K, Dahlem T, Grunwald DJ Index of experimental protocols for "Utah-Big Love" approach to construction of zinc finger nucleases. Zebrafish Model Organism Database (ZFIN), University of Oregon, Eugene, OR 97403–5274; URL: http://zfin.org/. Accessed 2011 Oct 10.
34. Meng X, Noyes MB, Zhu LJ, Lawson ND, Wolfe SA (2008) Targeted gene inactivation in zebrafish using engineered zinc-finger nucleases. Nat Biotechnol 26:695–701.
35. Parant JM, George SA, Pryor R, Wittwer CT, Yost HJ (2009) A rapid and efficient method of genotyping zebrafish mutants. Dev Dyn 238:3168–74.
36. Wittwer CT (2009) High-resolution DNA melting analysis: advancements and limitations. Hum Mutat 30:857–859.
37. Gupta A, Meng X, Zhu LJ, Lawson ND, Wolfe SA (2011) Zinc finger protein-dependent and -independent contributions to the in vivo off-target activity of zinc finger nucleases. Nucleic Acids Res 39:381–92.
38. MacDermot KD, Bonora E, Sykes N, Coupe AM, Lai CS, et al. (2005) Identification of FOXP2 truncation as a novel cause of developmental speech and language deficits. Am J Hum Genet 76:1074–80.
39. Vernes SC, Nicod J, Elahi FM, Coventry JA, Kenny N, et al. (2006) Functional genetic analysis of mutations implicated in a human speech and language disorder. Hum Mol Genet 15:3154–67.
40. Suh Y, Obernier K, Hölzl-Wenig G, Mandl C, Herrmann A, et al. (2009) Interaction between DLX2 and EGFR regulates proliferation and neurogenesis of SVZ precursors. Mol Cell Neurosci 42:308–14.
41. Akimenko MA, Ekker M, Wegner J, Lin W, Westerfield M (1994) Combinatorial expression of three zebrafish genes related to distal-less: part of a homeobox gene code for the head. J Neurosci 14:3475–86.
42. Sanek NA, Taylor AA, Nyholm MK, Grinblat Y (2009) Zebrafish zic2a patterns the forebrain through modulation of Hedgehog-activated gene expression. Development 136:3791–800.
43. Meyer MP, Smith SJ (2006) Evidence from in vivo imaging that synaptogenesis guides the growth and branching of axonal arbors by two distinct mechanisms. J Neurosci 26:3604–14.
44. Bonkowsky JL, Wang X, Fujimoto E, Lee JE, Chien CB, et al. (2008) Domain-specific regulation of foxP2 CNS expression by lef1. BMC Dev Biol 8:103.
45. Fujimoto E, Stevenson TJ, Chien CB, Bonkowsky JL (2011) Identification of a dopaminergic enhancer indicates complexity in vertebrate dopamine neuron phenotype specification. Dev Biol 352:393–404.
46. Gutnick A, Blechman J, Kaslin J, Herwig L, Belting HG, et al. (2011) The hypothalamic neuropeptide oxytocin is required for formation of the neurovascular interface of the pituitary. Dev Cell 21:642–54.
47. Wilson SW, Ross LS, Parrett T, Easter Jr SS (1990) The development of a simple scaffold of axon tracts in the brain of the embryonic zebrafish, Brachydanio rerio. *Development* 108:121–48.
48. Price CJ (2010) The anatomy of language: a review of 100 fMRI studies published in 2009. Ann N Y Acad Sci 1191:62–88.
49. Stevenson TJ, Trinh T, Kogelschatz C, Fujimoto E, Lush ME, et al. (2012) Hypoxia disruption of vertebrate CNS pathfinding through ephrinB2 Is rescued by magnesium. PLoS Genet 8:e1002638.
50. Cheng L, Chong M, Fan W, Guo X, Zhang W, et al. (2007) Molecular cloning, characterization, and developmental expression of foxp1 in zebrafish. Dev Genes Evol 217:699–707.
51. Li S, Weidenfeld J, Morrisey EE (2004) Transcriptional and DNA binding activity of the Foxp1/2/4 family is modulated by heterotypic and homotypic protein interactions. Mol Cell Biol 24:809–22.
52. Shu W, Lu MM, Zhang Y, Tucker PW, Zhou D, et al. (2007) Foxp2 and Foxp1 cooperatively regulate lung and esophagus development. Development 134:1991–2000.
53. Kimmel CB, Ballard WW, Kimmel SR, Ullmann B, Schilling TF (1995) Stages of embryonic development of the zebrafish. Dev Dyn 203:253–310.
54. Kwan KM, Fujimoto E, Grabher C, Mangum BD, Hardy ME, et al. (2007) The Tol2kit: A multisite gateway-based construction kit for Tol2 transposon transgenesis constructs. Dev Dyn 236:3088–3099.
55. Fisher S, Grice EA, Vinton RM, Bessling SL, Urasaki A, et al. (2006) Evaluating the biological relevance of putative enhancers using Tol2 transposon-mediated transgenesis in zebrafish. Nat Protoc 1:1297–305.
56. Sidi S, Sanda T, Kennedy RD, Hagen AT, Jette CA, et al. (2008) Chk1 suppresses a caspase-2 apoptotic response to DNA damage that bypasses p53, Bcl-2, and caspase-3. Cell 133:864–77.
57. Pfaffl MW (2001) A new mathematical model for relative quantification in real-time RT-PCR. Nucleic Acids Res 29:e45.
58. Liew M, Pryor R, Palais R, Meadows C, Erali M, et al. (2004) Genotyping of single-nucleotide polymorphisms by high-resolution melting of small amplicons. Clin Chem 50:1156–64.

CHAPTER 4

A SEROTONIN CIRCUIT ACTS AS AN ENVIRONMENTAL SENSOR TO MEDIATE MIDLINE AXON CROSSING THROUGH EPHRINB2

This is a paper submitted to the Journal of Neuroscience for publication. The authors are Lingyan Xing, Jong-Hyun Son, Tiffanie M. Dahl, Tamara J. Stevenson, Christina Lillesaar, Laure Bally-Cuif, and Joshua L. Bonkowsky

Abstract

Modulation of connectivity formation in the developing brain in response to external stimuli is poorly understood. Here, we show that the raphe nucleus and its serotonergic projections regulate pathfinding of commissural axons. We found that the raphe neurons extend projections towards midline crossing axons, and that when serotonergic signaling is blocked by pharmacological inhibition or by raphe neuron ablation, commissural pathfinding is disrupted. We demonstrate that the serotonin receptor *htr2a* is expressed on these commissural axons, and that genetic knock-down of *htr2a* disrupts crossing. We further show that knock-down of *htr2a*, or ablation of the raphe neurons, increases ephrinB2a protein levels in commissural axons. An *ephrinB2a* mutant can rescue midline crossing when serotonergic signaling is blocked. Furthermore, we found that regulation of serotonin expression in the raphe neurons is modulated in response to the developmental environment. Hypoxia causes the raphe to decrease serotonin levels, leading to a reduction in midline crossing. Increasing serotonin in the setting of hypoxia restored midline crossing. Our findings demonstrate an instructive role for serotonin in axon guidance acting through *ephrinB2a*, and reveal a novel mechanism for developmental interpretation of the environmental milieu in the generation of mature neural circuitry.

Introduction

Current models propose that neural circuitry development in the vertebrate brain is governed by an early life genetic program that constrains the range of potential connectivity and behaviors, but then is refined by experience-driven neuronal activity to

refine this template (Katz and Shatz, 1996). Recent evidence also shows a role for neuronal activity in the development of normal connectivity (Hanson and Landmesser, 2004; Suárez et al., 2014). However, it is not known whether intrinsic mechanisms exist to modulate developing CNS connectivity in response to exogenous developmental or environmental cues.

In the adult CNS the neurotransmitter serotonin (5-HT) is known to act as a molecular mediator of plasticity (Celada et al., 2013; Jitsuki et al., 2011). Intriguingly, in early development 5-HT neurons and their axon projections are widespread in the vertebrate CNS. Projections from the 5-HT raphe nuclei (nuclei B1-9) (Dahlström and Fuxe, 1964) arborize throughout the CNS (Steinbusch, 1981), including ascending projections in the telencephalon and descending innervation of the brainstem and spinal cord. Innervation occurs early in development (Lillesaar et al., 2009; Rubenstein, 1998), prior to the development of behaviors requiring 5-HT; and prior to 5-HT's roles in the refinement of sensory maps (Lesch and Waider, 2012; Toda et al., 2013).

These findings suggest a non-classical role for 5-HT in early development. Recent work has shown that 5-HT is necessary for neuron migration, dendrite arborization, and synapse formation (Matsukawa et al., 2003; Persico et al., 2001; Riccio et al., 2009; Vitalis et al., 2007;). A potential role in pathfinding has also been observed. In mouse thalamocortical neuron explants 5-HT caused a repulsive response to netrin-1, and over-expression of the 5-HT receptor *htr1B/1D* caused dorso-ventral shifting of the axon tracts (Bonnin et al., 2007). In rat raphe neuron explants, knockdown of the 5-HT transporter caused altered fasciculation and projections of axons (Witteveen et al., 2013).

Precise mechanisms and roles for 5-HT in pathfinding are poorly understood. Is

5-HT a modulator to fine-tune axon guidance, or does it play a more instructive role in pathway choice? Since 5-HT signaling activates second messenger systems, how is specificity of action achieved? 5-HT has been shown in *Aplysia* to increase expression of neurexin and neuroligin at the synapse by increased kinesin-mediated transport (Choi et al., 2011; Puthanveettil et al., 2008), supporting the possibility of a role for 5-HT in regulating cell-surface receptors responsible for axon guidance.

Another unresolved feature is whether in vertebrates neural connectivity can be modulated during development, for example by changes in 5-HT. Altered behavior in *C. elegans* can be caused by changes in 5-HT expression from environmental manipulation, apparently by alterations in neuropeptide and receptor expression in an extant neural circuit (Pocock and Hobert, 2010). In vertebrates no similar mechanism has been noted. A role for 5-HT in interpreting exogenous stimuli and altering neural circuits during development would represent an unexpected means for altering an organism's neurobehavioral repertoire in response to parental or developmental exposures.

To investigate a role for 5-HT in neural circuit development we applied the experimental tractability of the small vertebrate zebrafish (*Danio rerio*) to visualize axon-guidance decisions. Here we report that pharmacological blockade of 5-HT signaling, genetic ablation of the raphe neurons, or knock-down of 5-HT receptors lead to failure of midline axon crossing of telencephalic neurons. We further demonstrate that 5-HT's axon guidance role is mediated by downregulation of *ephrinB2a (efnB2a)* levels, as loss of 5-HT signaling led to increased *efnB2a* levels, which caused failure of commissural axons to cross the midline. 5-HT expression is decreased by hypoxia; restoration of serotonergic signaling rescued hypoxic-mediated disruption of midline axon crossing. Our results

show that raphe 5-HT neurons act as a sensor to alterations in the developmental milieu, and their projections regulate pathfinding of a separate circuit. Thus, our study demonstrates an instructive role for 5-HT in axon pathfinding, and identifies a novel mechanism of connectivity development in the CNS.

Materials and methods

Ethics statement

All zebrafish experiments were performed in accordance of guidelines from the University of Utah Institutional Animal Care and Use Committee (IACUC), regulated under federal law (the Animal Welfare Act and Public Health Services Regulation Act) by the U.S. Department of Agriculture (USDA) and the Office of Laboratory Animal Welfare at the NIH, and accredited by the Association for Assessment and Accreditation of Laboratory Care International (AAALAC).

Fish stocks and animal husbandry

Adult fish were bred according to standard methods. Embryos were raised at 28.5°C in E3 embryo medium with methylene blue, and embryos beyond 24 hpf were treated with phenylthiourea (PTU) to prevent pigment formation. For *in situ* staining and immunohistochemistry, embryos were fixed in 4% paraformaldehyde (PFA) in PBS overnight (O/N) at 4°C, washed briefly in PBS with 0.1% Tween-20, dehydrated stepwise in MeOH (25%, 50%, 75%, 100%), and stored in 100% MeOH at -20°C until use. Transgenic fish lines and alleles used in this paper were the following: Tg(*foxP2-enhancerA.2:egfp-caax*)^{zc69} (Stevenson et al., 2012); Tg(*foxP2-enhancerA.2:Gal4-*

VP16$_{413\text{-}470}$)^{zc72} (Stevenson et al., 2012); Tg(*myl7:EGFP*;*UAS:TagRFP-caax*)^{zc61}; *efnb2a*$^{hu3393/+}$ (Kettleborough et al., 2013; ENSDARG00000020164#hu3393); Tg(*UAS:Eco.NfsB-mCherry*)^{rw0144} (referred to as Tg(*UAS:NTR-mCherry*)) (Davison et al., 2007); Tg(*tph2:GAL4FF*)^{y228Tg} (Yokogawa et al., 2012); Tg(*fev:GAL4-GFP*)^{gy1} (generated from the *-3.2pet1* enhancer, Lillesaar et al., 2009). Lines are available upon request from the Zebrafish International Resource Center (ZIRC; Eugene, OR) or upon contact.

Hypoxia reagents

For induction and monitoring of hypoxia, embryonic zebrafish were placed in a sealed plexiglass chamber connected via a controller that monitored and adjusted nitrogen gas flow to a desired pO_2 set point (Biospherix Ltd.), using previously established protocols (Stevenson et al., 2012). Embryos were incubated in 1% O_2 from 24-36 hpf. Morphological staging was used to determine age at fixation for analysis.

Scoring TCPT axon errors; C/L1 and C/L2 intensity ratios

Evaluation of TCPT midline axon crossing defects was determined as previously described (Stevenson et al., 2012) with the following modifications: we measured the total fluorescence intensity (average intensity *x* area) of a rectangular area placed over the commissure or longitudinal tract. The rectangle (set size, 10 x 30 pixels in ImageJ) was placed over the midline of the commissural TCPT pathway or over the longitudinal axons immediately rostral to (L1) or caudal to (L2) their decussation into the TCPT. A confocal z-stack of 10 slices (step size 2 μm) was taken of the region using identical confocal

settings (20x objective, PMT range 400-600, imaging speed 12.5 ms/pixel), then we calculated the fluorescence of the average intensity projection. A ratio of the commissural vs. longitudinal axon intensity was calculated (C/L1, C/L2 ratio) (Figure 4.2D). Some experimental variation was noted, and so results were only directly compared for experiments performed on the same day.

Immunohistochemistry and *in situ* hybridization

Immunohistochemistry was performed as previously described (Bonkowsky et al., 2008; Stevenson et al., 2012; Xing et al., 2012). Antibodies used were: mouse anti-tubulin 1:250 (Developmental Studies Hybridoma Bank, 6G7), mouse monoclonal a-GFP 1:250 (Millipore, MAB3580), goat polyclonal a-ephrinB2a 1:20 (R&D Biosystems, AF1088), rabbit a-serotonin 1:500 (ImmunoStar, 20080), mouse a-HuC/D 1:250 (Molecular Probes, A21271), rabbit a-TagRFP 1:250 (Evrogen, AB234), Cy-3 a-rabbit 1:400 (Millipore, AP132C), Alexa 488 donkey a-mouse 1:400 (Invitrogen, A21202), Alexa 555 rabbit a-goat 1:100 (Invitrogen, A21429).

Tubulin immunohistochemistry was performed by fixation in 2% trichloroacetic acid overnight at 4°C. Embryos were washed with PBST four times for 5 minutes each, blocked for 1 hour (Roche western blocking reagent, 11921673001), and incubated with mouse ~~a~~-tubulin overnight at 4°C. After PBST washes, embryos were incubated with Alexa 488 donkey a-mouse overnight at 4°C.

Quantification of 5-HT in hypoxia/normoxia

Images were obtained with identical confocal settings for all embryos. Intensities were calculated in a rectangle of set size (70 x 100 pixels in ImageJ) placed over the raphe nuclei (rostral edge of the rectangle was placed at the rostral-most 5-HT raphe neurons) using average intensity projections of 5 z-slices (step size 2 μm). HuC/D intensity was also measured with the same z projections. 5-HT intensity level was normalized to HuC/D.

Quantification of ephrinB2a levels

a-ephrinB2a staining intensity was determined in control and ketanserin-treated embryos at 36 hpf; or control and Mtz-treated embryos at 64hpf; confocal images were obtained with identical confocal settings. Intensities were calculated in rectangles of fixed size, in control/ketanserin over the telencephalon (78 x 72 pixels), diencephalon (24 x 50 pixels), or lens (74 x 107 pixels), using average intensity projections of 11 z-slices starting at the equator of the lens and then extending 5 steps in dorsally and ventrally (11 z-slices total; step size 2 μm); and in control/Mtz, rectangles were over the telencephalon (85 x 110 pixels), diencephalon (34 x 64 pixels), and lens (105 x 165 pixels) using average intensity projections of 5 z-slices (5 slices from ventral-most edge of the lens; step size 2 μm).

In situ hybridization

Antisense digoxigenin-labeled RNA probes were prepared for *tph2* (ENSDARG00000057239), *htr2ab* (ENSDARG00000058165), *htr2aa*

(ENSDARG00000057029), and *htr2c* (ENSDARG00000018228) using standard methods (Bonkowsky and Chien, 2005). Probe for *tph2* was made from *pCR2.1TOPO z tphR* (*tph2*) D75 (from L. Bally-Cuif). To generate the *htr2ab, htr2aa,* and *htr2c* probes, cDNA from 3 dpf larvae was amplified with primers as follows: *htr2ab*, forward: 5'-GCAATGGGAGCGAAGAGAGA-3'; reverse: 5'-GGCCAGGTGTAACCGTAGAG-3'. *htr2aa*, forward: 5'-TCACACCTCCTTTTGGACGG-3'; reverse: 5'-TTAGCATTGCACGCATTCGG-3'; *htr2c*, forward: 5'-TAGACCTCGTTGGCTGGATG-3'; reverse: 5'-CACTAGAATCAGCAGGGCCG-3'. After gel purification, the fragment was cloned into a pCR4-TOPO TA vector (Invitrogen) and sequenced to confirm its identity. To make an antisense probe, the construct was linearized with SpeI and transcription performed using T7 polymerase.

In situ hybridization combined with immunohistochemistry on sections

In situ hybridization was performed as described above. After the *in situ* was completed, embryos were sequentially transferred to 5%, 15% and then 30% sucrose (in PBS). Embryos were then embedded in optimal cutting temperature compound (OCT, Tissue-TeK, 4583) using a dry ice ethanol bath, and stored at -80°C at least overnight. 20 µm sections were cut for immunostaining. Sections were boiled for 20 minutes with citrate buffer (10 mM sodium citrate, 0.05% Tween-20, pH 6.0) for antigen retrieval, then blocked for 30 minutes (1% BSA, 0.1% fish skin gelatin (Sigma G7765), 0.1% Tween-20 in PBS). The sections were incubated with primary antibody mouse a-GFP 1:100 at room temperature for one hour. After washing of the primary antibody with PBS 3 x 5 minutes, the secondary donkey a-mouse Alexa 488 (1:100) was incubated at room temperature for

one hour.

Sparse and ipsilateral neuron labeling

One-cell stage embryos were co-injected with plasmids for *UAS-lyn-TagRFP* (Yokogawa et al., 2012) and *foxP2-enhancerA.2:Gal4* (Stevenson et al., 2012). 25 pg of each plasmid was injected per embryo.

Microscopy, image analysis, and movie analysis

Image acquisition and analysis were performed as described previously (Bonkowsky et al., 2008). For 3-D images, confocal images were processed with FluoRender (Wan et al., 2012). Rendered images were exported as TIFFs and converted into avi files using ImageJ.

Morpholino injections and *htr2ab* mRNA expression analysis

One-cell stage embryos were injected with either 6 ng *htr2aa*, 6 ng *htr2ab*, or 2 ng *htr2c* splice-blocking morpholino (Gene Tools, Inc.). RT-PCR to test splice-blocking of morpholinos was performed as previously described (Xing et al., 2012). Sequences for the morpholinos were *htr2ab* mo:5'-ATGTAAAGAAACTCACCGTAGAGGA-3' (targeting gene ENSDARG00000058165); *htr2aa* mo: 5'-TAACCTGAAGAGGAGATACACATGC-3' (targeting gene ENSDARG00000057029); and *htr2c* mo: 5'- TCAAATCCGTGTTTCTCTGACCTAT-3' (targeting gene ENSDARG00000018228). RT-PCR to test splice-blocking of morpholinos was performed as previously described (Xing et al., 2012). Primers for testing *htr2ab*

morpholino efficacy were used to amplify the region encompassing exons 1 and 3 (forward: 5'-ATGGATTGCAATGGGAGCGA-3'; reverse: 5'-GATGAGCGGGACGAAAAACG-3').

TUNEL staining

Terminal deoxynucleotidyl transferase dUTP nick-end labeling (TUNEL) was performed on whole-mount larvae (ApopTag Fluorescein *in situ* Apoptosis Detection Kit; Millipore) as described (Lambert et al., 2012).

Drug treatment

Embryos were manually dechorionated at 24hpf. E3/PTU-containing solution was mixed with the respective compound: 500 mM ketanserin (Sigma, S006), 2 mM fluoxetine (Sigma F132), or 200 mM methysergide (Sigma, M137). Embryos were incubated with the compound from 24-72 hpf. Fixation with 4% PFA occurred at 72 hpf. Metronidazole (Mtz) (Sigma catalog no. M1547) was dissolved in 0.05% or 0.2% DMSO in standard E3/PTU-containing solution. Before 24 hpf, embryos were exposed to 5 mM Mtz in 0.2% DMSO. At 24 hpf, embryos were manually dechorionated, and exposed to 5 mM Mtz in 0.05% DMSO from 24-96 hpf. Fixation with 4% PFA occurred at 96hpf.

Quantitative RT-PCR

qPCR for *tph2* was performed on 36 hpf and 48 hpf embryos. Each reaction was performed in triplicate and the mean of replicates was calculated; results were normalized to the mRNA level of *tph2* in wild-type embryos with β-actin transcript levels as a

control. qRT-PCR reaction for *ephrinB2a* was performed on 48hpf embryos. Primers for *tph2* were forward 5′-TTTGTGGAGGTTGCAATGAA-3′ and reverse 5′-CAGTCCAGCCAGGAAGTCTC-3′. Primers for β-actin were forward 5′-CTCTTCCAGCCTTCCTTCCT-3′ and reverse 5′- CACCGATCCAGACGGAGTAT-3′. qRT-PCR reaction for *ephrinB2a* was performed on 48hpf embryos. Primers for *ephrinB2a* were forward 5'-CCCTACCAGTTACCCTCCCA-3' and reverse 5'-CTCTGAGCCGTTGTTGTTGC-3'.

htr2ab CRISPR/Cas9

One-cell stage embryos from a mating of Tg(*foxP2:egfp-caax*) outcrossed to wild type were injected with 1 ng Cas9 protein (PNA Bio, CP01) and 600 pg *htr2ab* sgRNA (Jao et al., 2013). sgRNA was targeted to the following sequence in *htr2ab*: GGTCATAATCATCACCGTGA. sgRNA synthesis followed the protocol as previously described (Jao et al., 2013). Embryos were collected at 24 hpf for mutation analysis using PCR and high-resolution melt analysis (HRMA) (Xing et al., 2012; Xing et al., 2014).

Genomic DNA from 24 hpf embryos was prepared as follows: embryos were incubated with 30 μl 50 mM NaOH at 95°C for 25 minutes; then cooled to 4°C, then 3 μl 1M Tris-HCl (pH8.0) was added. PCR reactions were performed in 96-well hard-shell plates (Bio-Rad, Inc.) in 10 μl volume: 4 μl 2.5x LightScanner Master Mix (Idaho Technology, Inc.), 5 pmol each primer (forward primer: 5′-GTCCAGAAGAACTGGGTGGC-3′; reverse primer: 5′-CTGGTCATCATGGCGGTGAG-3′), and 3 μl genomic DNA template extracted above. PCR reactions were covered with 30 μl mineral oil. PCR cycling conditions were: 2 min

at 95°C, followed by 28 cycles of 10 s at 95°C, 30 s at 68°C, ending with 95°C for 30 s and cooled to 15°C. HRMA was performed on a LightScanner-96 instrument (Idaho Technology, Inc.), from 60°C to 97°C with a temperature transition rate of 0.1°C/s. For sequencing the targeted region in F0 founders, PCR amplicons were cloned into the pCR4-TOPO TA vector (Invitrogen). Plasmids were isolated from individual colonies and Sanger sequenced.

Results

5-HT blockade causes commissural axon pathfinding errors

To study the role of 5-HT in axon pathfinding, we used the transgenic line *Tg(foxP2-enhancerA.2:egfp-caax)*, which expresses membrane-targeted GFP in a subset of neurons in the telencephalon (Stevenson et al., 2012). *Tg(foxP2-enhancerA.2:egfp-caax)* neurons project axons in the anterior commissure, longitudinal pathways, and the diencephalic tract of the commissure of the posterior tuberculum (TCPTc) (Wilson et al., 1990). The TCPTc axons start to extend at 24 hpf (hours post-fertilization); by 36-48 hpf axons are preparing to cross the midline; most axons have crossed by 72 hpf; and the commissure is fully formed by 96 hpf (Figure 4.1 A-D). To clarify the targets and pathways of these axons, we performed ipsilateral sparse labeling of the neurons labeled by *foxP2-enhancerA.2 by* transient expression of co-injected plasmids, *foxP2-enhancerA.2:Gal4* and *UAS:lyn-TagRFP* (Stevenson et al., 2012*;* Yokogawa et al., 2012) into one-cell stage embryos. We observed three different projection classes: a subset of axons that cross the midline as the TCPTc and target onto the contralateral neurons in the telencephalon; a subset that extends longitudinally into

Figure 4.1. Axons labeled by *foxP2-enhancerA.2:egfp-caax* and the TCPT commissure. Confocal images of whole-mount embryos, rostral top, scale bar, 50 µm. A-D) Tg(*foxP2-enhancerA.2:egfp-caax*) embryos, maximum intensity z-stack projections, a-GFP immunohistochemistry. A-C) Midline TCPT commissure (TCPTc) axon crossing begins around 36-48 hpf (arrowhead). D) By 72hpf the TCPTc is formed (arrow). E) Schematic illustration of three major axon pathways of *foxP2-enhancerA.2* neurons. 1, longitudinal axons; 2, TCPTc, tract of the commissure of the posterior tuberculum; 3, anterior commissure. F) Projection targets of *foxP2* neurons were determined by sparse ipsilateral neuron labeling (arrow) using co-injection of plasmids carrying *UAS:lyn-TagRFP* and *foxP2-enhancerA.2:Gal4* at the one-cell stage, stained for a-RFP. *foxP2* neurons project longitudinally; across the anterior commissure; or across the TCPTc.

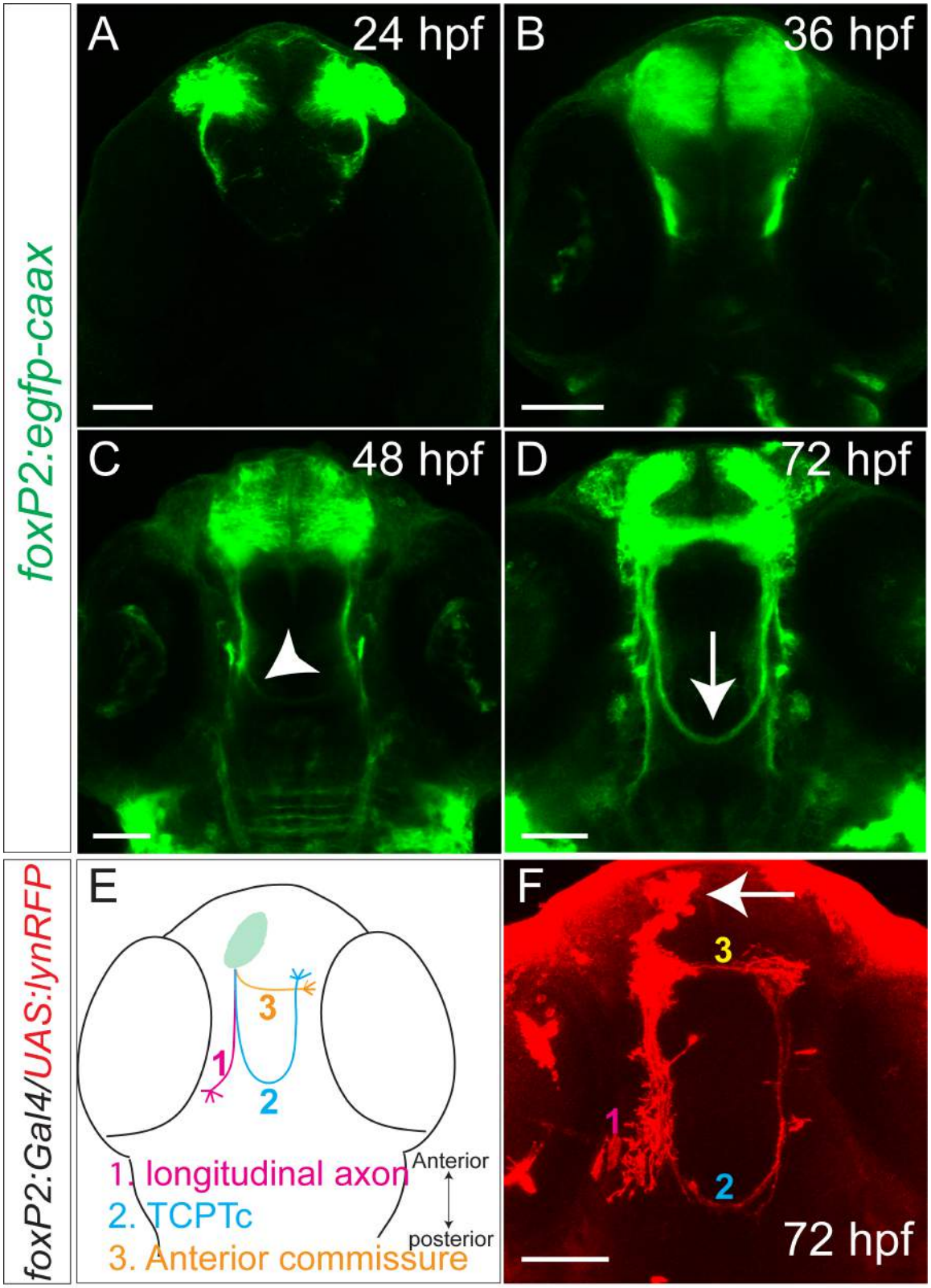
foxP2:egfp-caax
A
24 hpf
B
36 hpf
C
48 hpf
D
72 hpf
foxP2:Gal4/UAS:lynRFP
E
3
1
2
1. longitudinal axon
2. TCPTc
3. Anterior commissure
Anterior
posterior
F
3
1
2
72 hpf

the caudal diencephalon; and axons that cross directly in the anterior commissure onto neurons in the contralateral telencephalon (Figure 4.1E-F).

To test the effects of 5-HT on axon pathfinding, we tried a variety of pharmacological manipulations of 5-HT signaling. Embryos were dechorionated and incubated with different compounds from 24 to 72 hpf during the critical period for *foxP2-enhancerA.2* axon pathfinding. The nonspecific 5-HT receptor antagonist methysergide (Silberstein, 1998) caused defects in midline crossing of the TCPTc, but overall health of the embryos was compromised and it was unclear if the pathfinding errors were a secondary nonspecific effect. When we incubated embryos with the 5-HT receptor type 2 (hydroxytryptamine receptor 2, htr2) antagonist ketanserin (Brogden and Sorkin, 1990), there was no effect on overall mortality or development of the embryos. However, *Tg(foxP2-enhancerA.2:egfp-caax)* embryos treated with ketanserin had failure to form the TCPTc, or a reduction in the number of TCPTc axons crossing the midline (Figure 4.2A, B).

The effects of ketanserin were dose-dependent: levels of 200 mM had minimal effect on TCTPc pathfinding (data not shown), and 500 mM was used for experiments. We did not observe any overall difference in apoptosis in control compared to ketanserin-treated embryos (Figure 4.2C). Further, the reduction in crossing axons was not due to a loss of *foxP2* neurons, as control and ketanserin-treated embryos had the same number of telencephalic neurons (Figure 4.2C). We noted that the defects in axon guidance persisted at 5 dpf (days post-fertilization), indicating that the pathfinding errors were not due to a developmental delay.

To quantify the changes in commissure axon crossing, we calculated fluorescence

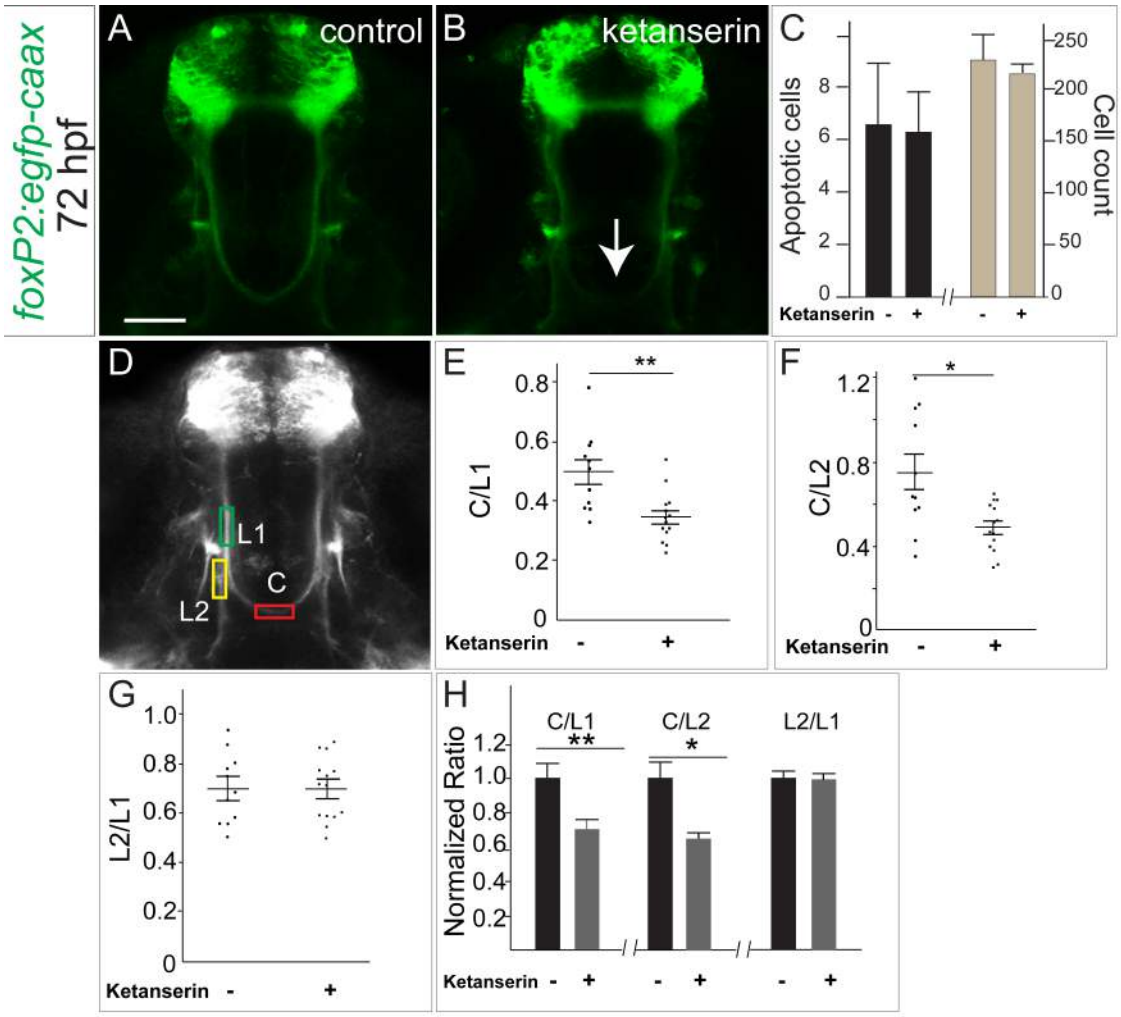

Figure 4.2. Commissural axon projections of TCPT neurons are disrupted by blockade of 5-HT signaling. (A, B) Tg(*foxP2-enhancerA.2:egfp-caax*) embryos, maximum intensity z-stack projections, a-GFP immunohistochemistry, rostral top, scale bar, 50 µm. TCPTc midline axon crossing is disrupted (arrow) when treated with ketanserin (B) compared to control (A). C) Ketanserin does not cause increased apoptosis in treated embryos or changes in overall cell counts in the telencephalon (TUNEL and TOPRO-3 staining). n = 5 each group. Error bars, standard deviation (apoptosis); standard error of the mean (cell counts). D) Confocal image of Tg(*foxP2-enhancerA.2:egfp-caax*) embryo, showing where measurements were made for the intensity of commissural (C), pre-crossing longitudinal (L1), and post-crossing (L2) axon tracts (see Methods for details). E-G) Scatterplots of results from individual embryos, showing the distribution of C/L results. n=11 and 14, respectively in control and ketanserin-treated group. *, $p < 0.05$, **, $p < 0.01$; Student's *t*-test. Error bars, SEM. E, F) Results of ketanserin-treated compared to control axon pathways, showing that in treated embryos the C/L ratio was decreased, indicating fewer TCPTc axons crossing the midline. G) No change was seen in the L2/L1 ratios between control and ketanserin-treated embryos, indicating that the misguided axons did not preferentially choose the longitudinal tract. H) Intensity ratio data shown with values normalized to that in controls.

intensity ratios of commissure to longitudinal axons (C/L ratios, Stevenson et al., 2012). Effects of ketanserin on the TCPTc ranged from minimal to complete loss of the TCPTc, and varied from embryo to embryo. We measured the signal intensity of the commissure axons, compared to the precommissure longitudinal tract axons (C/L1 ratio), and to the postcommissure longitudinal tract axons (C/L2 ratio) (Figure 4.2D-F). A lower C/L ratio indicates fewer TCPTc axons crossing the midline. Finally, we also compared the intensity of the precommissure longitudinal tract, to the postcommissure longitudinal tract, in control and ketanserin-treated embryos (L2/L1 ratio, Figure 4.2G). We reasoned that if axons in ketanserin-treated embryos were indeed aberrantly selecting the longitudinal pathway in preference to the TCPTc, we would see an increase of L2/L1 in treated embryos. To address this we examined individual embryo raw data ratios, shown as scatterplots (Figure 4.2E-G); as well as normalized ratios (Figure 4.2H). We found that embryos treated with ketanserin had both decreased C/L1 and C/L2 ratios (Figure 4.2E, F), consistent with the decrease in axons crossing the TCPTc. Additionally, in ketanserin-treated embryos, the L2/L1 ratio did not change (Figure 4.2G), suggesting that axons did not select the L2 longitudinal tract preferentially.

5-HT receptors are necessary for commissural axon crossing

Since we noted the effect of blocking 5-HT signaling, and in particular of the *htr2* antagonist ketanserin on midline axon crossing, we next determined which *htr2* receptors were expressed in *foxP2* neurons. More than 14 different 5-HT receptors are expressed in the vertebrate CNS (Barnes and Sharp, 1999). Ketanserin has high affinity

for serotonin type 2A receptors but can also bind with lower affinity to type 2C receptors (Saxena, 1995). Expression of *htr2aa*, *htr2ab*, and *htr2c* in the 48 hpf zebrafish CNS exhibit a spatial overlap in the telencephalon with *foxP2* neurons (Schneider et al., 2012). We used sections of *Tg(foxP2-enhancerA.2:egfp-caax)* embryos to perform double staining with immunohistochemistry for GFP, and *in situ* hybridization for either *htr2aa*, *htr2ab*, or *htr2c*. We found that all three receptors were co-expressed in *foxP2* neurons, as well as in *foxP2* axons as they extend caudally to form the TCPTc. As explained below, we focused analysis on *htr2ab* (Figure 4.3A-B").

To demonstrate the necessity of *htr2* for TCPTc axon guidance, and to determine which receptor subtype(s) were involved, we used morpholino knockdown of the different *htr2* receptors alone and in combination. Knock-down of *htr2aa* or *htr2c* did not affect the TPCTc (Figure 4.3F, G). However, knock-down of *htr2ab* led to a reduction in the C/L1 ratio of the TCPTc, suggesting that 5-HT signaling via *htr2ab* receptors is critical for axon midline crossing (Figure 4.3C, E). Since there was still some crossing of the TCPTc, we tried co-injection of *htr2ab* and *htr2aa* morpholinos. This caused disruption of embryogenesis and severe dysmorphism of the body axis, preventing analysis of pathfinding.

To confirm specificity of the *htr2ab* morpholino phenotype, we designed and used CRISPR/Cas9 gene disruption of *htr2ab* (Figure 4.3D). Injection of CRISPR/Cas9 can lead to high-frequency bi-allelic disruption of the targeted gene in somatic cells (Jao et al., 2013; Jinek et al., 2012). We co-injected Cas9 protein and an *htr2ab* short guide RNA (sgRNA) into one-cell stage embryos and found mutagenesis efficiencies up to 94.7% in

Figure 4.3. *htr2ab* is necessary for TCPTc formation. A-B", sections of 48hpf Tg(*foxP2-enhancerA.2:egfp-caax)* embryo, double-labeled for *htr2ab in situ* and a-GFP, rostral top, scale bar 50 mm. Bright field (A), fluorescent (A'), and merged images (A") show *htr2ab* expression in *foxP2* neurons and in axon tracts. B-B") shows higher magnification of boxed region in A". C) *htr2ab* splice-blocking morpholino targets exon 1/intron 1 boundary. Gel shows that morpholino partially blocks normal splicing (arrowhead). D) Schematic of *htr2ab* sgRNA used in CRISPR experiments. E) *htr2ab* knock-down causes decreased TCPTc midline axon crossing. C/L1 normalized ratio data of TCPTc crossing. *htr2ab* morpholino or sgRNA/Cas9 -injected embryos have lower C/L1 ratios, indicating failure of midline axon crossing. C/L1 ratio is rescued in embryos co-injected with *htr2ab* mRNA and sgRNA/Cas9. (n=11, 14, 10, 9, 11, respectively in columns. * $p < 0.05$, ** $p < 0.01$; Student's *t*-test for morpholino; one-way ANOVA with Turkey's post-hoc test for CRISPR. Error bars, SEM.) (F) Scatterplot of C/L1 ratios shows that morpholino mediated knockdown of *htr2aa* and *htr2ac* does not affect axon pathfinding. (G) Normalized C/L1 ratios in *htr2aa* and *htr2c* morpholino-injected embryos. H) High Resolution Melting Analysis (HRMA) (Xing et al., 2014) of PCR products shows that 36 out of 38 embryos injected with *htr2ab* sgRNA/Cas9 have an abnormal melt-curve indicating a mutation. I) Proportion of in-frame and out-of-frame mutations, sequenced from *htr2ab* PCR amplicons for two embryos (all PCR products had mutations). J) Sequences from cloned PCR amplicons from *htr2ab* CRISPR. The target site and protospacer adjacent motif (PAM) are highlighted in grey and blue, respectively. Representative sequences of *htr2ab* mutations in the F0 are shown. Insertions, deletions and point mutations are shown as respectively, red lower case letters, dashes, and upper case letters.

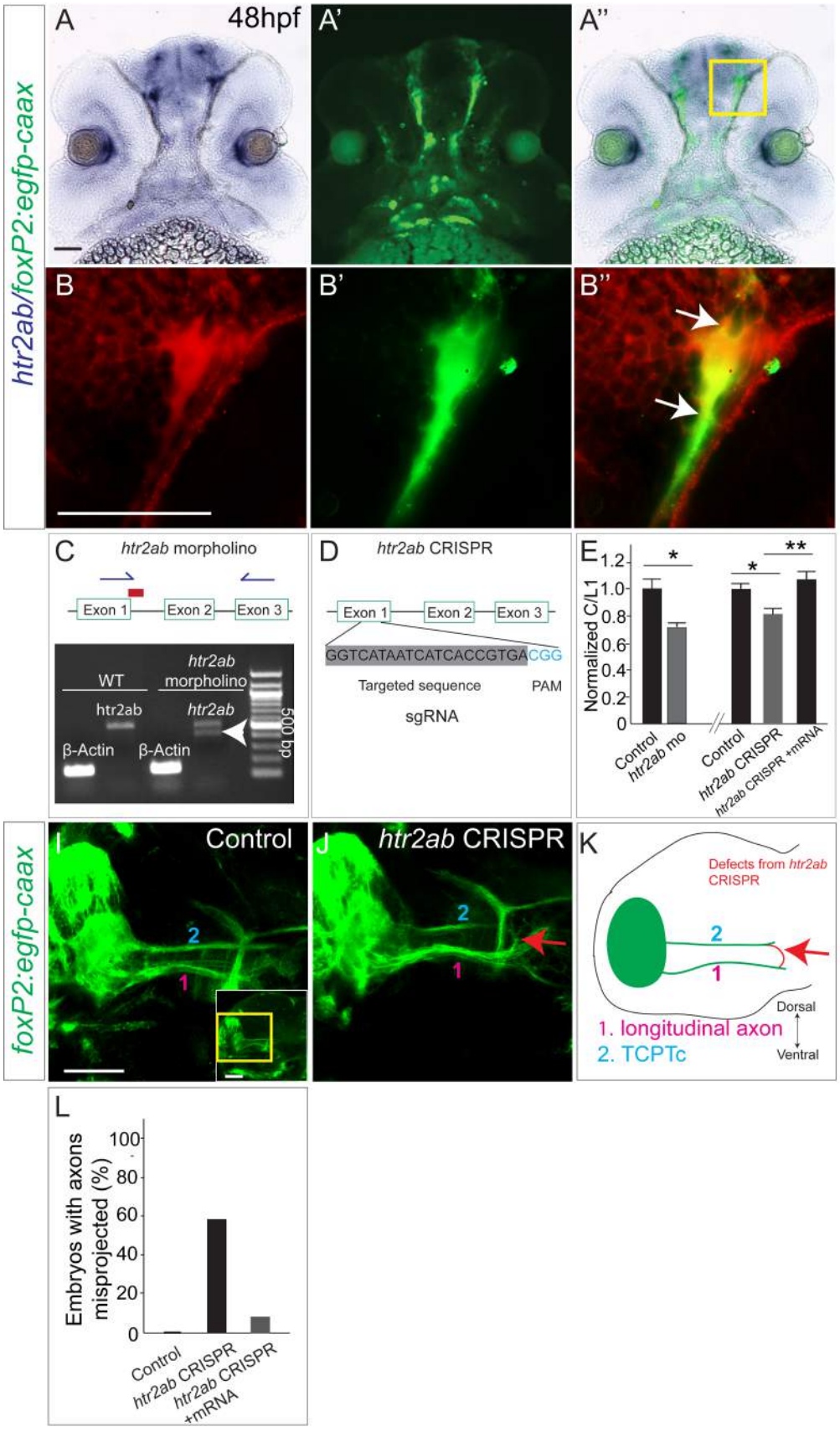
htr2ab/foxP2:egfp-caax
A
48hpf
A'
A''
B
B'
B''
C
htr2ab morpholino
Exon 1
Exon 2
Exon 3
WT
htr2ab morpholino
htr2ab
htr2ab
β-Actin
β-Actin
600 bp
D
htr2ab CRISPR
Exon 1
Exon 2
Exon 3
GGTCATAATCATCACCGTGACGG
Targeted sequence
PAM
sgRNA
E
Normalized C/L1
1.2
1.0
0.8
0.6
0.4
0.2
0
*
*
**
Control
htr2ab mo
Control
htr2ab CRISPR
htr2ab CRISPR +mRNA
foxP2:egfp-caax
I
Control
J
htr2ab CRISPR
2
1
K
Defects from htr2ab CRISPR
2
1
Dorsal
Ventral
1. longitudinal axon
2. TCPTc
L
Embryos with axons misprojected (%)
100
80
60
40
20
0
Control
htr2ab CRISPR
htr2ab CRISPR +mRNA

the F0 embryos (n= 36/38 injected embryos) (Figure 4.3H-**J**). To validate the extent of mutagenesis, we cloned 18 individual PCR amplicons each from two F0 embryos. Sanger sequencing showed that all 36 PCR products had mutations (deletions or insertions); 27/36 amplicons were outofframe and would cause a stop or an early protein truncation. The remaining 9 in-frame mutations caused a variety of short amino acid insertions or deletions.

We injected Tg(*foxP2-enhancerA.2:egfp-caax*) embryos with *htr2ab* CRISPR/Cas9 sgRNA; we found that F0 injected embryos had failure of TCPTc commissure formation, with a decreased C/L1 ratio (Figure 4.3E). The TCPTc formation defects induced by CRISPR/Cas9 sgRNA were rescued when co-injected with *htr2ab* mRNA (Figure 4.3E), indicating the specificity of CRISPR/Cas9 sgRNA. We validated that the CRISPR was still functional in the co-injected embryos by PCR analysis at the endogenous *htr2ab* locus, indicating that the rescue was due to the *htr2ab* mRNA, not due to failure of mutagenesis induced by CRISPR/Cas9 sgRNA. Thus, loss of *htr2ab*, either by morpholino knock-down or CRISPR gene disruption, leads to midline crossing errors in the TCPTc, supporting a role for 5-HT signaling in the TCPT axons as they decussate.

Raphe neuron serotonin expression is necessary for commissure formation

Since our data suggested a role for the *htr2ab* receptor and 5-HT signaling in midline crossing of TCPTc axons, we next tested if a source of 5-HT was available to the TCPTc axon growth cones during development. In zebrafish the dorsal raphe nucleus expresses 5-HT by 36 hpf and 5-HT axonal projections are widely distributed in the CNS

by 72 hpf (Lillesaar et al., 2009). To determine whether TCPTc axons encountered a 5-HT source, we performed immunostaining for 5-HT and for GFP in Tg*(foxP2-enhancerA.2:egfp-caax*) embryos. We found that serotonin-expressing neurons had projections neighboring the ends of TCPTc axons prior to their midline crossing (Figure 4.4A-A"). We confirmed this in confocal single slice high-resolution images (Figure 4.4B-B", C-E)**.**

In zebrafish, unlike mammals, several 5-HT nuclei are present in the CNS (Kaslin and Panula, 2001, McLean and Fetcho, 2004; Lillesaar, 2011), including pretectal and posterior tuberculum/hypothalamic nuclei (Figure 4.4A', arrowhead). To determine whether the raphe nuclei were the source of the serotonergic projections for the TCPTc axons, we used an enhancer for 5-HT neurons specific to the raphe nucleus, *-3.2pet1* (referred to as "*pet1*") (Lillesaar et al., 2009). We examined axon projections from the raphe 5-HT neurons to the TCPTc axons in triple-transgenic animals: Tg*(pet1:Gal4)*; Tg*(UAS:RFP-caax);* Tg*(foxP2-enhancerA.2:egfp-caax)*. We observed RFP-expressing axons from the raphe nuclei projecting to the TCPTc axons (Figure 4.4F-I), including in single slice confocal images, confirming that the raphe neurons are the likely source of 5-HT for TCPTc axons.

To determine whether the raphe neurons are necessary to provide 5-HT for TCPTc midline crossing, we performed targeted genetic ablation of the raphe. We used the cell-autonomous nitroreductase/metronidazole system (Curado et al., 2008; Pisharath and Parsons, 2009), driving expression of nitroreductase (Tg(*UAS:NTR-mCherry*)) in raphe 5-HT neurons using Tg(*tph2:Gal4*) (Yokogawa et al., 2012); and visualized expression of axons with *Tg(foxP2-enhancerA.2:egfp-caax*) (Figure 4.5A).

Figure 4.4. Serotonergic neurons project in close apposition to TCPTc commissural axon tips prior to midline crossing. A-B") Confocal images of whole-mount embryo at 48 hpf, rostral top, scale bar 50 μm. Tg(*foxP2-enhancerA.2:egfp-caax)* embryo double-labeled for a-GFP and for a-5-HT. Boxed region in A" is shown at higher resolution in B-B", as single confocal slice. Arrow points to serotonin-expressing axon projections (red) overlapping *foxP2* TCPTc developing axons (green). C-E) XZ and YZ plane projections from consecutive confocal slices confirm the overlap between 5-HT axons and TCPTc growth cones. F-G") Confocal images of Tg(*foxP2-enhancerA.2:egfp-caax)*; Tg(*pet1:Gal4*); Tg(*UAS:RFP-caax*) whole-mount embryo at 56hpf, rostral top, scale bar 50 mm, double immunohistochemistry for a-GFP and a-RFP, demonstrating that the raphe nucleus axons could provide 5-HT for *foxP2* axons. Boxed region in F' is shown in higher resolution G-G" as single confocal slice. Arrows (G) point to RFP expression from raphe nuclei overlapping TCPTc growth cone.

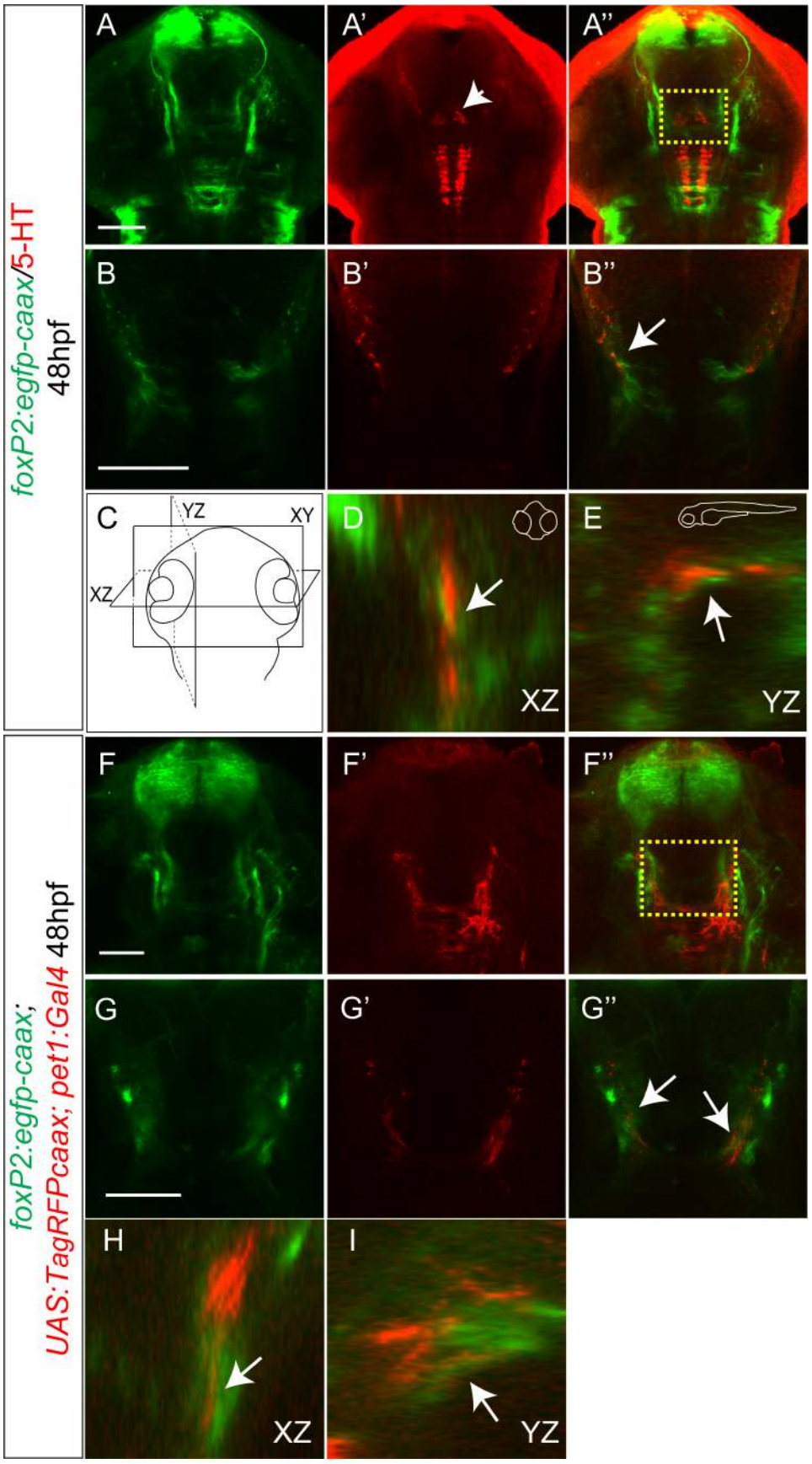
foxP2:egfp-caax/5-HT
48hpf
A
A'
A''
B
B'
B''
C
YZ
XY
XZ
D
XZ
E
YZ
foxP2:egfp-caax;
UAS:TagRFPcaax; pet1:Gal4 48hpf
F
F'
F''
G
G'
G''
H
XZ
I
YZ

Figure 4.5. Ablation of the 5-HT neurons causes TCPTc midline crossing defects. A) Schematic diagram of nitroreductase (NTR)/metronidazole (Mtz) experiments. *tph2:Gal4* embryos treated with Mtz from 0-96hpf; in double-transgenic animals (*tph2:Gal4*; *UAS:NTR-mCherry*), Mtz is converted to a toxic metabolite causing apoptosis of 5-HT/*tph2* neurons. B-G) Confocal images of whole-mount embryo at 96 hpf, rostral top, scale bar 50 μm. B) Embryos without Mtz treatment. C) Mtz treatment leads to axon crossing defects in embryos expressing *tph2:Gal4*/*UAS:NTR-mCherry*. D, F) Embryos without Mtz treatment, immunohistochemistry for mCherry (D) or 5-HT (F). E, G) Embryos expressing *tph2:Gal4*/*UAS:NTR-mCherry* treated with Mtz, immunohistochemistry for mCherry (E) or 5-HT (G). H) Normalized C/L1 ratios show that ablation of raphe nuclei leads to the failure of TCPTc axon crossing. ($n = 6, 8, 10$, respectively in columns. ** $p < 0.01$, *** $p < 0.001$, one-way ANOVA with Turkey's post-hoc test;. n.s., not significant. Error bars, SEM.)

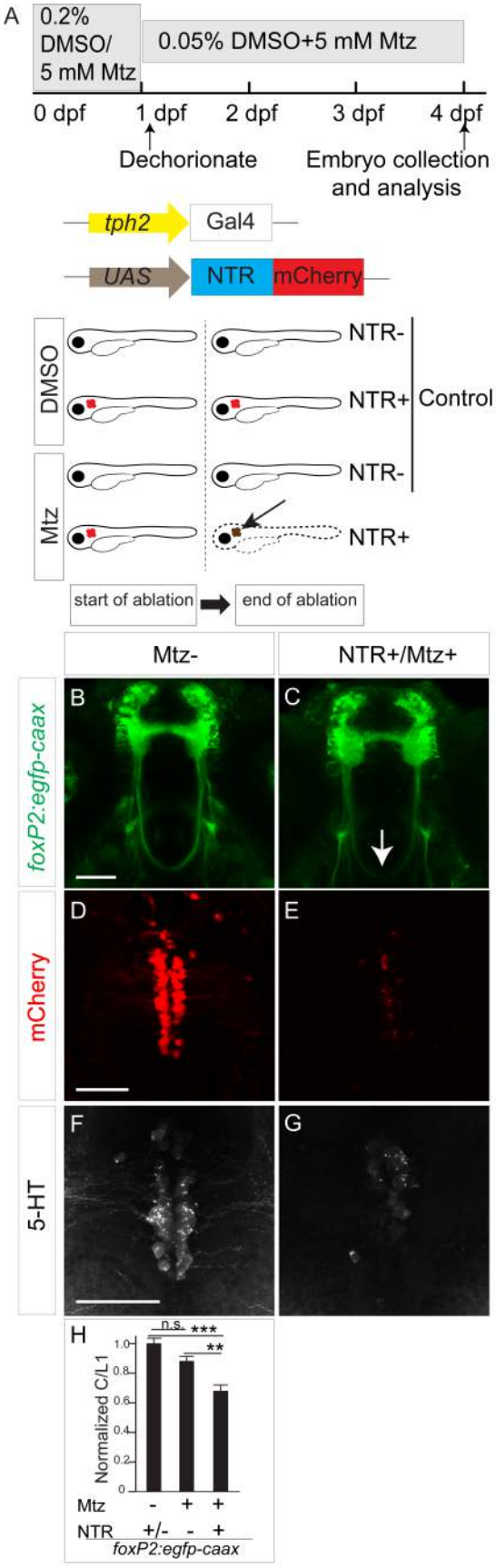
A
0.2% DMSO/ 5 mM Mtz
0.05% DMSO+5 mM Mtz
0 dpf
1 dpf
2 dpf
3 dpf
4 dpf
Dechorionate
Embryo collection and analysis
tph2
Gal4
UAS
NTR
mCherry
DMSO
Mtz
NTR-
NTR+
Control
NTR-
NTR+
start of ablation
end of ablation
Mtz-
NTR+/Mtz+
foxP2:egfp-caax
mCherry
5-HT
B
C
D
E
F
G
H
Normalized C/L1
n.s.
***
**
Mtz
NTR
foxP2:egfp-caax

We used the Tg(*tph2:Gal4)* line because we noted that Tg(*pet1:Gal4*) expressed in fewer 5-HT raphe neurons. In the absence of metronidazole, there was no ablation of raphe neurons and TCPTc axon pathfinding was normal (Figure 4.5B, D, F). With addition of metronidazole, ablation of raphe neurons occurred in embryos expressing nitroreductase, with loss of 5-HT and disruption of TCPTc midline crossing (Figure 4.5C, E, G). In embryos with no nitroreductase, metronidazole had no significant effect on midline axon crossing or on the number of 5-HT neurons. These results show that 5-HT is necessary for TCPTc midline crossing, and demonstrate that the raphe nucleus is the likely source of 5-HT.

ephrinB2a limits midline crossing and mediates 5-HT action on pathfinding

We had previously shown that the transmembrane ligand *ephrinB2a* is involved in TCPTc axon midline crossing, and that its ligand *ephA4a* is expressed in a complementary pattern to the TCPT axons in the CNS midline (Stevenson et al., 2012). The *ephrinB* family of ligands are known to be involved in midline commissure formation (Imondi and Kaprielian, 2001; Kadison et al., 2006). To test whether 5-HT's role in TCPTc midline axon guidance could be mediated by ephrinB2a, we obtained and characterized an *ephrinB2a* mutant allele, $efnB2a^{hu3393}$ from the Zebrafish Mutation Project (Wellcome Trust Sanger Institute; (Kettleborough et al., 2013). $efnB2a^{hu3393}$ is a nonsense mutation in exon 2 of *ephrinB2a* (T>A; C86X) (Figure 4.6A). $efnB2a^{hu3393}$ homozygotes ("$efnB2a^{-/-}$") are viable, and immunohistochemistry demonstrates loss of ephrinB2a protein (Figure 4.6B, C). Tubulin staining of homozygous mutants did not show gross defects in major axon tracts (Figure 4.6D-G). The TCPTc commissure

Figure 4.6. 5-HT mediates axon guidance through *ephrinB2a* (*efnB2a*). A) The *efnB2a*^{hu3393} allele is a nonsense mutation in the receptor-binding domain (exon 2) of *ephrinB2a* (T>A; C86X). SP, signal peptide. RBD, receptor-binding domain. TM, transmembrane domain. B-K, M, M') Confocal images, rostral top, scale bar 50 μm. B, C) efnB2 immunohistochemistry. efnB2 protein is absent in *efnB2a*$^{hu3393/hu3393}$ (*efnB2a*$^{-/-}$) embryo compared to WT. D-G) Acetylated tubulin immunohistochemistry does not show gross axon defects in *efnB2a*$^{-/-}$ embryos. D, E) Axons in dorsal brain. F, G) Axons in ventral brain. H-K) GFP immunohistochemistry in Tg(*foxP2-enhancerA.2:egfp-caax)* embryos shows that lack of efnB2 (in *efnB2a*$^{-/-}$ embryos, J, K) prevents ketanserin-induced midline crossing defects (arrow) compared to *efnB2a* heterozygotes (H, I). L) Quantification confirms that *efnB2a*$^{-/-}$ restores axon guidance in presence of ketanserin. (n = 10 per group. * $p < 0.05$, two-way ANOVA followed by Bonferroni post-test. Error bars, SEM.) M) *efnB2a*$^{-/-}$ mutant has normal raphe 5-HT expression compared to WT (M').

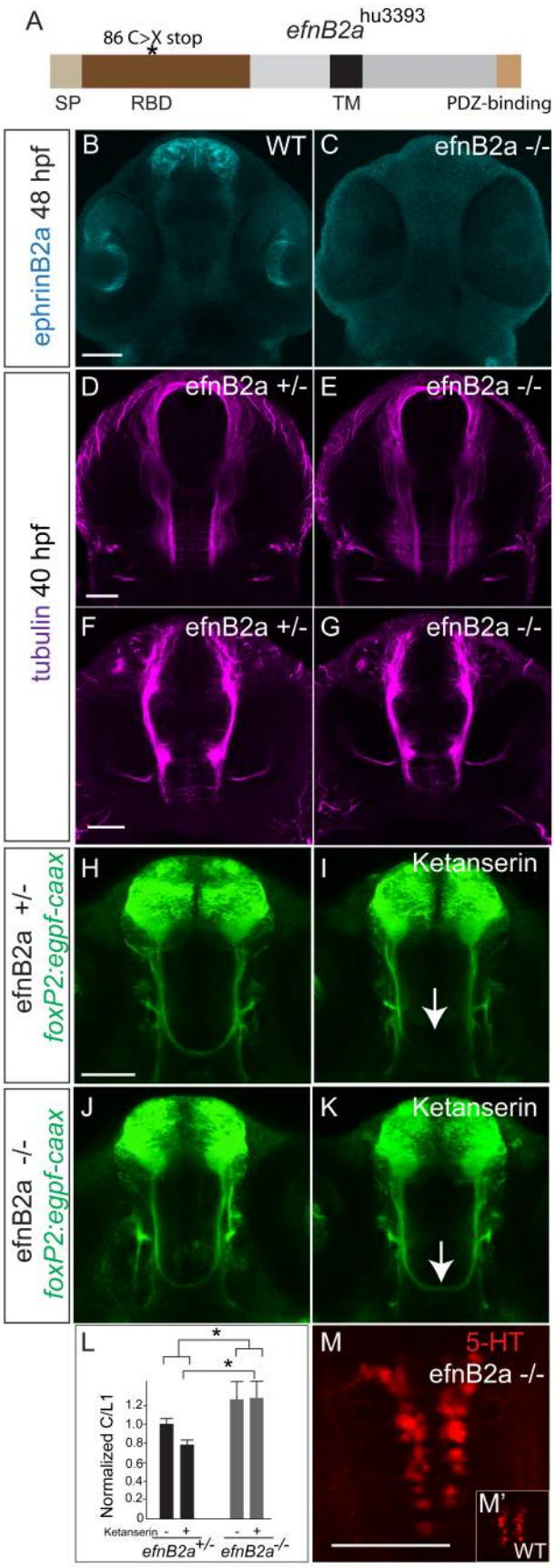
A
86 C>X stop
efnB2a hu3393
SP
RBD
TM
PDZ-binding
ephrinB2a 48 hpf
B WT
C efnB2a -/-
tubulin 40 hpf
D efnB2a +/-
E efnB2a -/-
F efnB2a +/-
G efnB2a -/-
efnB2a +/- foxP2:egpf-caax
H
I Ketanserin
efnB2a -/- foxP2:egpf-caax
J
K Ketanserin
L
Normalized C/L1
1.2
1.0
0.8
0.6
0.4
0.2
0
Ketanserin - + - +
efnB2a+/- efnB2a-/-
M 5-HT
efnB2a -/-
M'
WT

appeared normal on visual inspection in the homozygous *efnB2a*$^{-/-}$ background (Figure 4.6J), but there was a statistically significant increase in the number of crossing axons (Figure 4.6L).

Blockade of 5-HT signaling in *efnB2a*$^{+/-}$ heterozygotes by ketanserin causes TCPTc axon pathfinding defects similar to that seen in a wild-type background (Figure 4.6H, I, L). However, in *efnB2a*$^{-/-}$ homozygous mutants treated with ketanserin, TCPTc midline axon crossing was normal (Figure 4.6J-L). *efnB2a*$^{-/-}$ mutants do not have a change in raphe 5-HT expression (Figure 4.6M, M'). These results show a role for ephrinB2a in normally limiting midline axon crossing, and in mediating the action of 5-HT on the TCPTc decussation.

5-HT regulates ephrinB2a translation in the axon

How does 5-HT signaling interact with *ephrinB2a* regulation of TCPTc midline axon crossing? Axon guidance molecule expression can be regulated or modified by transcription, translation, or posttranslational processes (Winckler and Mellman, 2010; Jung et al., 2011; Hancock et al., 2014). 5-HT is able to stimulate translation in subcellular domains of target cells (Martin et al., 1997; Casadio et al., 1999; Miniaci et al., 2008). This could be a possible mechanism by which it could regulate axon guidance receptor activity.

To address these potential mechanisms, we examined levels of *ephrinB2a* in ketanserin-treated embryos. We found no significant difference in overall *ephrinB2a* RNA transcript levels by RT-PCR in whole embryos. However, after ketanserin treatment we noted increased ephrinB2a protein levels in embryos by quantification of

immunofluorescence levels, including in the telencephalon and TCPTc axons (Figure 4.7A-C), but not in the eyes. To demonstrate that ketanserin's effect on ephrinB2a levels was dependent on 5-HT, we performed ablation of raphe 5-HT neurons in Tg(*tph2:Gal4*); Tg(*UAS:NTR-mCherry*) embryos. We found that raphe neuron ablation led to an increase of ephrinB2a protein levels in the TCPTc axons, but not in the telencephalon and eyes (Figure 4.7D-G).

5-HT responds to hypoxia to decrease midline axon crossing

Since 5-HT has demonstrated roles in mediating adult plasticity, we considered whether 5-HT might also have a role in regulating axon guidance in response to environmental or developmental factors. Interpretation of external factors and changes to developing circuitry would be a mechanism by which a developing organism could modify its regulation of connectivity. Previous work from our lab demonstrated that hypoxia disrupts midline axon crossing by increasing levels of ephrinB2a (Stevenson et al., 2012). In nematodes hypoxia increases 5-HT expression, with a resultant activation of a latent sensory circuit (Pocock and Hobert, 2010). To test if hypoxia affects 5-HT expression we exposed developing zebrafish embryos to hypoxia from 24 to 36 hpf (Stevenson et al., 2012), and examined levels of 5-HT at 72 hpf. We found a decrease in 5-HT levels at 72 hpf (Figure 4.8A-D) but normal cell counts in the raphe. Hypoxia's effect on 5-HT expression was specific, since there were not effects on apoptosis or general embryo viability (Stevenson et al., 2012); and because levels of expression of the pan-neuronal marker Elav family members anti-HuC/D were unaffected (Figure 4.8C, D).

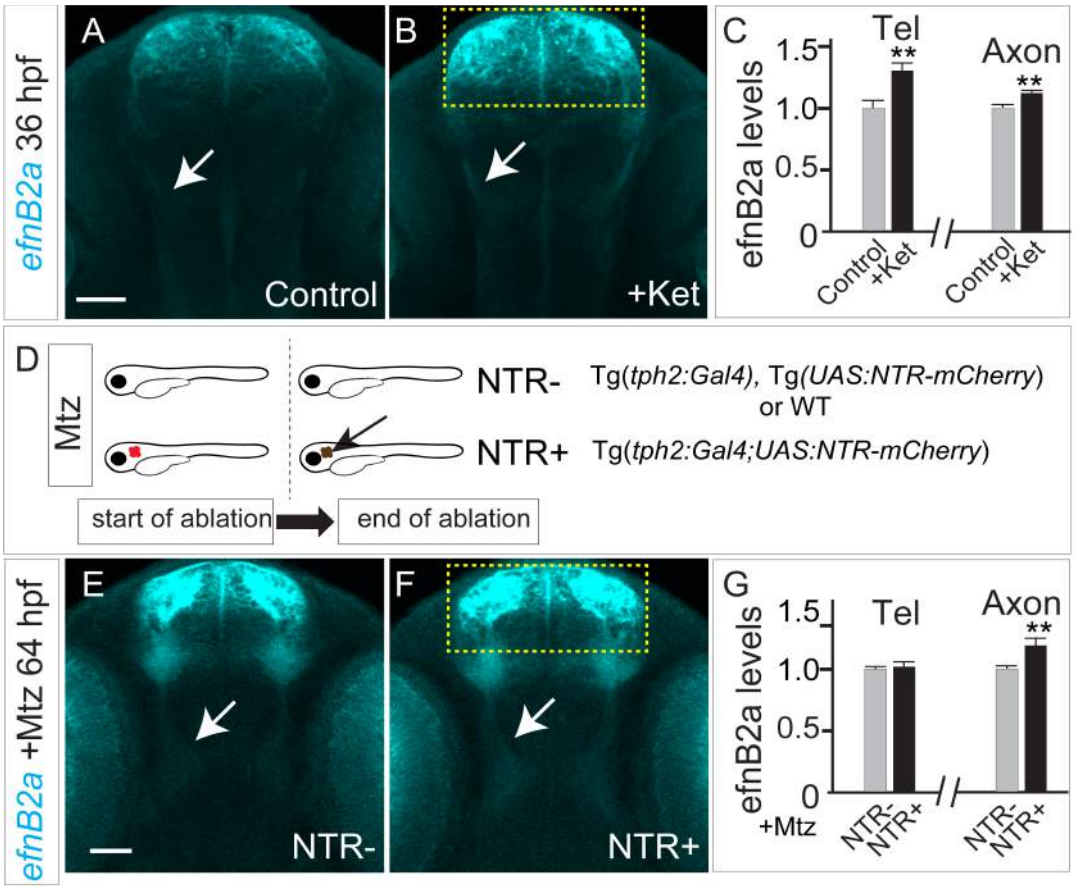

Figure 4.7. 5-HT regulates ephrinB2a (efnB2a) protein levels. A, B, E, F) Confocal images, 36hpf embryos, immunohistochemistry for a-efnB2a, rostral top, scale bar, 50 µm. A, B) efnB2a levels are increased in telencephalon (boxed region) and TCPTc axons (arrows) in embryos treated with ketanserin (B) compared to control (A). C) Quantification of ephB2a levels in telencephalon and TCPTc axons. (n = 20, 14, respectively in control and embryos treated with ketanserin. ** $p < 0.01$, Student's *t*-test. Error bars, SEM.) D) Schematic illustration of Mtz treatment in NTR- and NTR+ embryos. Genotypes in each group shown on right. Note that ablation can occur only when both *tph2:Gal4* and *UAS:NTR-mCherry* are expressed. E, F) efnB2a levels in TCPTc axons (arrows) are increased but not in the telencephalon (boxed region), in embryos expressing *tph2:Gal4/UAS:NTR-mCherry* (F) compared to embryos without *NTR* expression (E) following treatment with Mtz. G) Quantification of efnB2a levels in telencephalon and TCPTc axons. (n = 10, 12, respectively in NTR- and NTR+ embryos. ** $p < 0.01$, Student's *t*-test.)

Figure 4.8. 5-HT signaling is an interpreter of developmental environment to control TCPTc midline crossing. A-B') Hypoxia decreases 5-HT expression. Normoxia compared to hypoxia, confocal images of WT embryos at 48 hpf, maximal intensity z-stack projections, stained with 5-HT (A, B), stained with HuC/D (A', B'), rostral top, scale bar, 50 μm. C) 5-HT levels in raphe neurons (normalized to pan-neuronal marker HuC/D) are significantly decreased by hypoxia. (n = 6 per group, ** $p < 0.01$ Student's *t*-test.) D) HuC/D levels are not changed following hypoxia. (n = 6 per group. Error bars, SEM). E) Bright field *in situ* shows that *tph2* mRNA is specifically expressed in raphe. F) *tph2* mRNA levels (qRT-PCR) are decreased in 36 hpf and 48 hpf post-hypoxic embryos. (Error bars, SEM, three experimental replicates.) G-H), confocal images of Tg(*foxP2-enhancerA.2:egfp-caax*) show that fluoxetine (H) rescues axon guidance defects in hypoxic embryos (G). I) Normalized C/L1 ratio data confirms fluoxetine rescue of hypoxia effects. (n = 10, 13, 14, respectively in columns. * $p < 0.05$, ** $p < 0.01$, one-way ANOVA followed by Turkey's post-hoc test. Error bars, SEM.)

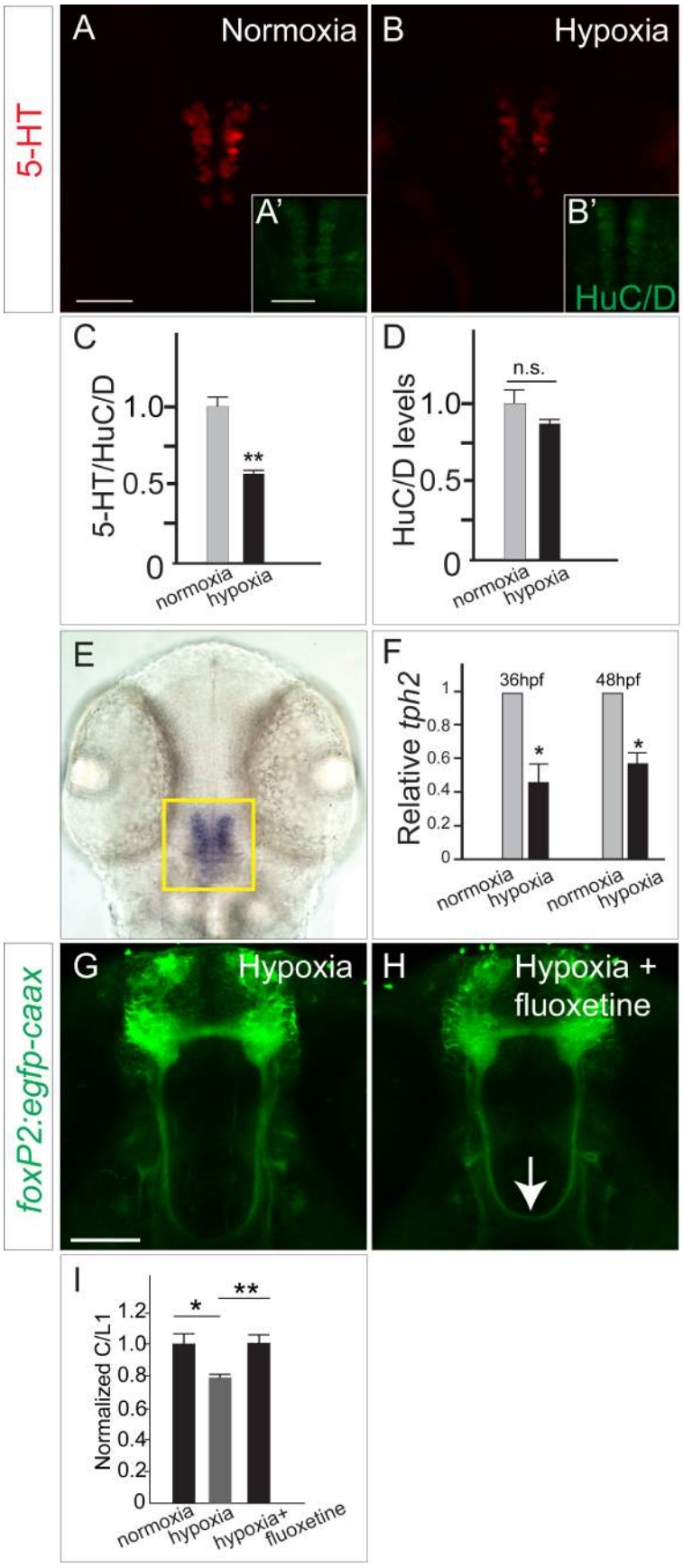
5-HT
A
Normoxia
A'
B
Hypoxia
B'
HuC/D
C
5-HT/HuC/D
1.0
0.5
0
**
normoxia
hypoxia
D
HuC/D levels
n.s.
1.0
0.5
0
normoxia
hypoxia
E
F
Relative tph2
36hpf
48hpf
1
0.8
0.6
0.4
0.2
0
*
*
normoxia
hypoxia
normoxia
hypoxia
foxP2:egfp-caax
G
Hypoxia
H
Hypoxia +
fluoxetine
I
Normalized C/L1
1.2
1.0
0.8
0.6
0.4
0.2
0
*
**
normoxia
hypoxia
hypoxia+
fluoxetine

Tryptophan hydroxylase (*tph*) is the rate-limiting enzyme for 5-HT biosynthesis; raphe neurons in zebrafish express the Tph ortholog *tph2* (Bellipanni et al., 2002; Teraoka et al., 2004). *tph* expression in other species has been shown to be responsive to hypoxia (Pocock and Hobert, 2010; Rahman and Thomas, 2009). Using qRT-PCR, we found that following hypoxia *tph2* RNA expression was decreased in the raphe nucleus. The decrease in *tph2* was present at 36 hpf, immediately following cessation of hypoxia, and persisted at 48 hpf (Figure 4.8E, F).

Since hypoxia decreased 5-HT levels, we reasoned that rescuing 5-HT signaling in hypoxia embryos should prevent midline axon crossing errors. To test this we incubated hypoxic embryos with fluoxetine, a selective 5-HT reuptake inhibitor (SSRI), which increases available 5-HT at the synapse. We found that fluoxetine incubation from 24hpf to 72hpf rescued the effect of hypoxia on midline axon crossing (Figure 4.8G-I). Hypoxia did not affect the overall distribution of raphe 5-HT axon projections. These data show that raphe neurons can respond to environmental hypoxia and modulate 5-HT expression, thereby altering neural circuit development.

Discussion

We have found that 5-HT and its receptor *htr2ab* provide instructive guidance for midline axon crossing, through down-regulation of ephrinB2a levels. 5-HT's role is sensitive to environmental cues, as developmental hypoxia decreases 5-HT expression from the raphe neurons and causes midline crossing defects. Our findings suggest that modification of the serotonergic system by early environmental exposures may contribute to permanent CNS connectivity alterations.

5-HT and *htr2ab* are necessary for axon guidance

The components of 5-HT signaling are conserved over 2 billion years of evolution from protozoa to mammals (Azmitia, 2007). During evolution 5-HT's roles and localization of action have become increasingly more specialized. In unicellular eukaryotes such as the ciliate protozoa *Tetrahymena,* 5-HT acts in intracellular signaling; in primitive metazoans such as *Planaria,* 5-HT has additional roles in hormonal cell-cell signaling; and in the nervous system of arthropods and vertebrates, 5-HT acts as a neurotransmitter at synapses (Hay-Schmidt, 2000; Turlejski, 1996). In mammals 5-HT signaling plays important roles in regulating behavior, memory consolidation, sleep, and appetite (Gingrich et al., 2003). Abnormalities in the 5-HT system in humans are associated with a range of neurobehavioral and neuropsychiatric disorders (Blasi et al., 2013; Harrington et al., 2013; Lesch and Waider, 2012).

Roles for 5-HT in early CNS development have recently been uncovered, including in neuron migration, dendrite arborization, and synapse formation (Matsukawa et al., 2003; Persico et al., 2001; Riccio et al., 2009; Vitalis et al., 2007). 5-HT signaling has been suggested to regulate axon guidance: in mice overexpression of 5-HT receptors causes a shift in thalamocortical axon tracts (Bonnin et al., 2007), and rats lacking the 5-HT transporter had altered raphe-prefrontal cortex pathways (Witteveen et al., 2013). We found that 5-HT acting through *htr2ab*, an excitatory G-protein coupled receptor, is necessary for normal midline axon crossing. We confirmed this finding using pharmacological blockade of *htr2* as well as with both morpholino and CRISPR/Cas9 knock-down of *htr2ab*. We found that the source of the 5-HT is from neurons of the raphe nucleus, by demonstrating close apposition of 5-HT axon termini to the termini of

TCPTc axons. Further, using cell-type specific genetic ablation we demonstrated that the raphe neurons are a necessary source of 5-HT TCPTc axon development. However, we cannot fully exclude the involvement of other 5-HT sources as well, for example the cell cluster located medially and anterior to the paraventricular organ (Lillesaar, 2009).

ephrinB2a mediates serotonin-associated axon pathfinding

ephrinB2 acts as a ligand for receptor tyrosine kinases (RTK) of the EphA and EphB families, inducing an intracellular signaling cascade in the RTK-expressing cell (Bashaw and Klein, 2010). EphrinB ligands are also known to "reverse" signal (Pasquale, 2008; Taylor et al., 2012), which we observed in previous studies on TCPTc pathfinding in the setting of hypoxia (Stevenson et al., 2012). Several studies have demonstrated that ephrinB signaling can function in midline crossing. For example, in Xenopus, ephrinB regulates ipsilateral sorting of retinal axons at the midline optic chiasm (Nakagawa et al., 2003); in chick, ephB2 expression at the midline repels axons at older ages (Cramer et al., 2006).

We found that pharmacological blockade of serotonergic signaling through its G-protein coupled receptor (GPCR) *htr2a*, or ablation of the raphe 5-HT neurons, increased ephrinB2a protein levels in the TCPTc axons. This increase in ephrinB2a could be due to increased transcription: both GPCRs and transcription factors including *Tbx5* and *VAX2* have been shown to alter ephrinB transcription levels (Jassen et al., 2006; Polleux et al., 2007). However, when we measured *ephrinB2a* mRNA levels using qRT-PCR we did not observe changes in embryos treated with *htr2a* antagonist; though we cannot exclude the possibility that local or subtle changes in *ephrinB2a* transcript levels are masked. Thus, our data support a role for 5-HT regulation of ephrinB2a protein levels. This could be by

increased translation of ephrinB2a, or by regulation of stability of ephrinB2a. Studies in *Aplysia* neuron cultures show that 5-HT can stimulate translation in subcellular domains of target cells (Casadio et al., 1999; Martin et al., 1997; Miniaci et al., 2008). This effect on translation could be through second messenger systems such as CPEB or CREB as in *Aplysia*; or alternatively 5-HT might exert its effect through miRNAs. *ephrinB2* can be regulated by multiple miRNAs (Wang et al., 2012), and drugs modifying the serotonergic system can alter miRNA expression (Baudry et al., 2010). miRNAs are present in axon growth cones and can alter local translation (Kaplan et al., 2013). Future studies could examine the interaction between serotonin signaling during development and effects on local translation and axon guidance.

Role of the raphe nucleus and serotonin in embryonic development

We observed that hypoxia disrupts axon connectivity by decreasing 5-HT synthesis. If serotonergic signaling is increased by blockade of 5-HT reuptake, then the effects of hypoxia on TCPTc midline crossing are prevented. Thus the raphe nucleus, through regulation of 5-HT levels, which in turn affects midline axon guidance, effectively act as a sensor to changes in the embryonic milieu. Interestingly, in the adult rat dorsal raphe 5-HT neurons also respond to the environment, acting as chemoreceptors to changes in blood pH/CO2 levels with altered firing patterns (Severson et al., 2003).

5-HT axon projections are widespread in early development during the period when extensive axon pathfinding is occurring (Lillesaar et al., 2009; Rubenstein, 1998); exposures to serotonergic drugs during gestation have been linked with increased risks for neurodevelopmental disorders (El Marroun et al., 2014; Gidaya et al., 2014;

Harrington et al., 2014; Rai et al., 2013); and polymorphisms in genes in the 5-HT signaling pathway are associated with a range of neuropsychiatric disorders (Kuzelova et al., 2010; Prasad et al., 2009; Sutcliffe et al., 2005). Loss or knock-out in early development of 5-HT neurons or other components of 5-HT signaling leads to diffuse CNS abnormalities with a wide range of behavioral phenotypes (Daubert and Condron, 2010; van Kleef et al., 2012). In the invertebrate *C. elegans* hypoxia can increase 5-HT expression and change a neural circuit response to gustatory sensation (Pocock and Hobert, 2010), providing evidence of biological relevance for an interaction between 5-HT signaling and neural circuits. These lines of evidence, in addition to the work presented here, are consistent with 5-HT acting to mediate changes in how connectivity develops. Future studies can examine the evolutionary and neurobiology significance of 5-HT's role for axon guidance, and its responsiveness to external conditions during development.

Conclusion

The findings here suggest a model in which serotonergic signaling, supplied by embryonic axon projections from the raphe nucleus, is necessary for normal midline axon crossing (Figure 4.9). In the presence of 5-HT, levels of ephrinB2a are decreased and axons are able to cross the midline. Conversely, if 5-HT levels are decreased, by pharmacological manipulation or through hypoxic exposure, ephrinB2a levels are higher (our data and Stevenson et al., 2012), and axons fail to cross the midline or take abnormal paths. Regulation of midline crossing is complex and includes interacting attractive and repulsive signaling (Evans and Bashaw, 2010). Recent work suggests the possibility for

Figure 4.9. Model. A) During development, TCPTc growth cones are exposed to 5-HT from raphe nuclei axon projections. 5-HT activates htr2ab in the TCPTc, decreasing expression of ephrinB2a, and allowing axons to cross the midline. B) When 5-HT signaling is inhibited by drug, knockdown, or hypoxia, the up-regulation of ephrinB2a expression prevents TCPTc axons crossing the midline.

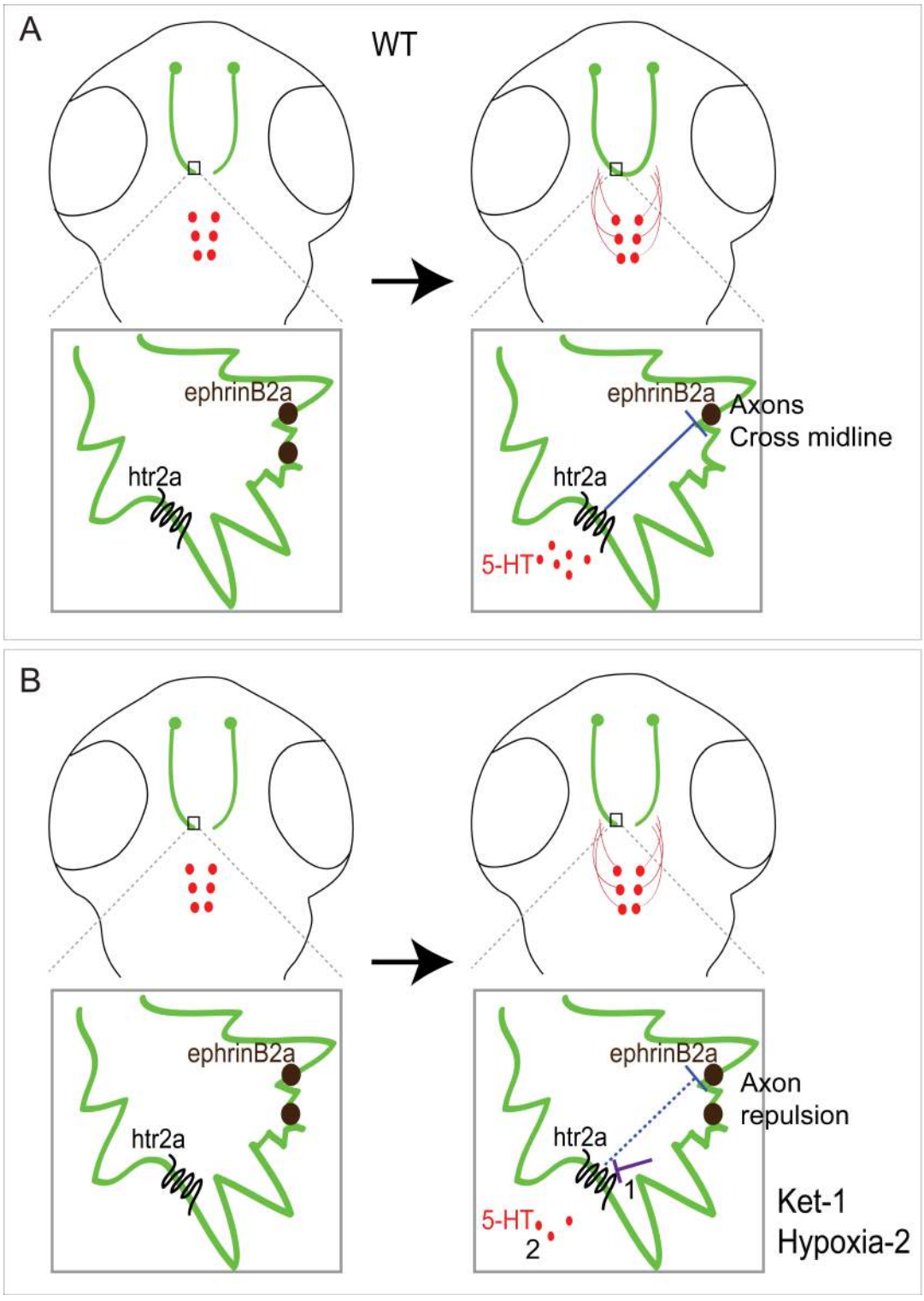
A
WT
ephrinB2a
htr2a
ephrinB2a
Axons
Cross midline
htr2a
5-HT
B
ephrinB2a
htr2a
ephrinB2a
Axon
repulsion
htr2a
1
5-HT
2
Ket-1
Hypoxia-2

unexpectedly more complex systems of axon guidance, including of balancing neuronal activity, although it is not clear if this applies to midline crossing (Suarez et al., 2014).

Our data show a novel link between the embryonic environment and early circuit formation. We provide evidence that 5-HT is instructive for CNS axon guidance and that 5-HT circuits regulate connectivity development. Our findings suggest that modification of the serotonergic system during early development can contribute to permanent CNS connectivity alterations.

References

Azmitia EC. (2007) Serotonin and brain: evolution, neuroplasticity, and homeostasis. Int. Rev. Neurobiol. 77:31-56.

Barnes, N.M., and Sharp, T. (1999). A review of central 5-HT receptors and their function. Neuropharmacology *38*, 1083–1152.

Bellipanni, G., Rink, E., and Bally-Cuif, L. (2002). Cloning of two tryptophan hydroxylase genes expressed in the diencephalon of the developing zebrafish brain. Mech. Dev. *119 Suppl* , S215–S220.

Bonkowsky, J.L., and Chien, C.-B. (2005). Molecular cloning and developmental expression of foxP2 in zebrafish. Dev. Dyn. *234*, 740–746.

Bonkowsky, J.L., Wang, X., Fujimoto, E., Lee, J.E., Chien, C.-B., and Dorsky, R.I. (2008). Domain-specific regulation of foxP2 CNS expression by lef1. BMC Dev. Biol. *8*, 103.

Bonnin, A., Torii, M., Wang, L., Rakic, P., and Levitt, P. (2007). Serotonin modulates the response of embryonic thalamocortical axons to netrin-1. Nat. Neurosci. *10*, 588–597.

Brogden, R.N., and Sorkin, E.M. (1990). Ketanserin. A review of its pharmacodynamic and pharmacokinetic properties, and therapeutic potential in hypertension and peripheral vascular disease. Drugs *40*, 903–949.

Casadio, A., Martin, K.C., Giustetto, M., Zhu, H., Chen, M., Bartsch, D., Bailey, C.H., and Kandel, E.R. (1999). A transient, neuron-wide form of CREB-mediated long-term facilitation can be stabilized at specific synapses by local protein synthesis. Cell *99*, 221–237.

Choi, Y.-B., Li, H.-L., Kassabov, S.R., Jin, I., Puthanveettil, S. V, Karl, K.A., Lu, Y., Kim, J.-H., Bailey, C.H., and Kandel, E.R. (2011). Neurexin-neuroligin transsynaptic interaction mediates learning-related synaptic remodeling and long-term facilitation in aplysia. Neuron *70*, 468–481.

Curado, S., Stainier, D.Y.R., and Anderson, R.M. (2008). Nitroreductase-mediated cell/tissue ablation in zebrafish: a spatially and temporally controlled ablation method with applications in developmental and regeneration studies. Nat. Protoc. *3*, 948–954.

Dahlström, A., and Fuxe, K. (1964). Localization of monoamines in the lower brain stem. Experientia *20*, 398–399.

Davison, J.M., Akitake, C.M., Goll, M.G., Rhee, J.M., Gosse, N., Baier, H., Halpern, M.E., Leach, S.D., and Parsons, M.J. (2007). Transactivation from Gal4-VP16 transgenic insertions for tissue-specific cell labeling and ablation in zebrafish. Dev. Biol. *304*, 811–824.

Hancock, M.L., Preitner, N., Quan, J., and Flanagan, J.G. (2014). MicroRNA-132 is enriched in developing axons, locally regulates Rasa1 mRNA, and promotes axon extension. J. Neurosci. *34*, 66–78.

Hanson, M.G., and Landmesser, L.T. (2004). Normal patterns of spontaneous activity are required for correct motor axon guidance and the expression of specific guidance molecules. Neuron *43*, 687–701.

Imondi, R., and Kaprielian, Z. (2001). Commissural axon pathfinding on the contralateral side of the floor plate: a role for B-class ephrins in specifying the dorsoventral position of longitudinally projecting commissural axons. Development *128*, 4859–4871.

Jao, L.-E., Wente, S.R., and Chen, W. (2013). Efficient multiplex biallelic zebrafish genome editing using a CRISPR nuclease system. Proc. Natl. Acad. Sci. U. S. A. *110*, 13904–13909.

Jinek, M., Chylinski, K., Fonfara, I., Hauer, M., Doudna, J.A., and Charpentier, E. (2012). A programmable dual-RNA-guided DNA endonuclease in adaptive bacterial immunity. Science *337*, 816–821.

Jitsuki, S., Takemoto, K., Kawasaki, T., Tada, H., Takahashi, A., Becamel, C., Sano, A., Yuzaki, M., Zukin, R.S., Ziff, E.B., et al. (2011). Serotonin mediates cross-modal reorganization of cortical circuits. Neuron *69*, 780–792.

Jung, H., O'Hare, C.M., and Holt, C.E. (2011). Translational regulation in growth cones. Curr. Opin. Genet. Dev. *21*, 458–464.

Kadison, S.R., Mäkinen, T., Klein, R., Henkemeyer, M., and Kaprielian, Z. (2006). EphB receptors and ephrin-B3 regulate axon guidance at the ventral midline of the embryonic

mouse spinal cord. J. Neurosci. *26*, 8909–8914.

Kaslin, J., and Panula, P. (2001). Comparative anatomy of the histaminergic and other aminergic systems in zebrafish (Danio rerio). J. Comp. Neurol. *440*, 342–377.

Katz, L.C., and Shatz, C.J. (1996). Synaptic activity and the construction of cortical circuits. Science *274*, 1133–1138.

Kettleborough, R.N.W., Busch-Nentwich, E.M., Harvey, S.A., Dooley, C.M., de Bruijn, E., van Eeden, F., Sealy, I., White, R.J., Herd, C., Nijman, I.J., et al. (2013). A systematic genome-wide analysis of zebrafish protein-coding gene function. Nature *496*, 494–497.

Van Kleef, E.S.B., Gaspar, P., and Bonnin, A. (2012). Insights into the complex influence of 5-HT signaling on thalamocortical axonal system development. Eur. J. Neurosci. *35*, 1563–1572.

Lambert, A.M., Bonkowsky, J.L., and Masino, M.A. (2012). The conserved dopaminergic diencephalospinal tract mediates vertebrate locomotor development in zebrafish larvae. J. Neurosci. *32*, 13488–13500.

Lesch, K.-P., and Waider, J. (2012). Serotonin in the modulation of neural plasticity and networks: implications for neurodevelopmental disorders. Neuron *76*, 175–191.

Lillesaar, C. (2011). The serotonergic system in fish. J. Chem. Neuroanat. *41*, 294–308.

Lillesaar, C., Stigloher, C., Tannhäuser, B., Wullimann, M.F., and Bally-Cuif, L. (2009). Axonal projections originating from raphe serotonergic neurons in the developing and adult zebrafish, Danio rerio, using transgenics to visualize raphe-specific pet1 expression. J. Comp. Neurol. *512*, 158–182.

Matsukawa, M., Nakadate, K., Ishihara, I., and Okado, N. (2003). Synaptic loss following depletion of noradrenaline and/or serotonin in the rat visual cortex: a quantitative electron microscopic study. Neuroscience *122*, 627–635.

McLean, D.L., and Fetcho, J.R. (2004). Ontogeny and innervation patterns of dopaminergic, noradrenergic, and serotonergic neurons in larval zebrafish. J. Comp. Neurol. *480*, 38–56.

Miniaci, M.C., Kim, J.-H., Puthanveettil, S. V, Si, K., Zhu, H., Kandel, E.R., and Bailey, C.H. (2008). Sustained CPEB-dependent local protein synthesis is required to stabilize synaptic growth for persistence of long-term facilitation in Aplysia. Neuron *59*, 1024–1036.

Persico, A.M., Mengual, E., Moessner, R., Hall, F.S., Revay, R.S., Sora, I., Arellano, J., DeFelipe, J., Gimenez-Amaya, J.M., Conciatori, M., et al. (2001). Barrel pattern formation requires serotonin uptake by thalamocortical afferents, and not vesicular

monoamine release. J. Neurosci. *21*, 6862–6873.

Pisharath, H., and Parsons, M.J. (2009). Nitroreductase-mediated cell ablation in transgenic zebrafish embryos. Methods Mol. Biol. *546*, 133–143.

Pocock, R., and Hobert, O. (2010). Hypoxia activates a latent circuit for processing gustatory information in C. elegans. Nat. Neurosci. *13*, 610–614.

Puthanveettil, S. V, Monje, F.J., Miniaci, M.C., Choi, Y.-B., Karl, K.A., Khandros, E., Gawinowicz, M.A., Sheetz, M.P., and Kandel, E.R. (2008). A new component in synaptic plasticity: upregulation of kinesin in the neurons of the gill-withdrawal reflex. Cell *135*, 960–973.

Rahman, M.S., and Thomas, P. (2009). Molecular cloning, characterization and expression of two tryptophan hydroxylase (TPH-1 and TPH-2) genes in the hypothalamus of Atlantic croaker: down-regulation after chronic exposure to hypoxia. Neuroscience *158*, 751–765.

Riccio, O., Potter, G., Walzer, C., Vallet, P., Szabó, G., Vutskits, L., Kiss, J.Z., and Dayer, A.G. (2009). Excess of serotonin affects embryonic interneuron migration through activation of the serotonin receptor 6. Mol. Psychiatry *14*, 280–290.

Rubenstein, J.L. (1998). Development of serotonergic neurons and their projections. Biol. Psychiatry *44*, 145–150.

Saxena, P.R. (1995). Serotonin receptors: subtypes, functional responses and therapeutic relevance. Pharmacol. Ther. *66*, 339–368.

Schneider, H., Fritzky, L., Williams, J., Heumann, C., Yochum, M., Pattar, K., Noppert, G., Mock, V., and Hawley, E. (2012). Cloning and expression of a zebrafish 5-HT(2C) receptor gene. Gene *502*, 108–117.

Silberstein, S.D. (1998). Methysergide. Cephalalgia *18*, 421–435.

Steinbusch, H.W. (1981). Distribution of serotonin-immunoreactivity in the central nervous system of the rat-cell bodies and terminals. Neuroscience *6*, 557–618.

Stevenson, T.J., Trinh, T., Kogelschatz, C., Fujimoto, E., Lush, M.E., Piotrowski, T., Brimley, C.J., and Bonkowsky, J.L. (2012). Hypoxia disruption of vertebrate CNS pathfinding through ephrinB2 Is rescued by magnesium. PLoS Genet. *8*, e1002638.

Suárez, R., Fenlon, L.R., Marek, R., Avitan, L., Sah, P., Goodhill, G.J., and Richards, L.J. (2014). Balanced interhemispheric cortical activity is required for correct targeting of the corpus callosum. Neuron *82*, 1289–1298.

Tayler, T.D., Pacheco, D.A., Hergarden, A.C., Murthy, M., and Anderson, D.J. (2012). A

neuropeptide circuit that coordinates sperm transfer and copulation duration in Drosophila. Proc. Natl. Acad. Sci. U. S. A. *109*, 20697–20702.

Teraoka, H., Russell, C., Regan, J., Chandrasekhar, A., Concha, M.L., Yokoyama, R., Higashi, K., Take-Uchi, M., Dong, W., Hiraga, T., et al. (2004). Hedgehog and Fgf signaling pathways regulate the development of tphR-expressing serotonergic raphe neurons in zebrafish embryos. J. Neurobiol. *60*, 275–288.

Toda, T., Homma, D., Tokuoka, H., Hayakawa, I., Sugimoto, Y., Ichinose, H., and Kawasaki, H. (2013). Birth Regulates the Initiation of Sensory Map Formation through Serotonin Signaling. Dev. Cell *27*, 32–46.

Vitalis, T., Cases, O., Passemard, S., Callebert, J., and Parnavelas, J.G. (2007). Embryonic depletion of serotonin affects cortical development. Eur. J. Neurosci. *26*, 331–344.

Wan, Y., Otsuna, H., Chien, C.-B., and Hansen, C. (2012). FluoRender: An Application of 2D Image Space Methods for 3D and 4D Confocal Microscopy Data Visualization in Neurobiology Research. IEEE Pac. Vis. Symp. 201–208.

Wilson, S.W., Ross, L.S., Parrett, T., and Easter, S.S. (1990). The development of a simple scaffold of axon tracts in the brain of the embryonic zebrafish, Brachydanio rerio. Development *108*, 121–145.

Winckler, B., and Mellman, I. (2010). Trafficking guidance receptors. Cold Spring Harb. Perspect. Biol. *2*, a001826.

Witteveen, J.S., Middelman, A., van Hulten, J.A., Martens, G.J.M., Homberg, J.R., and Kolk, S.M. (2013). Lack of serotonin reuptake during brain development alters rostral raphe-prefrontal network formation. Front. Cell. Neurosci. *7*, 143.

Xing, L., Hoshijima, K., Grunwald, D.J., Fujimoto, E., Quist, T.S., Sneddon, J., Chien, C.-B., Stevenson, T.J., and Bonkowsky, J.L. (2012). Zebrafish foxP2 zinc finger nuclease mutant has normal axon pathfinding. PLoS One *7*, e43968.

Xing, L., Quist, T.S., Stevenson, T.J., Dahlem, T.J., and Bonkowsky, J.L. (2014). Rapid and efficient zebrafish genotyping using PCR with high-resolution melt analysis. J. Vis. Exp. e51138.

Yokogawa, T., Hannan, M.C., and Burgess, H.A. (2012). The dorsal raphe modulates sensory responsiveness during arousal in zebrafish. J. Neurosci. *32*, 15205–15215.

CHAPTER 5

DISCUSSION

Summary

The work in this dissertation has advanced understanding of the molecular mechanisms involved in axon development. I developed a zebrafish developmental model to investigate the role of 5-HT and FoxP2 in axon guidance. I found that FoxP2 is not necessary for axon pathfinding in the defined axon TCPTc (Figure 5.1A) (see Chapter 3) (Figure 5.1B), but it can increase the expression levels of CNTNAP2. I also discovered that 5-HT is required for TCPTc axon guidance by inhibiting the protein levels of ephrinB2a (see Chapter 4) (Figure 5.1C).

In Chapter 2, I also show that PCR combined with high resolution melting analysis (HRMA) is a rapid and powerful technique for genotyping. HRMA can detect single point mutations, and is ideal for large-scale screening. It can be used in both embryonic and adult zebrafish to detect transgenes as well as mutations induced either by zinc finger nucleases (ZFNs), transcription activation-like effector nucleases (TALENs) or clustered regularly interspaced short palindromic repeats (CRISPR) (Dahlem et al. 2012; Parant et al. 2009; Xing et al. 2012; Xing, unpublished). Application of HRMA facilitates identification and characterization of genes involved in axon development.

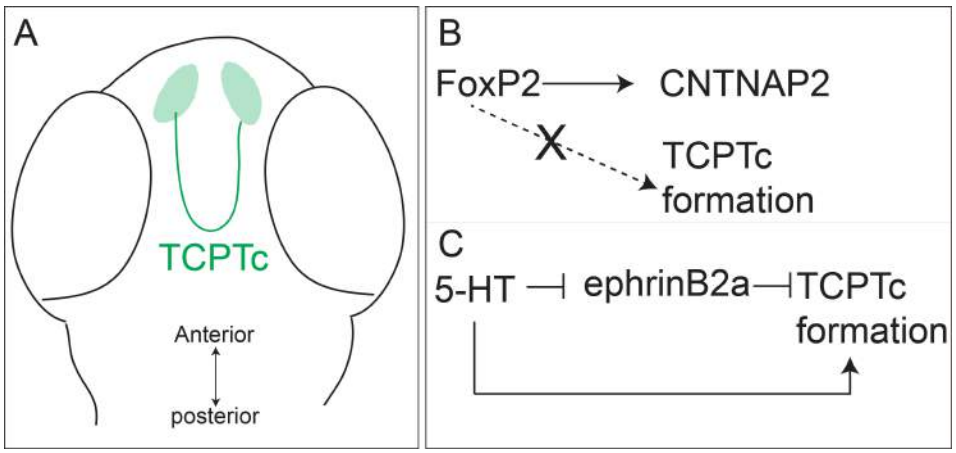

Figure 5.1. Model of regulation mechanisms involved in TCPTc formation. A. Illustration of TCPTc pathways in 72 hpf zebrafish. B. FoxP2 increases expression of CNTNAP2, but is not required for TCPTc formation (Chapter 3). C. 5-HT inhibits ephrinB2a protein levels and contributes to TCPTc formation (Chapter 4).

The role of FoxP2 in development

When the study was initiated, very little was known about the mechanism by which FoxP2 regulates early brain development. Though studies in multiple species, including human, mouse, and songbird, indicate that FoxP2 is necessary for brain development (Groszer et al., 2008; Haesler et al., 2004; Lai et al., 2001; Shu et al., 2005; Takahashi et al., 2003; Vargha-Khadem et al., 2005), only one single study tested the direct role of FoxP2 in development. This study identified FoxP2 as necessary for neurite outgrowth by a cell culture assay (Vernes et al., 2011). Our study finds that knock down of FoxP2 leads to a decreased expression level of CNTNAP2. Combined with the recent findings that FoxP2 is involved in neuronal differentiation and neurogenesis during development (Devanna et al., 2014; Tsui et al., 2013), our study suggests that FoxP2 plays a complex role in brain development, which might be mediated by a variety of downstream target signaling. The multiple developmental roles of FoxP2 thus might

account for the importance of FoxP2 in language development and processing.

A few studies have indicated that FoxP2 might be involved in axon development, since FoxP2 can target multiple axon guidance molecules, including EPHA2 and SEMA3B (Spiteri et al., 2007; Vernes et al., 2007, 2011). However, in axon tracts I identified in zebrafish, including the TCPTc and dopaminergic axons, I did not observe axon guidance defects in FoxP2 mutants. Though I did not find abnormal axon pathfinding in FoxP2 mutants, I cannot exclude the possibility that FoxP2 might exert subtle effects on axon pathfinding that our assays could not detect, nor the possibility that FoxP2 plays a role in other unidentified axon tracts. We can take advantage of multiple transgenic lines having been generated in zebrafish to address the general role of FoxP2 in the CNS axons. Studies are also required in order to test whether FoxP2 plays a conserved role in axon guidance among different species. The FoxP2 protein is highly conserved in mammals. In chimpanzees, FoxP2 differs from that in humans by the substitution of two amino acids (Enard et al., 2002). It is proposed that the two amino acid substitutions are critical for language and speech development in humans. Consequently, dissecting the developmental role of FoxP2 among different species will provide insight into the functional changes of FoxP2 during evolution. On the other hand, we should be cautious to interpret the novel function of FoxP2 in humans, since FoxP2 is also important for imitation of tutor songs in songbirds and appropriate ultrasonic vocalization in mice (Haesler et al., 2004; Shu et al., 2005; Teramitsu et al., 2004). The uniquely expressive power of human language must derive from the delicate interaction between FoxP2 and numerous other molecules, rather than from the role of the single molecule FoxP2.

Given our findings of decreased CNTNAP2 expression levels in FoxP2 mutants, and the role of CNTNAP2 in synaptic function (Groszer et al., 2008; Spiteri et al., 2007; Vernes et al., 2007), future studies will be needed to examine the role of FoxP2 in synaptic development. To elucidate the role of FoxP2 in synaptic development, numerous novel techniques can be employed. These include: GFP reconstitution across synaptic partners (GRASP), Fibronectin intrabodies generated with mRNA display (FingR), genetically encoded fluorescent synaptic proteins such as SYP (synaptophysin)-EGFP or Trans-Cellular Activation of Transcription (TCAT), currently being developed in our laboratory (Appelbaum et al., 2010; Bonkowsky et al., unpublished; Gross et al., 2013; Kim et al., 2012). These techniques provide a powerful means to visualize endogenous synapses in live zebrafish, and thus will promote our understanding of molecular mechanisms (including FoxP2) involved in synaptic formation and function. Elucidating the role of FoxP2 in axon guidance and/or synaptic formation will help us better understand the mechanism by which FoxP2 regulates early brain wiring and interpret how disruption of FoxP2 contributes to specific language impairment.

The role of 5-HT in axon development

I have shown that 5-HT is necessary for TCPTc formation with an *in vivo* system. This adds another piece of evidence that 5-HT is important for early brain development. Many studies have shown that the role of the neurotransmitter 5-HT is to function in adult physiology by modulation of synaptic strength (Gingrich et al., 2003; Lesch and Waider, 2012). However, more and more evidence demonstrates that 5-HT is involved in brain circuit formation by regulating neuronal migration, synapse formation, axonal

branching, and dendrite arborization (Matsukawa et al., 2003; Persico et al., 2001; Riccio et al., 2009; Vitalis et al., 2007). The critical role of 5-HT in early development may account for clinical outcomes in children exposed to prenatal selective serotonin reuptake inhibitors (SSRIs). Prenatal use of SSRIs have been found to result in susceptibility to autism or other developmental delays, particularly in boys (Harrington et al., 2014). Elucidating the role of 5-HT in early brain circuit formation will advance our knowledge of pathogenic mechanisms in many neurological disorders. However, to date, very few studies are available to examine the direct mechanism of 5-HT involved in development.

We found that 5-HT controls axon pathfinding through the regulation of the axon guidance receptor ephrinB2a. In the presence of 5-HT, levels of ephrinB2a are decreased, and axons are able to cross the midline. Conversely, when serotonergic signaling is decreased, by pharmacological manipulation or ablation of serotonergic neurons, ephrinB2a levels are increased and axons fail to cross the midline. We interpret this finding to mean that 5-HT regulates the protein levels of an axon guidance receptor, ephrinB2a, revealing a novel mechanism by which a monoamine is involved in development. Further studies will determine how 5-HT regulates ephrinB2a protein levels in axons. The regulation of axon guidance receptors by either protein synthesis or transport are important mechanisms in axon guidance (Dent and Gertler, 2003; Jung et al., 2012; Martin, 2004); these mechanisms are candidates for the regulation of ephrinB2a by 5-HT. Dissecting the mechanism by which 5-HT regulates axon guidance receptors will facilitate progress in understanding the role of 5-HT in early development and later behavior.

We found that in zebrafish 5-HT regulates axon guidance via 5-HTR2, distinct

from what has been observed in mice, in which 5-HT modulation of axon guidance is mediated by 5-HT1B/1D (Bonnin et al., 2007). This indicates that both excitatory (5-HTR2) and inhibitory (5-HTR1) receptors can be activated by 5-HT during development, adding to the complexity of networks regulated by 5-HT. HTR2 is a G-protein coupled receptor that activates phospholipase C and then catalyzes the conversion of phosphatidylinositol 4,5-bisphosphate (PIP2) into inositol trisphosphate (IP3) and di-glyceride (DAG). IP3 acts on a ligand-gated Ca^{2+} channel, resulting in the release of Ca^{2+} from the endoplasmic reticulum into the cytoplasm. I hypothesized that activation of this signaling pathway results in a decrease in ephrinB2a levels. However, when I tested the effect of Ca^{2+} release on ephrinB2a levels by inhibiting Ca^{2+} release from the intracellular sarcoplasmic reticulum with u73122 or 2-Aminoethoxydiphenyl borate, I did not observe altered ephrinB2 levels (data not shown). This indicates that 5-HT acts via a nonclassical pathway during axon guidance, suggesting that 5-HT plays an instructive role, not a modulatory role in midline axon crossing, in contrast to what has been found in mice (Bonnin et al., 2007). Bonnin's study showed that the second messenger cAMP mediates 5-HT modulation of axonal response to netrin-1. The distinct mechanisms found in mice and zebrafish show the diversity of 5-HT response during axon pathfinding. Future studies will determine how 5-HT interacts with the molecule ephrinB2a.

In the future, it will be of particular interest to expand this study to characterize the general role of 5-HT in the development of a variety of CNS axons. To achieve that, we can utilize multiple transgenic zebrafish lines generated in the lab to test whether the modification of serotonergic signaling leads to other axon guidance defects in the developing CNS. This will result in a better understanding of the role of 5-HT in brain

wiring. Based on the fact that deficiency of 5-HT synthesis by *tph2* knock out does not lead to gross cellular or morphological changes in brain architecture (Narboux-Nême et al., 2013), I expect a specific role for 5-HT will be found in only certain brain circuits. This specific role of 5-HT might be due to the spatial and temporal regulation of 5-HT in the CNS development.

The regulation of axon guidance by 5-HT under hypoxia

We found that a decreased level of 5-HT by hypoxia contributes to axon guidance defects. The finding suggests that modification of the serotonergic system by early environmental exposures contributes to permanent CNS connectivity alterations. Alteration of serotonergic signaling has been observed in many neurological disorders, such as autism, mental retardation, and depression (Berger-Sweeney and Hohmann, 1997), consistent with the potential role of 5-HT in early brain circuit formation (Matsukawa et al., 2003; Persico et al., 2001; Riccio et al., 2009; Vitalis et al., 2007). Our finding suggests that 5-HT could be a mediator, translating the environmental stimuli into neural circuit changes. This might explain the plasticity of the serotonergic system in response to the environment.

I discovered a novel neural circuit modified by 5-HT under hypoxic conditions. The axon guidance defects that I have observed under hypoxic conditions suggest that the developmental environment can manipulate neural circuits. Interestingly, the axon guidance defects in hypoxic zebrafish embryos recapitulate the phenotype observed in some premature infants by diffusion tensor imaging (DTI) (Yeatman et al., 2009), which indicates that the conserved circuits and/or pathways are affected by environmental stress.

Fluoxetine, a serotonin reuptake inhibitor, rescued axon guidance defects following hypoxia in our experiment. This indicates that early intervention is an efficient way to minimize brain abnormalities. Therefore, elucidating the role of 5-HT or other molecules in zebrafish development will help us understand the occurrence of neurodevelopmental disorders correlated to an adverse environment or a modified serotonergic system.

Conclusion

In this dissertation, I have shown the value of the HRMA technique for large-scale genotyping, and have examined the effects of FoxP2 and 5-HT in the developing zebrafish brain. PCR combined with HRMA promotes identification and characterization of genes involved in zebrafish brain development. FoxP2 can regulate the expression level of CNTNAP2, though it is not required for axon guidance. The developmental role of FoxP2 in the CNS could explain how FoxP2 contributes to language development. This work also reveals an important mechanism involved in midline axon crossing: 5-HT regulates axon guidance via ephrinB2a. Moreover, alteration of 5-HT levels by hypoxia contributes to axon guidance defects. This offers a novel mechanism by which the developmental environment manipulates the neural circuits.

Axon guidance is a critical process involved in brain wiring, and disruption of CNS connectivity may be associated with many neurological disorders. Consequently, uncovering the molecular mechanisms involved will facilitate progress toward understanding neurodevelopmental disorders and offer the possibility of improved therapeutic approaches.

Axon guidance is not a process mediated by a single receptor induced by

intracellular signaling, but involves networks of multiple axon guidance molecules and receptors. Future studies will first address whether other axon guidance molecules, such as Slit-Robo and Netrin-DCC/Unc5, are regulated by 5-HT and/or are involved in axon guidance defects under hypoxic conditions. Additional work will analyze how the complicated network of multiple axon guidance molecules and their receptors functions to cause disruption of axon guidance following hypoxia. Further studies are also necessary to analyze the potential interaction between 5-HT and FoxP2 or CNTNAP2 in order to better understand the role of molecular networks in the development of brain architecture.

References

Appelbaum, L., Wang, G., Yokogawa, T., Skariah, G.M., Smith, S.J., Mourrain, P., and Mignot, E. (2010). Circadian and homeostatic regulation of structural synaptic plasticity in hypocretin neurons. Neuron *68*, 87–98.

Berger-Sweeney, J., and Hohmann, C.F. (1997). Behavioral consequences of abnormal cortical development: insights into developmental disabilities. Behav. Brain Res. *86*, 121–142.

Bonnin, A., Torii, M., Wang, L., Rakic, P., and Levitt, P. (2007). Serotonin modulates the response of embryonic thalamocortical axons to netrin-1. Nat. Neurosci. *10*, 588–597.

Dahlem, T.J., Hoshijima, K., Jurynec, M.J., Gunther, D., Starker, C.G., Locke, A.S., Weis, A.M., Voytas, D.F., and Grunwald, D.J. (2012). Simple methods for generating and detecting locus-specific mutations induced with TALENs in the zebrafish genome. PLoS Genet. *8*, e1002861.

Dent, E.W., and Gertler, F.B. (2003). Cytoskeletal dynamics and transport in growth cone motility and axon guidance. Neuron *40*, 209–227.

Devanna, P., Middelbeek, J., and Vernes, S.C. (2014). FOXP2 drives neuronal differentiation by interacting with retinoic acid signaling pathways. Front. Cell. Neurosci. *8*, 305.

Enard, W., Przeworski, M., Fisher, S.E., Lai, C.S.L., Wiebe, V., Kitano, T., Monaco, A.P., and Pääbo, S. (2002). Molecular evolution of FOXP2, a gene involved in speech and language. Nature *418*, 869–872.

Gingrich, J.A., Ansorge, M.S., Merker, R., Weisstaub, N., and Zhou, M. (2003). New lessons from knockout mice: The role of serotonin during development and its possible contribution to the origins of neuropsychiatric disorders. CNS Spectr. *8*, 572–577.

Gross, G.G., Junge, J.A., Mora, R.J., Kwon, H.-B., Olson, C.A., Takahashi, T.T., Liman, E.R., Ellis-Davies, G.C.R., McGee, A.W., Sabatini, B.L., et al. (2013). Recombinant probes for visualizing endogenous synaptic proteins in living neurons. Neuron *78*, 971–985.

Groszer, M., Keays, D.A., Deacon, R.M.J., de Bono, J.P., Prasad-Mulcare, S., Gaub, S., Baum, M.G., French, C.A., Nicod, J., Coventry, J.A., et al. (2008). Impaired synaptic plasticity and motor learning in mice with a point mutation implicated in human speech deficits. Curr. Biol. *18*, 354–362.

Haesler, S., Wada, K., Nshdejan, A., Morrisey, E.E., Lints, T., Jarvis, E.D., and Scharff, C. (2004). FoxP2 expression in avian vocal learners and non-learners. J. Neurosci. *24*, 3164–3175.

Harrington, R.A., Lee, L.-C., Crum, R.M., Zimmerman, A.W., and Hertz-Picciotto, I. (2014). Prenatal SSRI Use and Offspring With Autism Spectrum Disorder or Developmental Delay. Pediatrics *133*, e1241–e1248.

Jung, H., Yoon, B.C., and Holt, C.E. (2012). Axonal mRNA localization and local protein synthesis in nervous system assembly, maintenance and repair. Nat. Rev. Neurosci. *13*, 308–324.

Kim, J., Zhao, T., Petralia, R.S., Yu, Y., Peng, H., Myers, E., and Magee, J.C. (2012). mGRASP enables mapping mammalian synaptic connectivity with light microscopy. Nat. Methods *9*, 96–102.

Lai, C.S.L., Fisher, S.E., Hurst, J.A., Vargha-Khadem, F., and Monaco, A.P. (2001). A forkhead-domain gene is mutated in a severe speech and language disorder. Nature *413*, 519–523.

Lesch, K.-P., and Waider, J. (2012). Serotonin in the modulation of neural plasticity and networks: implications for neurodevelopmental disorders. Neuron *76*, 175–191.

Martin, K.C. (2004). Local protein synthesis during axon guidance and synaptic plasticity. Curr. Opin. Neurobiol. *14*, 305–310.

Matsukawa, M., Nakadate, K., Ishihara, I., and Okado, N. (2003). Synaptic loss following depletion of noradrenaline and/or serotonin in the rat visual cortex: a quantitative electron

microscopic study. Neuroscience *122*, 627–635.

Narboux-Nême, N., Angenard, G., Mosienko, V., Klempin, F., Pitychoutis, P.M., Deneris, E., Bader, M., Giros, B., Alenina, N., and Gaspar, P. (2013). Postnatal growth defects in mice with constitutive depletion of central serotonin. ACS Chem. Neurosci. *4*, 171–181.

Parant, J.M., George, S.A., Pryor, R., Wittwer, C.T., and Yost, H.J. (2009). A rapid and efficient method of genotyping zebrafish mutants. Dev. Dyn. *238*, 3168–3174.

Persico, A.M., Mengual, E., Moessner, R., Hall, F.S., Revay, R.S., Sora, I., Arellano, J., DeFelipe, J., Gimenez-Amaya, J.M., Conciatori, M., et al. (2001). Barrel pattern formation requires serotonin uptake by thalamocortical afferents, and not vesicular monoamine release. J. Neurosci. *21*, 6862–6873.

Riccio, O., Potter, G., Walzer, C., Vallet, P., Szabó, G., Vutskits, L., Kiss, J.Z., and Dayer, A.G. (2009). Excess of serotonin affects embryonic interneuron migration through activation of the serotonin receptor 6. Mol. Psychiatry *14*, 280–290.

Shu, W., Cho, J.Y., Jiang, Y., Zhang, M., Weisz, D., Elder, G.A., Schmeidler, J., De Gasperi, R., Sosa, M.A.G., Rabidou, D., et al. (2005). Altered ultrasonic vocalization in mice with a disruption in the Foxp2 gene. Proc. Natl. Acad. Sci. U. S. A. *102*, 9643–9648.

Spiteri, E., Konopka, G., Coppola, G., Bomar, J., Oldham, M., Ou, J., Vernes, S.C., Fisher, S.E., Ren, B., and Geschwind, D.H. (2007). Identification of the Transcriptional Targets of FOXP2, a Gene Linked to Speech and Language, in Developing Human Brain. Am. J. Hum. Genet. *81*, 1144–1157.

Takahashi, K., Liu, F.-C., Hirokawa, K., and Takahashi, H. (2003). Expression of Foxp2, a gene involved in speech and language, in the developing and adult striatum. J. Neurosci. Res. *73*, 61–72.

Teramitsu, I., Kudo, L.C., London, S.E., Geschwind, D.H., and White, S.A. (2004). Parallel FoxP1 and FoxP2 expression in songbird and human brain predicts functional interaction. J. Neurosci. *24*, 3152–3163.

Tsui, D., Vessey, J.P., Tomita, H., Kaplan, D.R., and Miller, F.D. (2013). FoxP2 regulates neurogenesis during embryonic cortical development. J. Neurosci. *33*, 244–258.

Vargha-Khadem, F., Gadian, D.G., Copp, A., and Mishkin, M. (2005). FOXP2 and the neuroanatomy of speech and language. Nat. Rev. Neurosci. *6*, 131–138.

Vernes, S.C., Spiteri, E., Nicod, J., Groszer, M., Taylor, J.M., Davies, K.E., Geschwind, D.H., and Fisher, S.E. (2007). High-throughput analysis of promoter occupancy reveals direct neural targets of FOXP2, a gene mutated in speech and language disorders. Am. J.

Hum. Genet. *81*, 1232–1250.

Vernes, S.C., Oliver, P.L., Spiteri, E., Lockstone, H.E., Puliyadi, R., Taylor, J.M., Ho, J., Mombereau, C., Brewer, A., Lowy, E., et al. (2011). Foxp2 regulates gene networks implicated in neurite outgrowth in the developing brain. PLoS Genet. *7*, e1002145.

Vitalis, T., Cases, O., Passemard, S., Callebert, J., and Parnavelas, J.G. (2007). Embryonic depletion of serotonin affects cortical development. Eur. J. Neurosci. *26*, 331–344.

Xing, L., Hoshijima, K., Grunwald, D.J., Fujimoto, E., Quist, T.S., Sneddon, J., Chien, C.-B., Stevenson, T.J., and Bonkowsky, J.L. (2012). Zebrafish foxP2 zinc finger nuclease mutant has normal axon pathfinding. PLoS One *7*, e43968.

Xing, L., Quist, T.S., Stevenson, T.J., Dahlem, T.J., and Bonkowsky, J.L. (2014). Rapid and efficient zebrafish genotyping using PCR with high-resolution melt analysis. J. Vis. Exp. e51138.

Yeatman, J.D., Ben-Shachar, M., Bammer, R., and Feldman, H.M. (2009). Using diffusion tensor imaging and fiber tracking to characterize diffuse perinatal white matter injury: a case report. J. Child Neurol. *24*, 795–800.